Development of a chronology for open water reservoirs and subterranean cisterns in the Negev Highlands (Israel) using Optically Stimulated Luminescence

Construction — Utilization — Abandonment

Andrea Junge

Dissertation
zur Erlangung des akademischen Grades eines
Doktor der Naturwissenschaften
(Dr. rer. nat.)
am Institut für Geographie
der Justus-Liebig-Universität Gießen

JUSTUS-LIEBIG-
UNIVERSITÄT
GIESSEN

Gießen, Germany
Februar, 2024

©2024 – Andrea Junge
All Rights Reserved
Typesetting by LaTeX

Supervisor
Prof. Dr. Markus Fuchs
Justus-Liebig-Universität Gießen
Institut für Geographie
Senckenbergstraße 1
35390 Gießen
Germany

Abstract

Ancient open water reservoirs and subterranean cisterns are frequently occurring archaeological installations in drylands like the Negev Highlands, Israel. The former type are round open water reservoirs, which were dug into impermeable layers in foot slope areas and wadis. They may reach 10 m to 12 m in diameter and 4 m to 5 m in depth and were lined internally with unhewn stones and clay or marl that served as an aquiclude. In comparison, subterranean cisterns are rock-cut, excavated into soft limestone or chalk formations with a capacity of up to several hundred cubic meters. These two types of installations to collect and store water can sustain settlements, agriculture, and nomadic pastoralism under dry conditions. Despite the large number of cisterns and reservoirs in the Negev Highlands, they have scarcely been studied systematically.

Crucial for investigating water harvesting systems and their sediments is the establishment of robust chronologies of their life cycles. When the cisterns and water reservoirs are constructed, material is removed and deposited on an adjacent spoil pile. During precipitation events surface runoff from adjoining slopes erodes and transports sediments, which are then deposited in the reservoirs and cisterns. As long as they are maintained, the material is removed and also deposited on the spoil pile. After the cessation of maintenance, the installations were filled up with sediments.

The transport and deposition of sediments enables the application of optically stimulated luminescence (OSL) at the preferred dating method to determine the time of construction, utilisation and abandonment of reservoirs and cisterns. The interpretation of OSL ages is supported by micromorphological analyses and provides insights into the life cycles of the different installations, enabling a discussion about their chronology, the circumstance of construction and their purpose. The age determinations of ten studied installations allow the conclusion that the open water reservoirs were introduced into the Negev Highlands latest during the Intermediate Bronze Age with a continuing construction until Medieval times, while the construction of subterranean cisterns started during the Roman period, without interrupting the construction of further reservoirs. From this, it can be derived that the construction of different types of water collection and storage systems occurred in different contexts. While the construction of reservoirs could be carried out by small groups in a relatively short time, the building of cisterns required more technological knowledge, more individuals, and longer periods, facilitated by central authorities.

Zusammenfassung

Historische, an der Oberfläche befindliche Wasserreservoirs und unterirdische Zisternen sind häufig vorkommende archäologische Installationen in Trockengebieten wie den Negev Highlands in Israel. Die erstgenannten sind runde offene Wasserreservoirs, die in wasserstauende Schichten in Hanglagen und Wadis gegraben wurden. Sie erreichen Durchmesser von bis zu 10 bis 12 m und Tiefen von bis zu 4 m bis 5 m. Im Inneren wurden diese Wasserreservoirs häufig mit unbehauenen Steinen und Ton oder Mergel ausgekleidet, die als Aquiclude dienen. Im Vergleich dazu wurden unterirdische Zisternen in relativ weiche Kalkstein- oder Kreideformationen in den Fels gehauen und haben eine Kapazität von bis zu mehreren hundert Kubikmetern. Die beiden Arten von Installationen zur Sammlung und Speicherung von Oberflächenabfluss ermöglichten die Unterhaltung von Siedlungen, Landwirtschaft und nomadischer Viehzucht unter ariden Umweltbedingungen. Trotz der großen Anzahl von Zisternen und Reservoirs in den Negev Highlands wurden sie in der Vergangenheit jedoch kaum systematisch untersucht.

Entscheidend für die Untersuchung der Regenwasserspeicher und ihren Sedimenten ist die Festlegung robuster Chronologien ihrer Lebenszyklen. Bei der Konstruktion der Zisternen und Wasserreservoirs wurde Material entfernt und auf einem benachbarten Aushubhaufen oder -wall abgelagert. Bei Niederschlagsereignissen werden Sedimente von angrenzenden Hängen erodiert, durch den entstehenden Oberflächenabfluss in die Reservoirs und Zisternen transportiert und dort abgelagert. Während die Installationen gewartet wurden, wurde das akkumulierte Material entfernt und ebenfalls auf dem Aushubhaufen abgelagert. Nach dem Ende der Nutzung und Wartung wurden die Reservoirs und Zisternen teilweise vollständig durch den fuvialen Sedimenteintrag verfüllt.

Der Transport und die Ablagerung von Sedimenten ermöglichen die Anwendung der optisch stimulierten Lumineszenz (OSL) als bevorzugte Methode zur Bestimmung des Zeitpunkts der Konstruktion, Nutzung und Aufgabe von Reservoirs und Zisternen. Die Interpretation der OSL-Alter wird durch mikromorphologische Analysen unterstützt und ermöglicht Einblicke in die Lebenszyklen der verschiedenen Regenwasserspeicher, wodurch eine Diskussion über ihre Chronologie, die Umstände der Konstruktion und ihren Zweck ermöglicht wird.

Die Untersuchung und Altersbestimmungen von zehn Installationen lassen den Schluss zu, dass die offenen Wasserreservoirs spätestens während der Mittleren Bronzezeit in den Negev Highlands eingeführt und bis hinein ins Mittelalter errichtet wurden, während der Bau von unterirdischen Zisternen in der Römerzeit begann, ohne die Errichtung von weiteren Reservoirs zu unterbinden. Daraus kann abgeleitet werden, dass die Errichtung unterschiedlicher Arten von Systemen zur Sammlung und Speicherung von Oberflächenabfluss in verschiedenen Kontexten stattfand. Während der Bau von Reservoirs durch kleinen Gruppen von Personen in relativ kurzer Zeit durchgeführt werden konnte, erforderte der Bau von Zisternen mehr technologisches Wissen, eine größer Anzahl von Personen und längere Zeiträume, die durch zentrale Obrigkeiten bereitgestellt und gesteuert werden konnten.

Preface

This dissertation was written in the Department of Geography of Justus Liebig University Giessen. It is part of a research project called "Potential use of ancient cisterns for palaeoenvironmental research and geoarchaeology: the Negev Highlands, Israel" (originally: "Nutzungspotential historischer Zisternen für die Paläoumweltforschung und Geoarchäologie: Die Negev Highlands, Israel"). The initial phase of the project was financially supported by the German-Israeli-Foundation (GIF) and the main project was funded by the German Research Foundation (DFG, No. FU 417/33-1).
The conducted research is based on a cooperation between the Department of Geography (Physical Geography) of Justus Liebig University Giessen, the Institute of Archaeology of Tel Aviv University and the Department of Maritime Civilizations (Recanati Institute of Maritime Studies) of the University of Haifa. The interdisciplinary research team allowed a comprehensive study of ancient water reservoirs and cisterns in the Negev Highlands (Israel) from a geoarchaeological point of view. In the past, these installations to collect and store surface runoff were a major source of water to sustain drinking water needs, animal husbandry and agriculture in the arid region. Today, several hundreds of ancient water reservoirs and subterranean cisterns can be found all over the Negev Highlands. These witnesses of the settlement history in this area bear information about their time and context of construction, utilization and abandonment that has not been studied yet.
This dissertation is focused on the historical classification of these archaeological features by determining their time of construction, maintenance and cessation of use applying optically stimulated luminescence (OSL) dating. The results are presented in three peer-reviewed scientific articles and combined here as a cumulative dissertation.

I thankfully dedicate this dissertation to my wonderful parents.

"Rivers know this: There is no hurry.
We shall get there some day."

– A. A. Milne, Winnie the Pooh –

Acknowledgements

Even though, my name is written on the cover of this dissertation, the list of people that made my research possible is very long and I can only attempt to thank each and every single one.
I owe deep gratitude to my supervisor, Prof. Dr. Markus Fuchs, who encouraged me when I lost my confidence, who supported me when I needed help and asked me to go the extra mile when I put down my work prematurely. Besides this, a very special thank-you needs to be send to all the people, that worked with me side by side on this project: Prof. Dr. Ruth Shahack-Gross who spent as much time at the microscope to give her micromorphological insights to this project as she spent on being a helpful and supporting mentor, Prof. Dr. Israel Finkelstein whose knowledge about the Negev Highlands' archaeology cannot be replaced by a thousand books, Dr. Zachary C. Dunseth who taught me everything I know about archaeological excavations and was my 'mental support human' when the field work did not move as smoothly as a proper bucket line, and Dr. Johanna Lomax whose friendship and positivity enlightened the darker moments of my thesis, as well as the brighter. You were my greatest support and my greatest critics and without you not a single word would have been written – thank you very much.
During the many field campaigns, I was supported by countless excavation helpers from all around the globe. I am very grateful for all the relentless work you put into this research project and all the fun you brought into the field. Some honourable mentions are: Hadar Azrad, Omer Ze'evi-Berger, Eli Itkin, Abra Spiciarich, Angie Hudson, Brett Cohen and Ronnie Avidov from Tel Aviv University, Bastian Ringleb and Anna Geis from Justus Liebig University Giessen and Michael Stewart from Sacramento State, California.
Not only in the bright sun of the Negev, but also in the darkness of the luminescence lab, students brought diligence, interest and a lot of fun. In particular, I would like to thank Julian Herche, Salome Oehler and Manuel Pappusch. Further, I thank Matthias Schick for supporting me and my lab work from my bachelor and through my master thesis up to this dissertation, and Dr. Thomas Kolb for our constructive discussions about methodological questions and his moral support, when I needed it the most. For several years, my fellow PhD students Tilmann Wolpert and Raphael Steup went with me to conferences, through the easier and harder times of the first publications, and several hundred times to the cafeteria. Thank you very much for sharing these paths with me, you made them easier and a lot more pleasant.
I would like to thank all the amazing people I met on conferences and workshops that became the toughest rivals in discussions, helpful mentors, supportive colleagues, lovely friends or even all of this. These people are Dr. Lydia Krauß, Dr. Sebastian Kreutzer, Dr. Philipp Schulte, Prof. Dr. Julia Meister, Dr. Julian Struck, Dr. Sascha Scherer, Prof. Dr. Tony Reimann, Prof. Dr. André Kirchner, Benjamin Höpfer and countless others, that hopefully forgive me for not mentioning them specifically. You made the last years as educational for me as you made them cheerful. I am deeply thankful for getting to know each of you.

I am incredibly grateful for the opportunity to express my sincere thanks to Anna Pehlgrimm, Christopher-Ray Lenz, and Dr. Zachary C. Dunseth for your invaluable support and diligent efforts in proofreading this dissertation. I am truly thankful for your time, expertise, and dedication in helping me refine and enhance the content of my writing.

Furthermore, I would like to thank my friends and many flatmates I had over these last years. Especially Jochen Wahlers as my brother from another mother, Rebecca Linz as a friend of the first hour of my bachelor studies, Markus Karstädter as my best friend, Mareike Jannermann as my moral compass, Bastian Ringleb as the one with the best taste in fine dining, Roland Halder as the one that always shows up, Roman Bubholz as the one that never fails to make me laugh, Steffi Menges as the support I can always count on, Dr. Nele Raasch as the one who always had the tastiest wines, Luca Hikl as the one that I clicked with, Anamaria Halcea as the one who made me feel at home when I was far away, and Christopher-Ray Lenz as the one who saved me, when I got lost. Without each and every one of you, without all the adventures we lived through, without your patience to put up with my moods, this thesis would not have been possible. It is as simple as that.

Finally, I would like to express my deepest gratitude to my family and especially to my parents. All my life, I received nothing but support and encouragement from you. You are the people at the other end of the telephone in my darkest moments and you never stopped believing in me. You taught me to enjoy my life, as well as to work hard. You made me the person I am. Für all das danke und liebe ich euch sehr.

Contents

I Theoretical Background and Synopsis of Results **1**

1 Introduction **2**

2 Study Area **4**
2.1 Geology and Geomorphology 4
2.2 Climate 6
2.2.1 Present-day Climate 6
2.2.2 Paleoenvironmental Conditions 6
2.3 Archaeology 7

3 Objects of Study **9**

4 Methods **13**
4.1 Optically Stimulated Luminescence 13
4.1.1 Basic Principles 13
4.1.2 Application of OSL to Cisterns and Reservoirs 14
4.2 Micromorphology 16
4.3 Synergy of the Methods 16

5 Synopsis of the Results & Discussion **18**
5.1 General Results 18
5.2 Assessment of the Methodological Approach 21
5.3 Implications of Dating Results on Archaeological Interpretations 22

6 Conclusions & Outlook **23**

Bibliography **25**

II Publications **32**

First Study: ***Chronology of an ancient water reservoir and the history of human activity in the Negev Highlands, Israel*** **33**

Second Study: ***Construction and use of rock-cut cisterns: a chronological OSL approach in the arid Negev Highlands, Israel*** **47**

Third Study: ***The Archaeology and History of Rock-cut Cisterns and Open Water Reservoirs in the Negev Highlands*** **69**

Declaration **106**

List of Figures

2.1 Map of the souther Levant and the study area 5
2.2 Exemplary vegetation during different seasons in the Negev Highlands 6

3.1 Photographs of open water reservoirs and a subterranean cistern 10
3.2 Photographs of different features that are associated with ancient reservoirs and cisterns 12

4.1 Schematic drawings of the life cycle of an open reservoir 15

5.1 Summary of all OSL dating results from all studied sites 20

Part I

Theoretical Background and Synopsis of Results

1
Introduction

The Negev Highlands (Israel) are characterized by an active settlement history over the past millennia with strong oscillations in the degree of human activity (Greener et al., 2018), as well as semiarid to arid environmental conditions. To establish temporal or permanent settlements in this climate, the supply with water for drinking, animal husbandry and agriculture needed to be assured.

Perennial springs and wells in the area are scarce, often difficult to access and produce only a low flow of water, which makes them impractical for larger settlements (Rubin, 1988). Consequently, the construction of water harvesting and storage installations was necessary. Today, hundreds of ancient subterranean cisterns and open water reservoirs can be found throughout the Negev Highlands (Evenari et al., 1958; Haiman, 1994, 1995; Cohen, 1999; Cohen and Cohen-Amin, 2004) Even though water harvesting is a vital foundation to establish and sustain settlements in arid regions, water reservoirs and cisterns have rarely been studied in detail in the Negev Highlands in the past. Additionally, the age determinations of the construction of these installations were based on a few rare inscriptions within the installations, assessment of the plaster technology utilized or the proximity to sites from different settlement phases. The current dissertation describes a comprehensive investigation of five open water reservoirs and five subterranean cisterns to allow an understanding of the periods and circumstances in which they were constructed, used, and abandoned, as well as to establish a chronology of the different types of water harvesting installations. The age determinations are mainly performed using Optically Stimulated Luminescence (OSL) dating, supported by micromorphological analyses of thin section of the studied sediments.

This dissertation consists of three scientific papers published in peer-reviewed journals with a focus on (geo)archaeological research. The first study entitled "Chronology of an ancient water reservoir and the history of human activity in the Negev Highlands, Israel" (Junge et al., 2018) was published in *Geoarchaeology*. In this work, the initial and successful attempt to determine the age of an open water reservoir near Atar Haroa using OSL dating is described.

The second paper was published in the journal *Archaeological and Anthropological Sciences* under the title "Construction and use of rock-cut cisterns: a chronological OSL approach in the arid Negev Highlands, Israel" (Junge et al., 2021). This study focusses on two subterranean cisterns of the Borot

Hazaz cistern system. It was shown that the combination of OSL dating and micromorphological analyses can be successfully applied to rock-cut cisterns and their associated structures as well.
The third and final paper of this dating project was published in the *Bulletin of the American Schools of Oriental Research (BASOR)* entitled "The Archaeology and History of Rock-cut Cisterns and Open Water Reservoirs in the Negev Highlands" (Junge et al., 2023). It contains the OSL dating results of three further subterranean cisterns and four additional open water reservoirs, as well as a comprehensive discussion of the results and their meaning for the history of the Negev Highlands.
In this dissertation, the research papers are presented after a short presentation of the Negev Highlands as the study area and ancient cisterns and reservoirs as study objects, a brief introduction of the used methods and a synopsis of the results and conclusions that were obtained in this research project.

2
Study Area

2.1 Geology and Geomorphology

All the sites that were excavated and studied are situated in the Negev Highlands in the south of central Israel (Figure 2.1). The altitudes of this area range between 600 m above sea level (a.s.l.) in the north-eastern part to 1000 m a.s.l. in the southwest (Cohen, 1999). The Negev Highlands were formed due to the uplift of the area and faulting processes of the Dead Sea Rift from the Late Miocene to the Early Pleistocene (Itzhaki, 1982; Avni et al., 2006) resulting in a series of northeast-to-southwest oriented synclines and anticlines. After the lifting and faulting of the area, today's topography was formed by erosional processes during the Plio-Pleistocene resulting in the omnipresence of wadis and valley (Avni et al., 2006; Avni and Weiler, 2013; Bruins, 1986). The bedrock in the Negev Highlands is composed of marine deposits and rocks like dolomite, chalk, chert, limestone, and marl formations (Avni et al., 2006; Starinsky et al., 2010). The studied water harvesting systems are cut into these formations in the centre of the valleys or in foot slope positions.

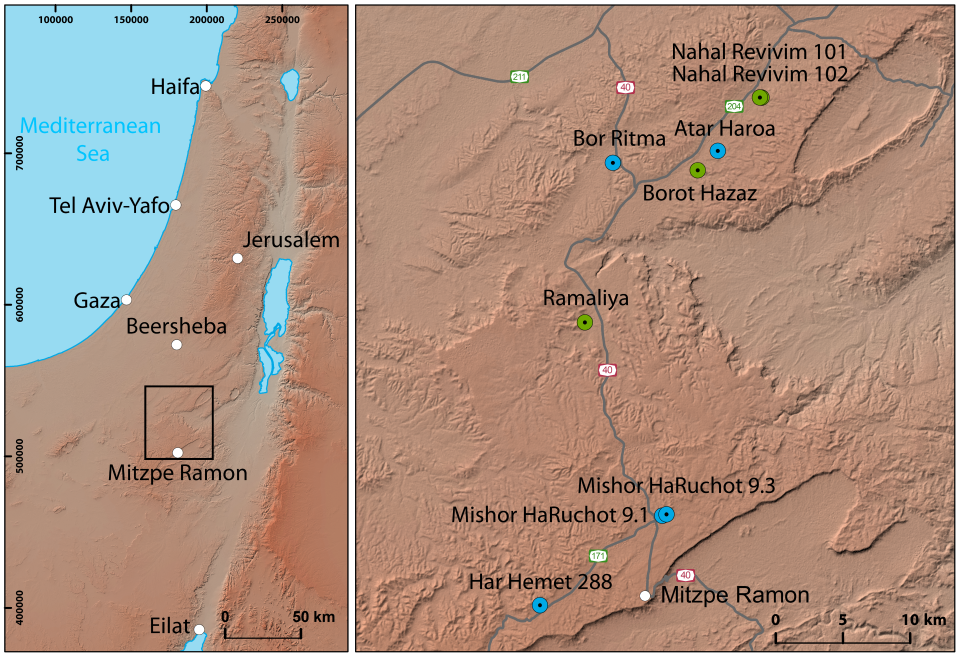


Figure 2.1: Left: map of the southern Levant marking the location of the investigated area in the Negev Highlands. Right: map of the investigated area showing the position of all studied subterranean cisterns and open water reservoirs. Reservoirs are marked as blue dots and rock-cut cisterns are marked as green dots.

2.2 Climate

2.2.1 Present-day Climate

The current climate in the Negev Highlands is characterized by arid environmental conditions represented by a sparse vegetation, especially during summer months (Figure 2.2 B & C). The mean annual air temperature ranges between 17 and 19 °C (with temperatures during summer up to 40 °C, and during winter down to 0 °C), with annual precipitation quantities between 80 and 150 mm (Kafle and Bruins, 2009). The majority of the rainfall occurs during late autumn, winter and early spring months (Figure 2.2 A & D) with strong variations from year to year (Avni et al., 2006; Goldreich, 2003; Bruins, 2012; Evenari et al., 1982; Shanan, 2000). The available precipitation is increased by fog and dew, which add an equivalent of 10 mm for each 100-m increase in elevation (Kidron, 1999).

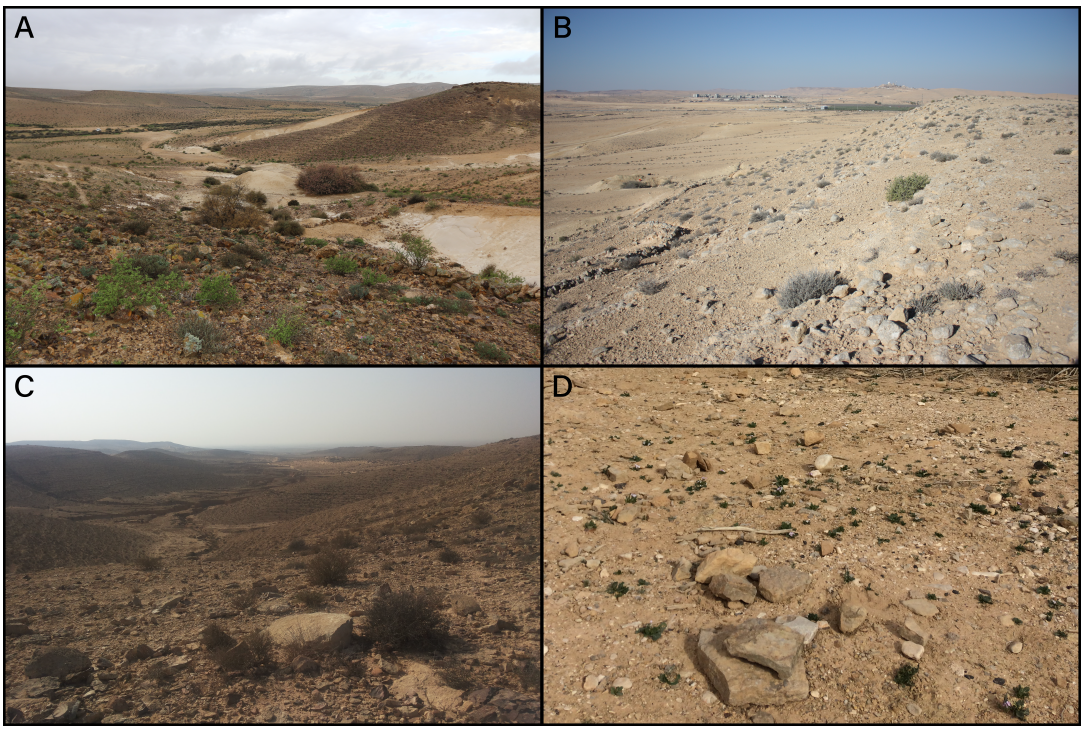


Figure 2.2: Exemplary vegetation during different seasons in the Negev Highlands. (A) View over Borot Hazaz cistern system in February 2018: fresh vegetation due to reoccurring precipitation events. (B) Mishor HaRuchot north of Mitzpe Ramon in April 2017: vanishing of vegetation due to the beginning of the dry season. (C) Landscape near Sede Boker in October 2015: only drought-resistant vegetation survived the dry season. (D) A small wadi north-west of Mitzpe Ramon in December 2019: some fresh vegetation occurs due to the first precipitation of the rain season.

2.2.2 Paleoenvironmental Conditions

The dry environmental conditions of the Negev Highlands allowed only a sparse development of paleoenvironmental archives to be used for temperature and precipitation reconstructions in this area. Therefore, paleoenvironmental reconstructions based on archives in the surrounding areas

need to be applied to get an understanding of the past climate in the studied area. In spite of the spatial proximity of these areas to the Negev Highlands, the reconstructions need to be viewed with caution, because Israel is characterized by a strong north-to-south rainfall gradient, causing strongly different precipitation regimes within a few kilometres (Ziv et al., 2014). Additionally, published paleoenvironmental reconstructions covering the Levante show in parts inconsistent results and draw contrasting conclusions (e.g. Bar-Matthews et al., 2003; Bookman et al., 2004; Finné et al., 2011; Kagan et al., 2015; Langgut et al., 2014; Litt et al., 2012; Migowski et al., 2006; Neumann et al., 2010; Orland et al., 2009).
Even though the palaeoenvironmental reconstructions show oscillations in mean annual temperature and amount of precipitation in the study area during the last 6000 years, the necessity for installations to collect and store water to sustain life has always been present.

2.3 Archaeology

The Negev Highlands have a long history of human settlement dating back thousands of years. It is characterized by strong oscillations in the degree of human activity. Phases with large numbers of stone-built remains are understood as phases of high settlement activity, while phases with no or only few left-behind structures are interpreted as times of low human activity. In the studied region, geopolitical, historical, and economic factors are suggested as the main reasons for the oscillations, while climate change is discarded as a primary cause (Greener et al., 2018).
The main settlement waves over the last five millennia occurred during the Early and Intermediate Bronze Ages (ca. 3600–1950 B.C.E.), the Iron Age II (late 10^{th}–late 9^{th} centuries B.C.E.) and the Byzantine to Early Islamic periods (4^{th}–11^{th} centuries C.E.) (Finkelstein, 1995; Cohen, 1999; Cohen and Cohen-Amin, 2004; Ben-Yosef et al., 2016; Rosen, 2017; Avni, 2014).
In past research it was suggested, that human activity during the first phase was interrupted during the Early Bronze III, but today's understanding is there was an ongoing settlement that lasted from Early Bronze I until the Intermediate Bronze Age (ca. 3600–2200 B.C.E.; Cohen, 1999; Gidding, 2016; Ben-Yosef et al., 2016; Dunseth et al., 2017, 2018; Finkelstein et al., 2018). This period is characterized by remains of larger and smaller sites, tumuli fields, and animal pens (Haiman, 1992, 1996; Cohen, 1999). During this period, subsistence was based on animal husbandry and copper industry, while no evidence for agricultural activity could be found (Dunseth et al., 2018; Vardi and Rosen, 2020).
The settlement activity during the Iron Age II is represented by remains of settlements, isolated houses and animal pens, and enclosed forts (Cohen and Cohen-Amin, 2004; Boaretto et al., 2010; Shahack-Gross et al., 2014). Additionally, some studies discuss opportunistic farming (Haiman, 1994, 2012b) or the cultivation of agricultural terrasses (Haiman, 2012b; Avni et al., 2013; Bruins and van der Plicht, 2017; Bruins and Van Der Plicht, 2017) during the Iron Age II.
The onset of the third activity wave is connected to the establishment of widespread permanent sites during the Byzantine period (Tepper et al., 2018). Besides permanent settlements and even larger towns, the phase is also characterized by isolated farms and separate animal pens (Rubin, 1990; Avni, 2014). During the Byzantine through Early Islamic periods, subsistence activities ranged from horticulture and dry-farming to animal husbandry and pastoral activities, to industry and circum-Mediterranean trade (Avni et al., 2013; Kraemer, 1958; Mayerson, 1994; Shahack-Gross et al., 2014; Bar-Oz et al., 2019; Dunseth et al., 2019; Marom et al., 2019; Blevis et al., 2021; Butler et al., 2020; Fuks et al., 2020; Lantos et al., 2020; Langgut et al., 2021).

These activity phases are interrupted by phases that are characterized by only very few left-behind stone-built constructions. It is assumed, that the human activity in the region did not completely cease during these phases, but it shifted from sedentary settlements to rather transitory (likely pastoral-nomadic) communities (e.g. Rosen et al., 2005; Saidel and Erickson-Gini, 2014; Bruins et al., 2018).

These periods of decreased settlement activity in the study area are the second half of the Intermediate Bronze Age, continuing during the Middle and Late Bronze Ages until the beginning of the Iron Age (ca. 2200–950 B.C.E.), a phase covering the Iron Age IIB–C, the Persian period, and most of the Hellenistic period (ca. 800–200 B.C.E.), and finally, the medieval period until the Ottoman period (starting ca. 11^{th} C.E.).

3
Objects of Study

The numerous installations to collect and store surface runoff in the Negev Highlands can be distinguished into two main types: open water reservoirs (Figure 3.1 A & B) and rock-cut subterranean cisterns (Figure 3.1 C) (Evenari et al., 1958; Haiman, 1994, 1995; Cohen, 1999; Cohen and Cohen-Amin, 2004).

Both types are dug into the ground – open reservoirs at the surface and rock-cut cisterns underneath the surface – to store surface runoff from nearby slopes that is generated during high precipitation events. When the installations were constructed, the removed material was deposited on spoil piles (Figure 3.2 A & B) near the reservoirs or cisterns. To enlarge the catchment area of the installations and increase the efficiency of water collection, small channels were built along the adjacent slopes above the structures to lead the water into the cisterns and reservoirs. Usually, the channels were made of sediments and stacked field stones (Figure 3.2 C), but in some case, natural bed rock surfaces were used as channels (Figure 3.2 D) or they were cut into the bed rock. With the surface runoff, sediments from the catchment area are washed into installations. In the past, the accumulated sediments were removed and added on top of the spoil pile in order to maintain the cisterns and reservoirs. At some sites, sedimentation pools (Figure 3.2 E & F) between the channels and the installations can be found. These were installed to reduce the water's flow velocity to allow the coarser sediments to be deposited before the water reaches the cisterns or reservoirs. While the operating principles and functionality of open water reservoirs and subterranean cisterns are relatively similar, there are differences in their sizes, efficiency, assumed chronology, and minor variances in their construction.

The open water reservoirs are the more primitive installations and therefore believed to be the initial form of rainwater harvesting in the area (Evenari et al., 1958). The reservoirs are usually dug into the Ora or Tamar formation, consisting of relatively impermeable marl that serves as an aquiclude for the stored water. The round man-made basins are up to twelve meters wide, four to five meters deep and the walls are often lined with local stones to stabilize them (Evenari et al., 1958; Rubin, 1988). Due to the permeable nature of the marl material open water reservoirs are built into, and the lack of a covering roof, the water loss due to infiltration and evaporation is relatively high. Based on frequent proximity of reservoirs to Iron Age settlements and sherds

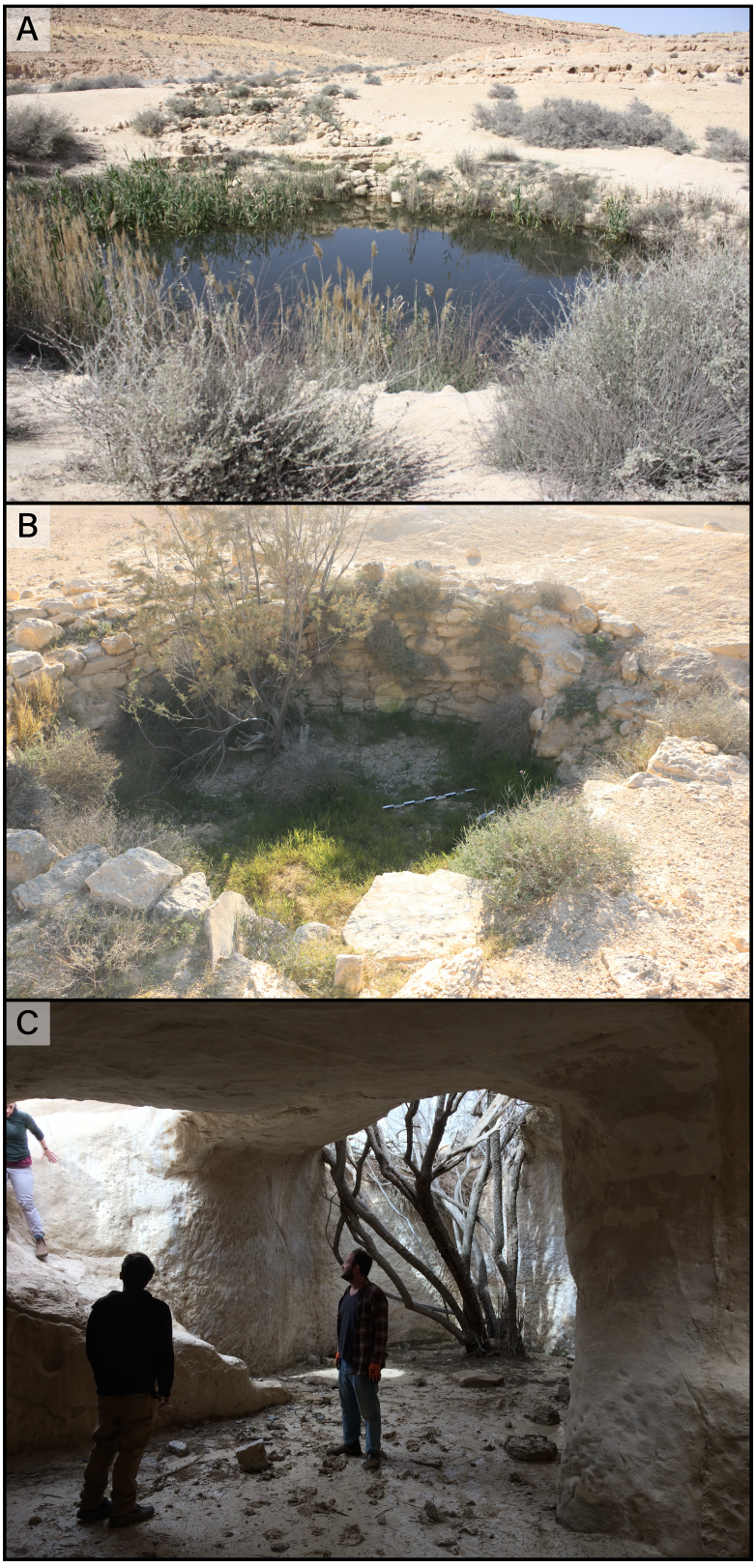


Figure 3.1: (A) The preserved and still maintained open water reservoir Bor Hemet and (B) the reservoir Mishor HaRuchot, that was filled with sediments after abandonment. (C) Cistern III of the Borot Hazaz cistern system that was maintained in modern times.

from this period scattered on the surface around the reservoirs, it was assumed that there is a chronological connection between these Iron Age sites and the reservoirs (e.g. Evenari et al., 1958; Haiman, 1994, 2012a; Cohen and Cohen-Amin, 2004). A more recent study associated them with the Early and Intermediate Bronze Ages, based on spatial correlations as well (Ore et al., 2020).
The subterranean cisterns are assumed to be the advancement of the open reservoirs, because they exhibit a higher level of efficiency and their construction is technically more challenging. The cisterns are cut into the soft chalk material of the Horsha or Menuha formation and have usually a rectangular or sometimes polygonal floor area. The sizes of the subterranean cisterns differ greatly resulting in water holding capacities of less than 100 up to over 1000 cubic metres (Junge et al., 2023). The larger cisterns are equipped with a rock-cut pillar to support the roof and in some cases the walls and floor of the cisterns were covered with plaster (cement). Due to the applied plaster technology and sporadic inscription within the cisterns, they have been placed traditionally in the Nabatean to Byzantine periods (Rubin, 1988). The cement lining on the inside of the cisterns and the soft chalk they were cut into made them more effective in holding the collected water than the open reservoirs, because the walls are less permeable. Additionally, the roof protects the water from contamination and high evaporation rates during the hot summers, resulting in a more effective water storage in the subterranean cisterns in comparison to the open water reservoirs.
For both types of water storing systems in the Negev Highlands, the dating in the past was based only on circumstantial (vicinity to other sites) or archaeological (inscriptions and sherds) evidence, but not on chronometric dating. More recently, Lucke et al. (2019) published the ages of a clean out spoil pile of a structure described as an open cistern using OSL dating. The determined ages are 1060-940 C.E. and 730-590 C.E., while the associated pottery finds were placed in the Byzantine-Islamic periods. The authors concluded a cleaning of the structure over the last 1300 years until recently, based on the shallow accumulation within the water harvesting installation (Lucke et al., 2019).
Tepper et al. (2020) determined the age of a subterranean cistern that belongs to an agricultural system in the vicinity of the ancient village Shivta. The associated spoil pile consists only of maintenance material that was dated to the 16^{th} century C.E. representing the utilization of the cistern. Since no construction material could be identified, the construction time of the installation could not be determined by chronometric dating. The shallow accumulation within the cistern yielded an age of 60 $\pm$ 10 years, suggesting a cleaning in modern times.
This sparse chronometric data of the possible construction times of ancient water reservoirs and subterranean cisterns does not allow to assess the full life cycle of the installations or if the different types of structures were introduced in a specific order.

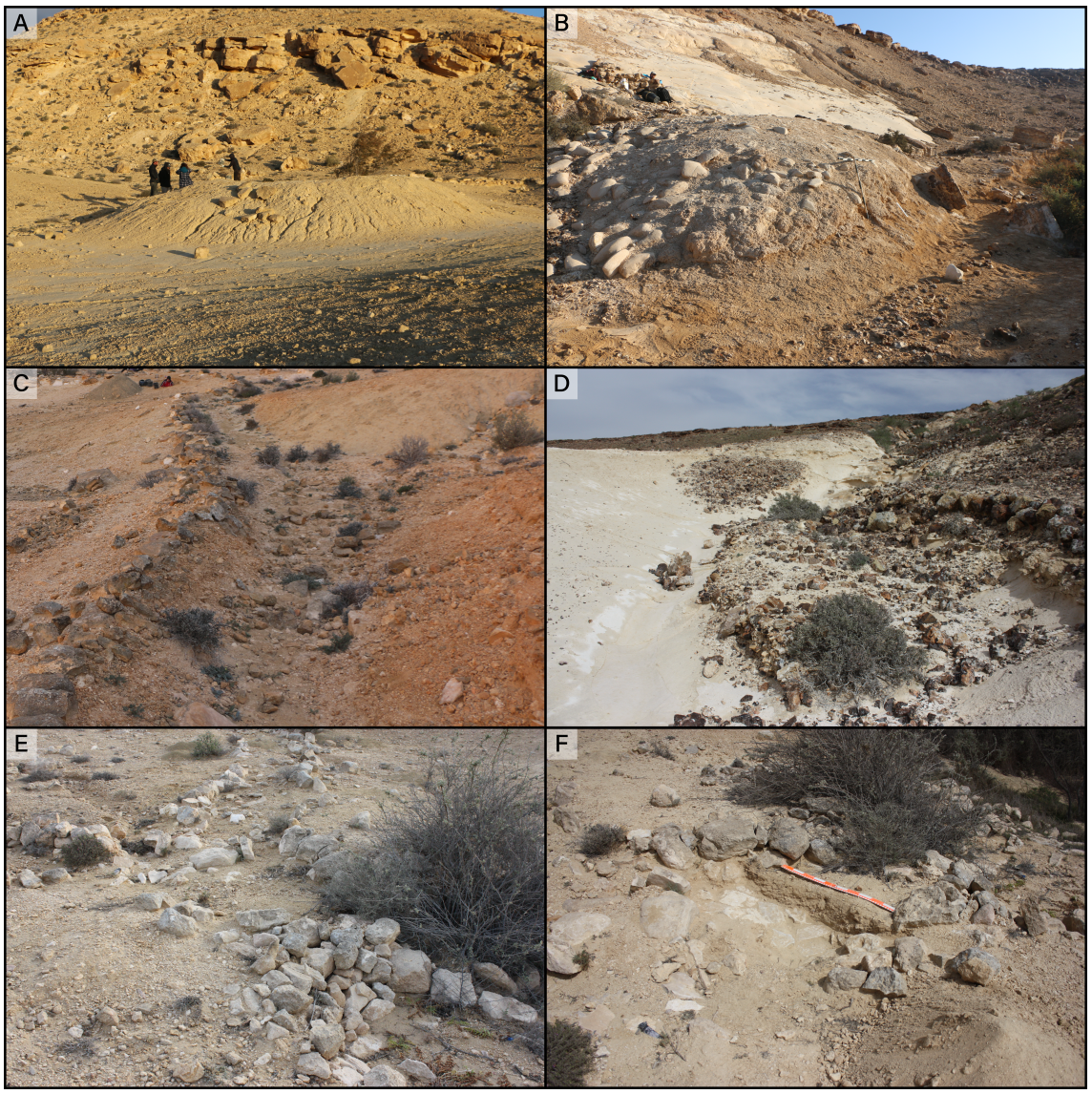


Figure 3.2: (A) The spoil pile of the Mishor HaRuchot 9.3 reservoir and (B) the spoil pile of the cistern Nahal Revivim 101, which was eroded on the front by water flooding the wadi. (C) The remains of a channel leading to the Mishor HaRuchot 9.3 reservoirs built of sediments and stacked field stones and (D) the natural bed rock surface used as a channel at the Borot Hazaz cistern system (left half of the photography). (E) A filled sedimentation pool at the reservoir Mishor HaRuchot 9.1 and (F) the same sedimentation pool partially excavated exposing the flooring stones.

4
Methods

4.1 Optically Stimulated Luminescence

4.1.1 Basic Principles

Luminescence dating is a chronometric dating method that is based on the storage of energy from ionizing radiation within certain minerals such as quartz and feldspar, which act like natural dosimeters (e.g. Wagner, 1998; Walker, 2005). The ionizing radiation originates either from cosmic radiation or from the decay of radioactive elements that are omnipresent in natural sediments (e.g. Prescott and Hutton, 1994; Wagner, 1998). For the latter, the radiation primarily results from the decay of radionuclides that occur naturally as part of the decay chains of uranium (^{238}U and ^{235}U), thorium (^{232}Th), as well as the decay of potassium (^{40}K) with a small contribution of rubidium (^{87}Rb) (Aitken, 1985). The energy is stored within the minerals due to the redistribution of electrons in defects within the mineral's crystal lattice from lower to higher energy levels (Aitken, 1998). This process causes an accumulation of energy within the natural dosimeters, but it can only take place while the minerals are not exposed to light as it is the case when they are buried by overlying sediments. The trapped electrons within the crystal lattice of the minerals are (partially) released back to lower energy levels when the material is stimulated by exposure to light. This release, regardless of whether it is happening in nature or conducted in the laboratory, is referred to as bleaching (Aitken, 1998). In nature, the reset of the luminescence clock usually happens during the erosion, transport, and deposition of material. With the stimulation induced movement of electrons from higher to lower energy levels, energy is released in form of light which is the luminescence signal. This can be measured in the laboratory and is referred to as the palaeodose or equivalent dose (D_e) given in the unit Gray (Gy) (Duller, 2008).
To calculate the age (equation 4.1) as the time passed since the last reset of the luminescence clock in kiloyears (ka), not only the accumulated luminescence signal (D_e) needs to be determined, but also the rate of accumulation as the environmental dose rate ($\dot{D}$) given in Gray per kiloyear (Aitken, 1998; Duller, 2008).

$$\text{Age [ka]} = \frac{\text{Equivalent dose } (D_e) \text{ [Gy]}}{\text{Environmental doserate } (\dot{D}) \text{ [Gy/ka]}} \tag{4.1}$$

By the use of OSL dating, the time of the last deposition and overlay of sediments containing quartz or feldspar within the time frame of ca. 50 up to 1 million years can be determined (Ballarini et al., 2003; Madsen et al., 2005; Bøtter-Jensen et al., 2004). A description of the preparation process and measurement setup for the OSL dating is given in Junge et al. (2018, 2021).

4.1.2 Application of OSL to Cisterns and Reservoirs

Concerning subterranean cisterns and open water reservoirs, the construction, maintenance and even their cessation of use is strongly connected to the transport, deposition, and overburden of sediments. This makes the processes connected to the life cycle of these structures available for age determination using OSL dating.

Before a cistern or reservoir is constructed in the foot slope area (Figure 3.2 A &B), the landscape developed, and the time of their natural deposition can be deterimend by OSL dating. This allows the dating of the pre-construction time of the installation which can help to constrain the construction period of this feature. With the construction of the cistern or reservoir (Figure 3.2 C), sediments or crumbled bedrock are removed and deposited on a spoil pile close to the installation. During this process, the material is exposed to sunlight and can undergo bleaching. The bleaching can be supported by post-depositional mixing of the spoil pile material due to humans walking over the spoil during the construction. Additionally, aeolian sediments may be incorporated into the spoil during the time-consuming construction process. The construction material and aeolian sediments of the spoil pile can be used to determine the time of the construction of the cistern or reservoir. During the use of the installations, precipitation erodes sediments from the adjacent slope's surfaces and transports them into the cisterns and reservoirs (Figure 3.2 D & E). The material is bleached during the transportation process – if it takes place during daytime – and gets overburden within the installations until maintenance is conducted. When subterranean cisterns or open water reservoirs are maintained, the sediment refill is removed and deposited on top of the spoil pile (Figure 3.2 F & G). The bleaching during this process allows the determination of the time of active maintenance of the installations and therefore the time of their use. After the last maintenance activity, the sediments within the reservoirs and cisterns are not removed anymore and they get filled in completely (Figure 3.2 H, I & J). Since the material accumulated within the installations is bleached during erosion, transport and deposition, the time of cessation of maintenance can be determined by OSL dating as well.

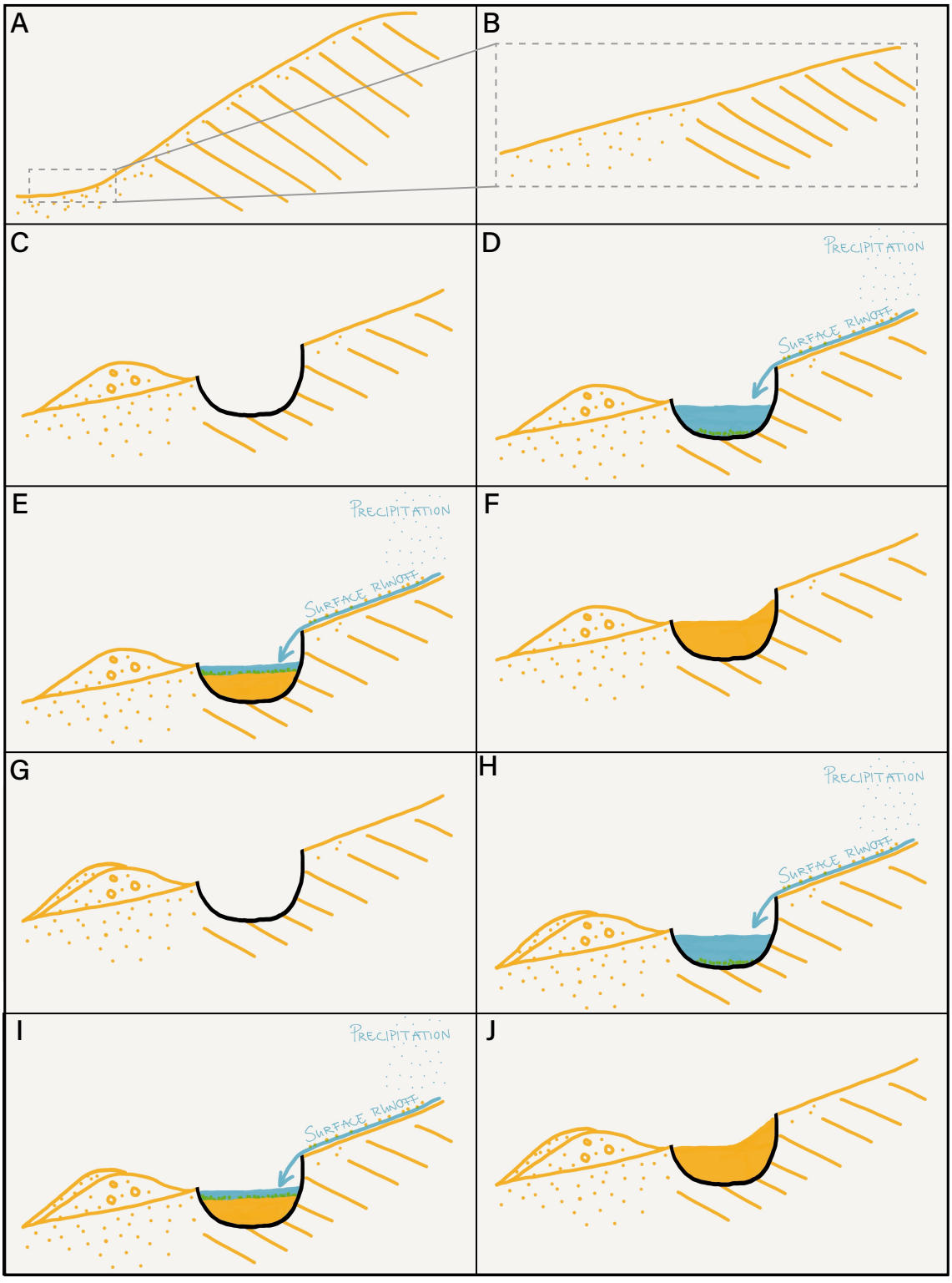


Figure 4.1: Schematic drawings of the life cycle of an open reservoir. The reservoirs are often constructed in the foot slope area (A & B). When the reservoir is constructed, the material is deposited on an adjacent spoil pile (C). While the reservoir is in use, sediments are washed into the installations with the water from the slopes (D & E). To keep the structure in use, the refill sediments are removed and deposited on the spoil pile as well (F & G). When the reservoir is no longer maintained, it refills completely (H, I & J).

4.2 Micromorphology

Micromorphology is a technique used in different fields like soil sciences, geomorphology and archaeology, that focusses on studying the small-scale features of soil, sediment, and rock samples. It involves the examination of thin sections of these materials at a microscopic level to gain insights into their small-scale features to reveal details about their structure, formation, and post-depositional processes (Elias and Alderton, 2020; Stoops, 2003).
In archaeology and related sciences, micromorphology is used to study the formation and history of archaeological sites. It can reveal the processes of human activities such as the construction and use of buildings, the deposition of waste materials and occupation horizons, and agricultural activities. Micromorphology can also provide insights into the natural post-depositional processes that have affected archaeological sites, such as erosion, post-depositional mixing and weathering (Banerjea et al., 2015).
In geomorphology, micromorphology is used to study the processes that shaped the Earth's surface. It can reveal details about how sediments are transported, deposited and eroded, and how landscapes and soils have evolved over time (Stoops, 2018).
In general, micromorphology is a valuable method for understanding complex processes that shape both natural and human-made environments. It can be used in combination with other analytical techniques such as geochemical analysis, physical analyses of sediments, and chronometric dating methods to provide a comprehensive picture of the history and development of landscapes and archaeological sites (e.g. Karkanas and Goldberg, 2017; Kühn et al., 2013; Mentzer and Quade, 2013)).

4.3 Synergy of the Methods

To date the different phases of the life cycle of cisterns and reservoirs, OSL samples were collected throughout the profiles within the installations and through the spoil piles. The sampling of the spoil piles was focussed on the transitions between palaeosurface and lowermost construction material in the spoil pile, the transition between construction and the first maintenance material, and the last maintenance material on top of the spoil pile. Within the installations, the most significant sample was collected from the lowermost sediment accumulation. Further samples where collected if the transitions were not clearly identified or larger sediment bodies were not covered by samples. This sampling approach provides the best estimation for the time periods covered by pre-construction, construction, maintenance, and abandonment of each studied site.
The foundation of this strategy is the correct specification of the respective contexts associated with the different life cycle phases of the reservoir or cistern. However, the identification and distinction of the deposits from different phases is not always visible to the unaided eye. To address this issue, OSL dating and micromorphological analyses were combined, to support the interpretation of the determined ages with sedimentological evidence. By analysing the structure of the sediments on a micro-scale, it is possible to distinguish between natural deposits and sediment movement by humans, and can it be used to identify the transition between the palaeosurface and the construction material of the spoil pile. Further, micromorphological analyses allow the identification of the contact zone between construction and maintenance deposits, and the characterisation of construction material as relocated foot slope material and maintenance material as relocated fluvial accumulation. Additionally, post-depositional processes, such as micro- or macro-animal activity,

can be identified using micromorphological analyses to interpret age under- or overestimations in the OSL results correctly. Further to this, the post-depositional incorporation of quarts grains can be detected to gain a better understanding of the sedimentation process, that is actually dated. By the fusion of the OSL and micromorphology results, the drawn interpretations are more reliable and show a higher concideration of the sedimentological evidence.

5

Synopsis of the Results & Discussion

5.1 General Results

In this project, it was possible to study the life cycles of five open water reservoirs and five subterranean cisterns in the Negev Highlands (Fig. 7), giving the first understanding of the chronology of these installations. A detailed description of findings obtained for the open water reservoir near Atar Haroa are presented in Junge et al. (2018) and the subterranean cisterns I and IV of the cistern system Borot Hazaz are published in Junge et al. (2021). The remaining sites were published en bloc in Junge et al. (2023).

At some sites, the age determinations of the entire life cycle (pre-construction, construction, maintenance, and abandonment) were in parts hampered due to the absence of the associated spoil pile, recent maintenance activities inside the installations or preservational reasons. For example, at the Ramaliya cistern, no spoil pile was preserved, and consequently neither the pre-construction time by dating the palaeosurface below the spoil pile nor the construction or maintenance time by establishing the ages of the spoil pile could be determined. At other sites, the cessation of maintenance was not determined by dating the accumulation within the cisterns and reservoirs, as there were indications that there has been recent use and maintenance, therefore the excavation and sampling of the material seemed unpromising (e.g. Bor Ritma reservoir) or the vegetation on top of the sediment refill was too lush and should not have been removed or destroyed for nature conservation reasons (Borot Hazaz cistern IV). At the Mishor HaRuchot reservoir, the sediment refill within the structure was excavated, but it was recently maintained and refilled which was indicated by modern trash within the sediment accumulation. For that reason, no OSL sampling was conducted for the sediment accumulation within this reservoir. In the case of the spoil pile of Borot Hazaz's cistern I, the spoil pile was deposited on bed rock, therefore no palaeosurface could be sampled and no pre-construction time could be determined.

Aside from life cycle phases that were not dated, in some cases the resulting ages did not follow the expected order of pre-construction, construction, maintenance and abandonment. This is often caused by methodological problems concerning the OSL dating. These are addressed in chapter 5.2 Assessment of the Methodological Approach.

Despite these difficulties and limitations, it was found that the age determination of the studied cisterns and reservoirs could be successfully carried out by the use of OSL dating supported by micromorphological analyses of the studied sediments. The overall dating results (Figure 5.1) cover a wide range of time with a pre-construction age in the Early Holocene for one of the installations up to dating results in the last century, with several ages indicating the ongoing refill of the cisterns and reservoirs. The human activity concerning the studied sites is represented by sediment depositions during construction and maintenance of the structures. Concerning the sites studied in this project, these cover a time frame from the late Early Bronze Age III (or latest the Intermediate Bronze Age) to modern times, starting with the construction of the first open water reservoirs (Mishor HaRuchot 9.1). In general, the different studied open water reservoirs were constructed over a long period covering the Early Bronze Age III to Middle Bronze Age, the Iron Age to Persian period and even during Early Islamic period to Medieval times (Figure 5.1, upper part). The active utilization represented by maintenance of the respective reservoirs, often persisted over several centuries or even millennia, followed by the cessation of maintenance or abandonment, that cannot be connected to a specific period for the studied reservoirs.

The construction of the studied subterranean cisterns clusters around the Late Roman to Early Medieval periods with only short utilization phases, probably caused by the late construction of these installations (Figure 5.1, lower part).

For the sites researched in this study, it is clear that the simpler open reservoirs were implemented earlier than the subterranean cistern. Hence, in parts, the assumption about the chronological order from simpler reservoirs to more advanced subterranean cisterns is supported by the current project. Additionally, it needs to be outlined, that even after the introduction of subterranean cistern as a more efficient runoff harvesting and storage structure, already existing open water reservoirs were not only kept in use, but even new reservoirs were constructed (e.g. Haroa Reservoir & Bor Ritma Reservoir). However, it should be noted that only a limited number of sites were excavated and therefore it cannot be ruled out that the chronology of the different types is biased or does not show the full picture. Additionally, the gaps in time where none of the studied installations were constructed, are no evidence for a general inactivity during these phases, but could likely be caused by the limited number of reservoirs and cisterns studied.

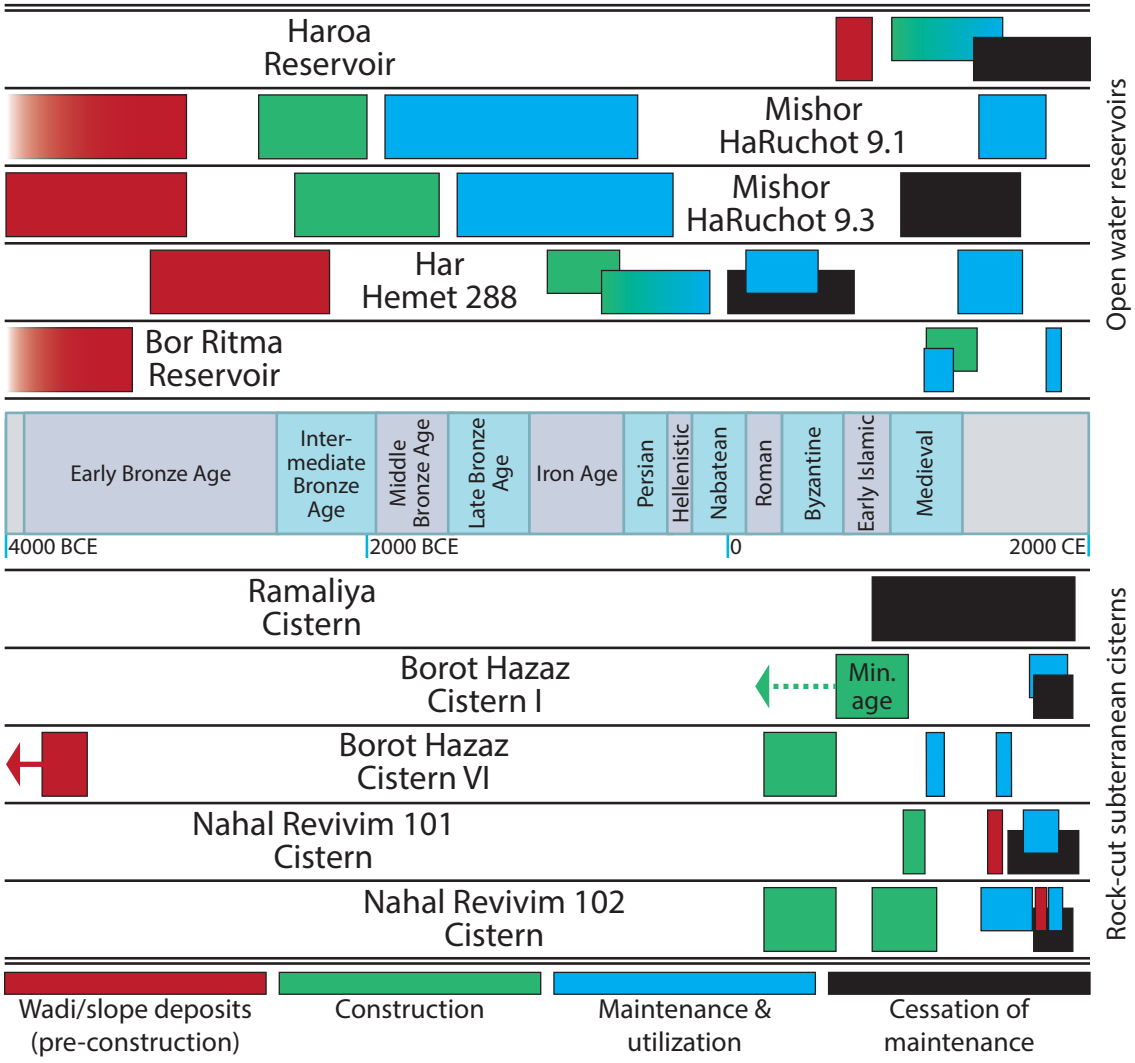


Figure 5.1: Summary of all OSL dating results from all studied open water reservoirs (top) and rock-cut subterranean cisterns (bottom). The ages are assigned to the different events assocciated to the deposition of the sampled sediments: pre-construction wadi or slope deposits (red), sediments removed and deposited during construction (green), refill sediments removed from the installations and deposited during maintenance and utilization (blue), and sediment refill within the installations representing the cessation of maintenance (black). Detailed data from the Haroa reservoir can be found in Junge et al. (2018), for the Borot Hazaz cisterns in Junge et al. (2021) and for the Mishor HaRochot 9.1 & 9.3 reservoirs, the Bor Ritma reservoir, the Ramaliya cistern, and the Nahal Revivim 101 & 102 cisterns in Junge et al. (2023).

5.2 Assessment of the Methodological Approach

The OSL dating studies conducted at other archaeological sites in the Negev Highlands have already demonstrated the high suitability of coarse-grained quartz for OSL dating (e.g. Porat et al., 2006; Junge et al., 2016; Dunseth et al., 2017)). The luminescence characteristics of the dated material in this region provide an excellent basis for the age determination of sediments associated with the life cycles of cisterns and reservoirs. Despite the promising characteristics of the coarse-grain quartz material, methodological problems concerning incomplete bleaching and post-depositional mixing appear, that can cause age over- and underestimations.

Insufficient or incomplete bleaching can be connected to the fast transport of large amounts of material which results in an inadequate exposure of single quartz grains to sunlight. The occurrence of incomplete bleaching is not limited to any particular mode of transportation and deposition at the studied sites, as it is found in all sections, including fluvial sediment accumulations within cisterns and reservoirs, channels and sedimentation pools, as well as sediments accumulated in spoil piles transported and deposited by humans.

In the case of the spoil piles, incomplete bleaching may occur due to insufficient exposure to sunlight resulting from the rapid movement of sediments in large quantities over short distances by humans. Depending on the used tools and the degree of humidity of the moved sediments, the material might be moved in lumps, shielding a majority of the grains from any sunlight exposure during transport. Fluvial transported sediments accumulated in the channels, pools, cisterns and reservoirs may also show evidence of incomplete bleaching, despite being transported as individual grains, due to the short transport distances resulting from the small catchment size and the high transport capacity generated by high-energy rainfall events. Additionally, the dominant carbonate lithology of the Negev Highlands often results in aggregates or carbonate coatings of the grains, reducing the likelihood of bleaching individual grains. In many but not all cases (e.g. sediment fill of the reservoir Har Hemet 288), the application of the bootstrap minimum age model (MAM, Cunningham and Wallinga, 2012) allows the correction of the age overestimation by emphasizing the well-bleached sub-samples in the D_e calculation.

Post-depositional mixing by animal burrowing may result in age over- or underestimation due to the incorporation of grains from under- or overlying strata into the sampled layer. In this study, these processes were detected using micromorphological analyses and could therefore be taken into account in the interpretation of the OSL results.

Incomplete bleaching, as well as post-depositional mixing is often indicated in the D_e distribution of a sample by outliers with higher or lower doses, causing wide distributions of the D_e values and consequently high values for the relative standard deviation (RSD). This effect is amplified for younger samples, because the RSD tends to increase with decreasing D_e values, because the unbleached residual doses are relatively high compared to the dose accumulated since the last bleaching event. Hence, even the smallest residual doses due to incomplete bleaching or the incorporation of grains from other layers can cause wide distributions for low D_e values, as they frequently occured in this project.

Beside the effects of incomplete bleaching and post-depositional mixing on the D_e distribution, a heterogeneous microdosimetry can also cause an increase in the RSD, especially when very low contents of U, Th, and K occur, as is the case for the studied sediments (Mayya et al., 2006). Therefore, the width of the distribution of D_e values should not consequently be interpreted as poor bleaching during transport and deposition, but can be caused by radioactive hot spots in the

samples sediments.
For a few of the ages, inversions like the younger ages of the pre-construction material in comparison to the construction material of the cisterns Nahal Revivim 101 & 102 (Figure 5.1, lower part) no explanation could be found. This indicates in general, that too much emphasis should not be placed on individual dating results, but the results should rather be viewed as a whole.

5.3 Implications of Dating Results on Archaeological Interpretations

The given OSL dating results indicate the introduction of open water reservoirs in the Negev Highlands during the 4^{th} to 3^{rd} millennium B.C.E., suggesting the development of these installations by pastoral groups. Due to the construction of the studied water reservoir over several millennia, the chronological connection of reservoirs to other ancient sites in their spatial proximity (e.g. Ore et al. (2020)) is partially supported by the dating results. However, the reservoirs that have no corresponding sites from their construction period in their vicinity challenges the conventional assumption that the dating of open water reservoirs in the Negev Highlands can be based solely on their proximity to archaeological remains. Additionally, the presented ages suggest that certain open reservoirs were built and maintained during the "empty periods" of settlement in the Negev Highlands, indicating human activity in the area during these eras even when there are no visible remains of stone constructions from an archaeological standpoint. The activity during these periods was likely focused on nomadic pastoralism, indicating a continuous human presence in the region for the past five thousand years (Finkelstein, 1995).
The introduction of the subterranean cisterns during the Late Roman to Early Medieval period did not replace the open water reservoirs but added more sophisticated system to collect and store surface runoff. The introduction and construction of cisterns during the Nabatean period, as it has been implied by a few inscriptions, was not supported by the OSL dating conducted in this study. Due to the relatively abrupt occurrence of subterranean cisterns, their advanced technology, and their short period of construction during specific socio-political circumstances (development of trade routes during the Late Roman period, 2^{nd}–3^{rd} centuries C.E.), it is suggested that the technology diffused into the Negev Highlands.
The construction and maintenance of open reservoirs, being dug into impermeable chalk or marl, did not require extensive manpower and could be accomplished with relative ease, even by smaller groups. It is possible that open reservoirs could have been created in a relatively short amount of time by the use of simpler tools, whereas subterranean cisterns were a more complex endeavor, requiring a significant investment of labor and expertise. The Byzantine-Early Islamic towns and villages in the Negev region showcased sophisticated stone architecture, urban planning, and infrastructure, suggesting the involvement of central authorities who could mobilize larger groups of workers. Accordingly, it can be inferred that the differences in technology between reservoirs and cisterns are based on different social structures.

6
Conclusions & Outlook

This research project presents a comprehensive examination of the history of installations to collect and store surface runoff in the Negev Highlands. While focusing on a limited selection of five subterranean cisterns and five open water reservoirs, this project represents the most extensive attempt to date to evaluate the traditional age determinations of these structures and to establish their chronology and life cycles.

The use of OSL dating as the primary method allows for dating the actual time periods of sediment repositioning associated with the construction, utilization represented by maintenance, and cessation of maintenance of the cisterns and water reservoirs. The interpretation of OSL results is supported by the use of micromorphological analyses. These analyses make it possible to identify the deposition mode of the respective sediments more clearly, helping to make statements about post-depositional mixing and the subsequent introduction of grains to a sediment layer, and support the identification of causes for age inversions occuring at some of the sites.

The combination of methods allows to answer the central research questions of this project regarding the time of introduction of cisterns and reservoirs into the Negev Highlands and the order of their introduction. It could be shown that reservoir construction – contrary to conventional wisdom – was not restricted to the Iron Age, but started at least as early as the Early Bronze Age or Intermediate Bronze Age and continued until Medieval times. Furthermore, the results indicate that the reservoirs were not only constructed and utilized during periods of active settlement, but were also used and maintained during times characterized by the absence of archaeological remains. The construction time of subterranean cisterns which was originally believed to be confined to the Nabatean and Byzantine periods, can be placed in the Late Roman until early Medieval times based on the OSL dating results.

The results demonstrate that subterranean cisterns were indeed introduced after the open water reservoirs. However, cisterns did not replace the water reservoirs. It is shown that even after the introduction of cisterns, reservoirs continued to be used and new ones were even constructed.

The differences in size, technological complexity, material that needed to be cut through and time of introduction between the open reservoirs and subterranean cisterns allows a differentiation of the contexts they were constructed in. The smaller, less complex reservoirs, often hewn into foot

slope deposits or marl, could have been constructed by a few people in relatively short periods of time, pointing towards pastoral groups constructing them. The subterranean cisterns on the other hand were cut into solid rock layers and have capacities of up to 1000 cubic meters. Consequently, their construction is dependent on a larger group of people, specific skills and technologies, and an extended period of time. This suggests that their construction was planned and executed under the control of central authorities, as was found in the region, for example, in the Byzantine Empire and the Early Islamic period.

Besides evaluating the conventional age determination of the construction of the installations, OSL dating also enables the determination of the time of active use represented by maintenance activities and the cessation of maintenance. This reveals the information that the open reservoirs were periodically maintained, sometimes over centuries and even after the introduction of subterranean cisterns, while the cisterns have only short maintenance phases, which can be related to their later introduction. The determination of the time of cessation of maintenance of both types of installations is often hampered by disturbance of the accumulation within the structures, but it can be shown, that they were often used until Medieval times and later.

In general, it can be demonstrated that the use of OSL dating allows for the successful evaluation and even correction of archaeological age estimation. Unlike archaeological dating or dating based on circumstances, it was shown, that OSL dating can also determine the periods of maintenance, as well as the time of cessation of use.

Future research in the field of ancient open reservoirs and subterranean cisterns should involve the excavation and age determination of additional sites and their associated sediments, in order to facilitate a decision on whether the determined construction phases are universally applicable for the installations in the Negev Highlands and whether reservoirs were built throughout the entire period since their introduction, or whether there were indeed times when no construction took place. Considering the potential for dating the deposits within the installations and the water-logging characteristics of these sediment accumulations, which could potentially enable the preservation of environmental proxies, the use of the installations and their sediment infillings as an environmental archive should be examined. This is to bridge the gap in paleoenvironmental reconstruction in the Negev Highlands region.

Bibliography

Aitken, M. J. (1985): Thermoluminescence Dating, Academic Press, London, England.

Aitken, M. J. (1998): Introduction to optical dating: the dating of Quaternary sediments by the use of photon-stimulated luminescence, Oxford University Press, Oxford, England.

Avni, G. (2014): The Byzantine-Islamic transition in Palestine: an archaeological approach, Oxford University Press, Oxford, England.

Avni, G.; Porat, N.; Avni, Y. (2013): Byzantine–Early Islamic agricultural systems in the Negev Highlands: Stages of development as interpreted through OSL dating, Journal of Field Archaeology, 38, 4, 332–346.

Avni, Y.; Porat, N.; Plakht, J.; Avni, G. (2006): Geomorphic changes leading to natural desertification versus anthropogenic land conservation in an arid environment, the Negev Highlands, Israel, Geomorphology, 82, 3-4, 177–200.

Avni, Y.; Weiler, N. (2013): The Geological map of Israel 1:50,000: Sede Boqer sheet (18-IV), Ministry of Energy and Water Resources, Earth and Marine Research Administration, Geological Survey, Jerusalem, Israel.

Ballarini, M.; Wallinga, J.; Murray, A.; Van Heteren, S.; Oost, A.; Bos, A.; Van Eijk, C. (2003): Optical dating of young coastal dunes on a decadal time scale, Quaternary Science Reviews, 22, 10-13, 1011–1017.

Banerjea, R. Y.; Bell, M.; Matthews, W.; Brown, A. (2015): Applications of micromorphology to understanding activity areas and site formation processes in experimental hut floors, Archaeological and Anthropological Sciences, 7, 89–112.

Bar-Matthews, M.; Ayalon, A.; Gilmour, M.; Matthews, A.; Hawkesworth, C. J. (2003): Sea–land oxygen isotopic relationships from planktonic foraminifera and speleothems in the Eastern Mediterranean region and their implication for paleorainfall during interglacial intervals, Geochimica et Cosmochimica Acta, 67, 17, 3181–3199.

Bar-Oz, G.; Weissbrod, L.; Erickson-Gini, T.; Tepper, Y.; Malkinson, D.; Benzaquen, M.; Langgut, D.; Dunseth, Z. C.; Butler, D. H.; Shahack-Gross, R.; et al. (2019): Ancient trash mounds unravel urban collapse a century before the end of Byzantine hegemony in the southern Levant, Proceedings of the National Academy of Sciences, 116, 17, 8239–8248.

Ben-Yosef, E.; Gidding, A.; Tauxe, L.; Davidovich, U.; Najjar, M.; Levy, T. E. (2016): Early Bronze Age copper production systems in the northern Arabah Valley: New insights from archaeomagnetic study of slag deposits in Jordan and Israel, Journal of Archaeological Science, 72, 71–84.

Blevis, R.; Bar-Oz, G.; Tepper, Y.; Zohar, I. (2021): Fish in the desert: Identifying fish trade routes and the role of Red Sea parrotfish (Scaridae) during the Byzantine and Early Islamic periods, Journal of Archaeological Science: Reports, 36, 102808.

Boaretto, E.; Finkelstein, I.; Shahack-Gross, R. (2010): Radiocarbon results from the Iron IIA site of Atar Haroa in the Negev Highlands and their archaeological and historical implications, Radiocarbon, 52, 1, 1–12.

Bookman, R.; Enzel, Y.; Agnon, A.; Stein, M. (2004): Late Holocene lake levels of the Dead Sea, Geological Society of America Bulletin, 116, 5-6, 555–571.

Bøtter-Jensen, L.; McKeever, S.; Wintle, A. (2004): Optically stimulated luminescence dosimetry, Elsevier, United Kingdom.

Bruins, H.; Segal, I.; van der Plicht, J. (2018): Bronze chisel at horvat haluqim (central negev highlands) in a sequence of radiocarbon dated late bronze to iron I layers, in Mining for ancient copper: Essays in memory of Beno Rothenberg, 16–27.

Bruins, H. J. (1986): Desert environment and agriculture in the central Negev and Kadesh-Barnea during historical times (Published PhD Dissertation), Stichting Midbar Foundation, Nijkerk, Netherlands, University of Wageningen, Wageningen, Netherlands.

Bruins, H. J. (2012): Ancient desert agriculture in the Negev and climate-zone boundary changes during average, wet and drought years, Journal of Arid Environments, 86, 28–42.

Bruins, H. J.; van der Plicht, J. (2017): Iron Age agriculture- a critical rejoinder to "Settlement Oscillations in the Negev Highlands Revisited: the Impact of Microarchaeological Methods", Radiocarbon, 59, 1, 1–16.

Bruins, H. J.; Van Der Plicht, J. (2017): Dating of Iron Age agriculture in the Negev Highlands: a response to Shahack-Gross and Finkelstein, Radiocarbon, 59, 4, 1233–1239.

Butler, D. H.; Dunseth, Z. C.; Tepper, Y.; Erickson-Gini, T.; Bar-Oz, G.; Shahack-Gross, R. (2020): Byzantine—Early Islamic resource management detected through micro-geoarchaeological investigations of trash mounds (Negev, Israel), PloS one, 15, 10, e0239227.

Cohen, R. (1999): Ancient settlement of the central Negev: The Chalcolithic Period, the Early Bronze Age and the Middle Bronze I (IAA Reports 6, Vol. I), Israel Antiquities Authority, Jerusalem, Israel.

Cohen, R.; Cohen-Amin, R. (2004): Ancient settlement of the Negev Highlands: The Iron Age and the Persian period (IAA REports 20, Vol. II), Israel Antiquities Authority, Jerusalem, Israel.

Cunningham, A. C.; Wallinga, J. (2012): Realizing the potential of fluvial archives using robust OSL chronologies, Quaternary Geochronology, 12, October, 98–106.

Duller, G. A. (2008): Luminescence Dating: guidelines on using luminescence dating in archaeology.

Dunseth, Z. C.; Finkelstein, I.; Shahack-Gross, R. (2018): Intermediate Bronze Age subsistence practices in the Negev Highlands, Israel: Macro-and microarchaeological results from the sites of Ein Ziq and Nahal Boqer 66, Journal of Archaeological Science: Reports, 19, 712–726.

Dunseth, Z. C.; Fuks, D.; Langgut, D.; Weiss, E.; Melamed, Y.; Butler, D. H.; Yan, X.; Boaretto, E.; Tepper, Y.; Bar-Oz, G.; et al. (2019): Archaeobotanical proxies and archaeological interpretation: A comparative study of phytoliths, pollen and seeds in dung pellets and refuse deposits at Early Islamic Shivta, Negev, Israel, Quaternary Science Reviews, 211, 166–185.

Dunseth, Z. C.; Junge, A.; Lomax, J.; Boaretto, E.; Finkelstein, I.; Fuchs, M.; Shahack-Gross, R. (2017): Dating archaeological sites in an arid environment: A multi-method case study in the Negev Highlands, Israel, Journal of Arid Environments, 144, 156–169.

Elias, S.; Alderton, D. (2020): Encyclopedia of Geology, Academic Press.

Evenari, M.; Aharoni, Y.; Shanan, L.; Tadmor, N. H. (1958): The Ancient Desert Agriculture of the Negev: III. Early Beginnings, Israel Exploration Journal, 8, 4, 231–268.

Evenari, M.; Shanan, L.; Tadmor, N. (1982): The Negev: The Challenge of a Desert, Harvard University Press, Cambridge, Massachusetts, 2nd edition edition.

Finkelstein, I. (1995): Living on the fringe: The archaeology and history of the Negev, Sinai and neighboring regions in the Bronze and Iron Ages, Sheffield Academic Press, Sheffield, England.

Finkelstein, I.; Adams, M. J.; Dunseth, Z. C.; Shahack-Gross, R. (2018): The archaeology and history of the Negev and neighbouring areas in the third millennium BCE: a new paradigm, Tel Aviv, 45, 1, 63–88.

Finné, M.; Holmgren, K.; Sundqvist, H. S.; Weiberg, E.; Lindblom, M. (2011): Climate in the eastern Mediterranean, and adjacent regions, during the past 6000 years — A review, Journal of Archaeological Science, 38, 12, 3153–3173.

Fuks, D.; Bar-Oz, G.; Tepper, Y.; Erickson-Gini, T.; Langgut, D.; Weissbrod, L.; Weiss, E. (2020): The rise and fall of viticulture in the Late Antique Negev Highlands reconstructed from archaeobotanical and ceramic data, Proceedings of the National Academy of Sciences, 117, 33, 19780–19791.

Gidding, A. D. (2016): Approaches to Production and Distribution in Anthropological Archaeology: Views from the Early Bronze Age of Jordan and Israel, University of California, San Diego.

Goldreich, Y. (2003): The Climate of Israel. Observations, Research and Applications, Kluwer Academics/Plenum Publisher, New York.

Greener, A.; Finkelstein, I.; Langgut, D. (2018): Settlement oscillations along the desert fringes of the southern Levant : impact of climate versus economic and historical factors, Ugarit-Forschungen, 49, 165–196.

Haiman, M. (1992): Cairn burials and cairn fields in the Negev, Bulletin of the American Schools of Oriental Research, 287, 1, 25–45.

Haiman, M. (1994): The Iron Age II sites of the western Negev highlands, Israel Exploration Journal, 36–61.

Haiman, M. (1995): Agriculture and Nomad-State Relations in the Negev Desert in the Byzantine and Early Islamic Periods, Bulletin of the American Schools of Oriental Research, 297, 29–53.

Haiman, M. (1996): Early Bronze Age IV settlement pattern of the Negev and Sinai deserts: view from small marginal temporary sites, Bulletin of the American Schools of Oriental Research, 303, 1, 1–32.

Haiman, M. (2012a): Dating the agricultural terraces in the southern Levantine deserts—The spatial-contextual argument, Journal of Arid Environments, 86, 43–49.

Haiman, M. (2012b): Geopolitical Aspects of the Negev Desert in the 11th–10th Centuries BCE, The Ancient Near East in the 12th–10th Centuries BCE: Culture and History, 199–206.

Itzhaki, Y. (1982): The geological history of the Negev, in Evenari, M.; Shanan, L.; Tadmor, N. (editors), The Negev: The Challenge of a Desert, Harvard University Press, Cambridge, Massachusetts, 2nd edition edition, 76–94.

Junge, A.; Dunseth, Z. C.; Shahack-Gross, R.; Finkelstein, I.; Fuchs, M. (2021): Construction and use of rock-cut cisterns: a chronological OSL approach in the arid Negev Highlands, Israel, Archaeological and Anthropological Sciences, 13, 9, 1–21.

Junge, A.; Dunseth, Z. C.; Shahack-Gross, R.; Finkelstein, I.; Fuchs, M. (2023): The archaeology and history of rock-cut cisterns and open water reservoirs in the Negev Highlands, Bulletin of the American Society of Overseas Research, 389, 1, 191–216.

Junge, A.; Lomax, J.; Shahack-Gross, R.; Dunseth, Z. C.; Finkelstein, I.; Fuchs, M. (2016): OSL Age Determination of Archaeological Stone Structures Using Trapped Aeolian Sediments: A Case Study from the Negev Highlands, Israel, Geoarchaeology, 31, 6, 550–563.

Junge, A.; Lomax, J.; Shahack-Gross, R.; Finkelstein, I.; Fuchs, M. (2018): Chronology of an ancient water reservoir and the history of human activity in the Negev Highlands, Israel, Geoarchaeology, 33, 6, 695–707.

Kafle, H. K.; Bruins, H. J. (2009): Climatic trends in Israel 1970–2002: warmer and increasing aridity inland, Climatic Change, 96, 1-2, 63–77.

Kagan, E. J.; Langgut, D.; Boaretto, E.; Neumann, F. H.; Stein, M. (2015): Dead Sea Levels during the Bronze and Iron Ages, Radiocarbon, 57, 2, 237–252.

Karkanas, P.; Goldberg, P. (2017): Soil Micromorphology, Springer Netherlands, Dordrecht, 830–841.

Kidron, G. J. (1999): Altitude dependent dew and fog in the Negev Desert, Israel, Agricultural and Forest Meteorology, 96, 1-3, 1–8.

Kraemer, C. J. (1958): Excavations at Nessana/3 Non-literary papyri, Excavations at Nessana (Auja Hafir, Palestine);[these vols. contain the report of the excavations at Nessana, the modern Auja Hafir, in the Negeb in Palestine].

Kühn, P.; Techmer, A.; Weidenfeller, M. (2013): Lower to middle Weichselian pedogenesis and palaeoclimate in Central Europe using combined micromorphology and geochemistry: the loess-paleosol sequence of Alsheim (Mainz Basin, Germany), Quaternary Science Reviews, 75, 43–58.

Langgut, D.; Neumann, F. H.; Stein, M.; Wagner, A.; Kagan, E. J.; Boaretto, E.; Finkelstein, I. (2014): Dead Sea pollen record and history of human activity in the Judean Highlands (Israel) from the Intermediate Bronze into the Iron Ages (~2500–500 BCE), Palynology, 38, 2, 280–302.

Langgut, D.; Tepper, Y.; Benzaquen, M.; Erickson-Gini, T.; Bar-Oz, G. (2021): Environment and horticulture in the Byzantine Negev Desert, Israel: sustainability, prosperity and enigmatic decline, Quaternary International, 593, 160–177.

Lantos, S.; Bar-Oz, G.; Gambash, G. (2020): Wine from the Desert: Late-Antique Negev Viniculture and the Famous Gaza Wine, Near Eastern Archaeology, 83, 1, 56–64.

Litt, T.; Ohlwein, C.; Neumann, F. H.; Hense, A.; Stein, M. (2012): Holocene climate variability in the Levant from the Dead Sea pollen record, Quaternary Science Reviews, 49, 95–105.

Lucke, B.; Sandler, A.; Vanselow, K. A.; Bruins, H. J.; Abu-Jaber, N.; Bäumler, R.; Porat, N.; Kouki, P. (2019): Composition of modern dust and holocene aeolian sediments in archaeological structures of the Southern Levant, Atmosphere, 10, 12, 762.

Madsen, A. T.; Murray, A. S.; Andersen, T. J.; Pejrup, M.; Breuning-Madsen, H. (2005): Optically stimulated luminescence dating of young estuarine sediments: a comparison with 210Pb and 137Cs dating, Marine Geology, 214, 1-3, 251–268.

Marom, N.; Meiri, M.; Tepper, Y.; Erickson-Gini, T.; Reshef, H.; Weissbrod, L.; Bar-Oz, G. (2019): Zooarchaeology of the social and economic upheavals in the Late Antique-Early Islamic sequence of the Negev Desert, Scientific reports, 9, 1, 1–10.

Mayerson, P. (1994): Monks, Martyrs, Soldiers and Saracens. Papers on the Near East in Late Antiquity (1962-1993), Jerusalem.

Mayya, Y.; Morthekai, P.; Murari, M. K.; Singhvi, A. (2006): Towards quantifying beta microdosimetric effects in single-grain quartz dose distribution, Radiation Measurements, 41, 7-8, 1032–1039.

Mentzer, S. M.; Quade, J. (2013): Compositional and isotopic analytical methods in archaeological micromorphology, Geoarchaeology, 28, 1, 87–97.

Migowski, C.; Stein, M.; Prasad, S.; Negendank, J. F. W.; Agnon, A. (2006): Holocene climate variability and cultural evolution in the Near East from the Dead Sea sedimentary record, Quaternary Research, 66, 3, 421–431.

Neumann, F. H.; Kagan, E. J.; Leroy, S. A. G.; Baruch, U. (2010): Vegetation history and climate fluctuations on a transect along the Dead Sea west shore and their impact on past societies over the last 3500 years, Journal of Arid Environments, 74, 7, 756–764.

Ore, G.; Bruins, H.; Meir, I. (2020): Ancient cisterns in the Negev Highlands: Types and spatial correlation with Bronze and Iron Age sites, Journal of Archaeological Science: Reports, 30, 102227.

Orland, I. J.; Bar-Matthews, M.; Kita, N. T.; Ayalon, A.; Matthews, A.; Valley, J. W. (2009): Climate deterioration in the Eastern Mediterranean as revealed by ion microprobe analysis of a speleothem that grew from 2.2 to 0.9 ka in Soreq Cave, Israel, Quaternary Research, 71, 1, 27–35.

Porat, N.; Rosen, S. A.; Boaretto, E.; Avni, Y. (2006): Dating the Ramat Saharonim late Neolithic desert cult site, Journal of Archaeological Science, 33, 10, 1341–1355.

Prescott, J. R.; Hutton, J. T. (1994): Cosmic ray contributions to dose rates for luminescence and ESR dating: large depths and long-term time variations, Radiation measurements, 23, 2-3, 497–500.

Rosen, S. A. (2017): Revolutions in the Desert. The Rise of Mobile Pastoralism in the Southern Levant.

Rosen, S. A.; Savinetsky, A. B.; Plakht, Y.; Kisselava, N. K.; Khassanov, B. F.; Pereladov, A. M.; Haiman, M. (2005): Dung in the desert: Preliminary results of the Negev Holocene Ecology Project, Current Anthropology, 46, 2, 317–326.

Rubin, R. (1988): Water conservation methods in Israel's Negev desert in late antiquity, Journal of Historical Geography, 14, 3, 229–244.

Rubin, R. (1990): The Negev as a settled land: Urbanization and settlement in the desert in the Byzantine period., Jerusalem, Israel.

Saidel, B. A.; Erickson-Gini, T. (2014): A note on the excavation of an Ottoman and British Mandate period Bedouin campground at Nahal Be'erotayim West in the Negev desert, Israel, Arabian archaeology and epigraphy, 25, 1, 138–145.

Shahack-Gross, R.; Boaretto, E.; Cabanes, D.; Katz, O.; Finkelstein, I. (2014): Subsistence economy in the Negev Highlands: the Iron Age and the Byzantine/Early Islamic period, Levant, 46, 1, 98–117.

Shahack-Gross, R.; Finkelstein, I. (2015): Settlement oscillations in the Negev Highlands revisited: the impact of microarchaeological methods, Radiocarbon, 57, 2, 253–264.

Shahack-Gross, R.; Finkelstein, I. (2017): Iron Age agriculture in the Negev Highlands? Methodological and factual comments on Bruins and van der Plicht 2017a (Radiocarbon Vol. 59, Nr. 1), Radiocarbon, 59, 4, 1227–1231.

Shanan, L. (2000): Runoff, erosion, and the sustainability of ancient irrigation systems in the Central Negev Desert., in Hassan, M. A.; Slaymaker, O. (editors), The hydrology-geomorphology interface: Rainfall, floods, sedimentation, land use, IAHS Publications, Jerusalem, Israel, 75–106.

Starinsky, A.; Zilberman, E.; Braun, M.; Sneh, A. (2010): Geological map of Israel 1: 50,000: Revivim sheet 18-II, Jerusalem: State of Israel, Ministry of National Infrastructure, Geological Survey.

Stoops, G. (2003): Guidelines for analysis and description of soil and regolith thin sections, Soil Science Society of America, Madison, Wisconsin.

Stoops, G. (2018): Chapter 1 - Micromorphology as a Tool in Soil and Regolith Studies, in Stoops, G.; Marcelino, V.; Mees, F. (editors), Interpretation of Micromorphological Features of Soils and Regoliths (Second Edition), Elsevier, second edition edition, 1–19.

Tepper, Y.; Erickson-Gini, T.; Farhi, Y.; Bar-Oz, G. (2018): Probing the Byzantine/Early Islamic Transition in the Negev: The Renewed Shivta Excavations, 2015–2016, Tel Aviv, 45, 120–152.

Tepper, Y.; Porat, N.; Bar-Oz, G. (2020): Sustainable farming in the Roman-Byzantine period: Dating an advanced agriculture system near the site of Shivta, Negev Desert, Israel, Journal of Arid Environments, 177, 104134.

Vardi, J.; Rosen, S. A. (2020): The Intermediate Bronze Age Lithic Industry from Ein Ziq: Implications for Cultural Affinities, Function, and Chronology, Mitekufat Haeven: Journal of the Israel Prehistoric Society, 50, 223–252.

Wagner, G. A. (1998): Age determination of young rocks and artifacts: physical and chemical clocks in quaternary geology and archaeology, Springer Science & Business Media.

Walker, M. (2005): Quaternary dating methods, John Wiley and Sons.

Ziv, B.; Saaroni, H.; Pargament, R.; Harpaz, T.; Alpert, P. (2014): Trends in rainfall regime over Israel, 1975–2010, and their relationship to large-scale variability, Regional Environmental Change, 14, 1751–1764.

Part II

Publications

First Study

Chronology of an ancient water reservoir and the history of human activity in the Negev Highlands, Israel

Andrea Junge, Johanna Lomax, Ruth Shahack-Gross,
Israel Finkelstein, & Markus Fuchs

Geoarchaeology, Volume 33, Issue 6, Pages 695-707, November/December 2018

Manuscript Received: 20^{th} June 2017
Manuscript Revised: 4^{th} December 2017
Manuscript Accepted: 4^{th} April 2018
First Published: 7^{th} June 2018

Received: 20 June 2017 | Revised: 4 December 2017 | Accepted: 4 April 2018

DOI: 10.1002/gea.21682

RESEARCH ARTICLE

WILEY Geoarchaeology An International Journal

Chronology of an ancient water reservoir and the history of human activity in the Negev Highlands, Israel

Andrea Junge[1] | Johanna Lomax[1] | Ruth Shahack-Gross[2]* | Israel Finkelstein[3]* | Markus Fuchs[1]*

[1]Department of Geography, Justus-Liebig-University Giessen, Giessen, Germany

[2]Department of Maritime Civilizations, Recanati Institute of Maritime Studies, University of Haifa, Haifa, Israel

[3]Institute of Archaeology, Tel Aviv University, Tel Aviv, Israel

Correspondence
Andrea Junge, Department of Geography, Justus-Liebig-University Giessen, Senckenbergstrasse 1, 35390 Giessen, Germany.
Email: andrea.junge@geogr.uni-giessen.de

*Project directors.

Scientific editing by Andreas Lang

Abstract

In antiquity, the development of techniques to collect and store water was fundamental to sustain life in arid regions. One way to overcome the problem of water supply in the desert was to construct water reservoirs and cisterns which collect surface runoff during rare rain events. Indeed, open reservoirs and rock-cut cisterns are widely spread over the arid zone of the Negev Highlands. They were an important component of human activity in the area. Today, they can serve as sedimentary archives for archaeological and paleoenvironmental reconstruction. To shed more light on this valuable archive, the chronology of an ancient stone-lined, open reservoir was established by optically stimulated luminescence dating. By determining the age of the deposition of sediments associated with the reservoir, it was possible to constrain its construction (8th–11th centuries C.E.), duration of use (up to ca. 15th century C.E.), and final refilling (from the 15th century C.E. to the modern era). These results indicate that most human activity related to the reservoir occurred between the 8th-to-11th and the 15th centuries C.E., when permanent settlements are not recorded archaeologically in the region, suggesting that the studied water reservoir was primarily utilized by pastoral nomads.

KEYWORDS

ancient water harvesting system, Atar Haroa, Levant, OSL, pastoral nomads

1 | INTRODUCTION

Establishment of settlements in arid and semi-arid regions depends on accessibility to a sufficient amount of water, fundamental for drinking, domestic use, as well as farming and herding. Precipitation in the study area (Figure 1) — the arid Negev Highlands — is low (ca. 100–150 mm annually) and characterized by a high seasonal and year-to-year variability (Evenari, Shanan, & Tadmor, 1982; Goldreich, 2003). Perennial springs in the region are scarce and usually characterized by low flow of water. Consequently, they are not sufficient or reliable enough to sustain large-scale human activity (Rubin, 1988). Natural bedrock depressions in wadis, which are filled with surface runoff during rain events, provide another source of water in the region, but they are not large enough or reliable enough to support a significant population.

To enable expansion of human activity in the Negev Highlands, several techniques to collect and store ground and surface water were developed. Groundwater is carried by shallow aquifers and can be reached by pits dug in wadis where the aquifer is close to the surface, or by wells if the water-bearing layer is deeper (Evenari et al., 1982). At a certain moment in history, the Negev inhabitants started constructing artificial reservoirs and cisterns, together with channels that collected surface runoff from nearby slopes. Researchers (e.g., Evenari, Aharoni, Shanan, & Tadmor, 1958) postulated sequential (chronological) development in the introduction of these reservoirs. According to conventional theory, the first to be established are round open water reservoirs, which were dug into impermeable layers of clay or marl that served as an aquiclude. These depressions, which may reach 10 m to 12 m in diameter and 4 m to 5 m in depth, were then lined internally with unhewn stones. These open reservoirs are believed to date to the Iron Age IIA (ca. late 10th–9th B.C.E.; for numerical dates see Boaretto, Finkelstein, & Shahack-Gross, 2010; Finkelstein & Piasetzky, 2010), a period which is characterized by a wave of settlement in the region. This dating was based on the observation that the open water reservoirs are found in proximity to Iron Age sites (e.g., Cohen & Cohen-Amin, 2004; Evenari et al., 1958; Haiman, 1991; Lender, 1990). Next came subterranean cisterns, which were rock-cut into soft chalk formations. One sub-type of the subterranean cisterns is known as the "bell-shaped cistern", with an average capacity of 25–50 m^3. The second subtype is often rectangular with a capacity of hundreds of cubic meters. The size of cisterns of the latter sub-type made it necessary to leave rock-cut pillars in their midst in order to support the overlying bedrock. The walls of these cisterns, locally termed

 © 2018 Wiley Periodicals, Inc.

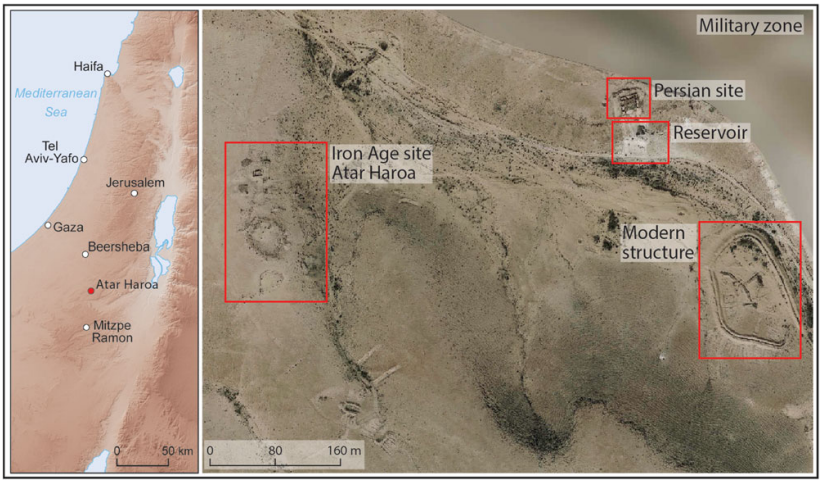


FIGURE 1 Map of the southern Levant and a satellite image close-up of the study area showing the reservoir under study, the Iron Age IIA site of Atar Haroa, and the Persian period "fortress" site (Survey of Israel, 2007). [Color figure can be viewed at wileyonlinelibrary.com]

kharaba in Arabic, are often plastered. Some of the rock-cut cisterns include Nabatean and Byzantine inscriptions and are thus dated to the Roman–Byzantine period (ca. 2nd–7th centuries C.E.). They are considered to be the final refinement of the rainwater harvesting installations in the region (Evenari et al., 1982; Rubin, 1988).

Numerical age determination of the different types of reservoirs and cisterns known in the Negev Highlands is fundamental for understanding the nature of ancient settlement systems in the region. Hitherto, the theory regarding developmental stages of rainwater harvesting installations from open reservoirs to rock-cut cisterns was based on modern notions of the technological complexity or ability of ancient societies. Thus, dating water installations based on proximity to settlement sites is highly hypothetical, as in most cases sites of different periods are found in their vicinity.

No attempt has been made so far to determine the age of the reservoirs and cisterns in the Negev Highlands by numerical dating methods. Beyond the Negev, the only published study that determined numerically the age of deposits filling subterranean cisterns by optically stimulated luminescence (OSL) dating in the Levant was conducted by Kraushaar, Ollesch, Siebert, Vogel, and Fuchs (2015). They successfully determined the rate of sediment transportation into two rock-cut subterranean cisterns in northern Jordan, establishing the onset of sediment accumulation within the cisterns to 760 to 860 C.E., indicating the time of their abandonment. Another attempt to determine the age of a cistern was made by Lichtenberger, Lindroos, Raja, and Heinemeier (2015). In their study, the usage (2nd–3rd centuries C.E.), repair (3rd–6th centuries C.E.), and abandonment (6th–7th centuries C.E.) of a cistern in Jordan was constrained by radiocarbon dating of the cistern's wall mortar and charcoal remains found within several layers of the mortar.

The present study focuses on the investigation of an open water reservoir located near the Iron Age site of Atar Haroa (Figure 1). According to the chronological development paradigm presented above, this reservoir is considered to have served the water requirements of this site and thus assumed to have been constructed during the Iron Age IIA (mainly 9th century B.C.E.; Boaretto et al., 2010). OSL dating was applied in order to test the preliminary assumption and shed light on the time of construction, utilization, and final refilling of this reservoir.

OSL dating provides the possibility to determine the last accumulation of sedimentary deposits due to the zeroing of the luminescence signal when the sediment grains are exposed to sunlight during transportation and deposition. In case of an open water reservoir, the resetting of the signal can be achieved during three main processes:

1. When sediments were removed in order to dig the reservoir and piled around it as a spoil pile. In this case, the age of the lowermost sediments in contact with the paleosurface will indicate the date of construction of the installation.
2. When sediments were washed into the reservoir, they were then removed during its use for maintenance purposes and placed on the spoil pile. In this case, the removed spoil material is expected to be somewhat stratified and its ages should reflect the time period of the reservoir's use and maintenance.
3. When sediments were washed into the reservoir but have not been removed. Assuming that reservoirs would have been cleaned of sediments while functioning, the age of the lowermost sediment within the reservoir will indicate either its abandonment or a declining use of this installation.

In the current study, all three phases in an open reservoir's life cycle are addressed: construction, use, and abandonment. OSL sampling is based on field observations on the stratigraphy of the sediments below and within the spoil pile around the water reservoir, as well as on the sediments that accumulated within the reservoir. Micromorphology of sediments from the spoil pile and the fill within the installation supports and amplifies field observations about the sedimentary processes associated with the reservoir.

2 | STUDY AREA

2.1 | Geomorphology and geology

The altitude of the Negev Highlands ranges between 600 m a.s.l. in the northeast to 1,000 m a.s.l. in the southwest (Figure 1). The present topography was formed following the uplift of the highlands and faulting processes of the Dead Sea Rift from the Late Miocene to the Early Pleistocene (Avni, Porat, Plakht, & Avni, 2006; Itzhaki, 1971). The region is characterized by a series of northeast-to-southwest-oriented anticlines and synclines. The bedrock mainly consists of Cretaceous and Eocene marine carbonates, traversed by wadis, which are the result of erosion processes over the Plio-Pleistocene (Avni et al., 2006; Avni & Weiler, 2013; Bruins, 1986). During the Late Pleistocene and Early Holocene, eolian sediments primarily from the Sinai and the Sahara accumulated across the Negev Highlands (Avni, Porat, & Avni, 2012; Avni et al., 2006; Crouvi, Amit, Enzel, Porat, & Sandler, 2008; Roskin, Tsoar, Porat, & Blumberg, 2011). Following this, the eolian sediments were partially eroded and mixed with local sediments, resulting in the formation of thick alluvial deposits in the wadis (Avni, Porat, & Avni, 2013).

The studied water reservoir is situated on a footslope between an elongated hill and a wadi (Figure 2) ca. 550 m a.s.l. It was dug below a thick escarpment of chert (Campanian, Mishash Formation) into a thin chalky-marly layer (Santonian, Menuha Formation; Avni & Weiler, 2013), the latter serving as the aquiclude.

2.2 | Modern and past climate

In this study, the OSL dating of the water reservoir yielded results covering the last 1,500 years. The modern climate, as well as the climate record of the last two millennia, is considered below to emphasize the aridity of the area. These are important considerations for both life sustainability in the region and the effect of humidity on OSL age calculations.

Present day climate in the study area is characterized by mean annual air temperature between 17°C and 19°C (hot summers, up to 40°C and cool winters down to freezing) and annual precipitation between 80 mm and 150 mm (Kafle & Bruins, 2009). Most of the rain falls during the winter months — roughly October to April (Avni et al., 2006; Goldreich, 2003) with strong year-to-year variations (Bruins, 2012; Evenari et al., 1982; Shanan, 2000). Fog and dew add to the annual precipitation an equivalent of 10 mm for each 100 m increase in elevation (Kidron, 1999).

Recent paleoclimate reconstructions for the Late Holocene in the Dead Sea region are inconclusive and contrasting conclusions were drawn (Bar-Matthews, Ayalon, Gilmour, Matthews, & Hawkesworth, 2003; Bookman, Enzel, Agnon, & Stein, 2004; Finné, Holmgren, Sundqvist, Weiberg, & Lindblom, 2011; Kagan, Langgut, Boaretto, Neumann, & Stein, 2015; Langgut et al., 2014; Litt, Ohlwein, Neumann, Hense, & Stein, 2012; Migowski, Stein, Prasad, Negendank, & Agnon, 2006; Neumann, Kagan, Leroy, & Baruch, 2010; Orland et al., 2009). A phase of decrease in precipitation at the beginning of the 1st millennium C.E. in comparison to the preceding period and today's climate

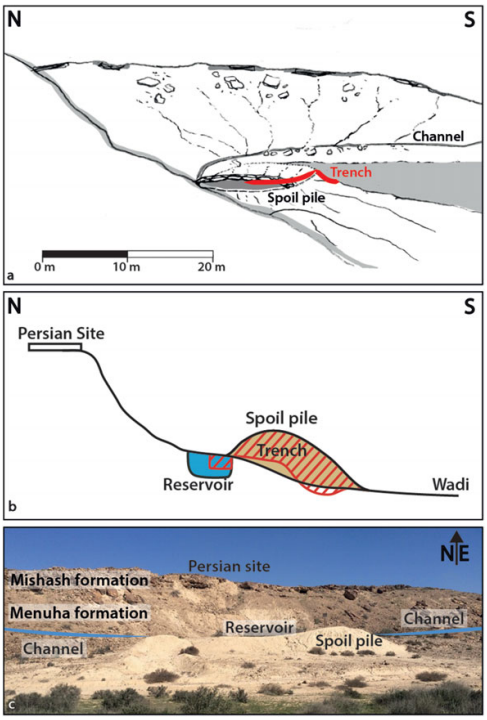


FIGURE 2 (a) Sketch of the reservoir at the footslope with channels bounding the catchment area. The trench cut from the center of the reservoir through the spoil pile is marked in red. (b) Schematic drawing (not to scale) of a topographic cross section of the reservoir. The cross section shows the position of the trench in relation to the reservoir, the spoil pile, and the paleosurface. (c) Photograph from the wadi facing the reservoir, showing the structure and associated geological formations, Persian period "fortress" site, and water conduits. [Color figure can be viewed at wileyonlinelibrary.com]

is postulated by Bar-Matthews and Ayalon (2004) and Orland et al. (2009) based on isotopic compositions of speleothems (Soreq Cave), by Bookman et al. (2004) based on the reconstruction of Dead Sea lake levels using sedimentological parameters, and also by Neumann et al. (2010) based on sedimentological and palynological analyses of cores from the Dead Sea shore. Whereas Bar-Matthews et al. (2003) reconstruct drier conditions over the majority of the last two millennia based on analyses of isotopic compositions of speleothems (Peqiin Cave), Neumann et al. (2010) and Bookman et al. (2004) reconstruct strong oscillations of the Dead Sea levels that are explained by variation in precipitation. Orland et al. (2009) describe a second phase of decreasing rainfall at about 400 C.E., possibly followed by further variations. Based on sedimentological and in parts also palynological investigations of sediment cores from the Dead Sea and its shore, Heim, Nowaczyk, Negendank, Leroy, and Ben-Avraham (1997) and Migowski et al. (2006) reconstruct the occurrence of significant arid events between 500 and 1,600 C.E., or between 500 and 1,200 C.E., respectively.

Despite these inconsistent reconstructions, it can be said that the climate in the last two millennia is as arid as current conditions, with a

few slightly drier phases. Therefore, the need for water harvesting and the construction of water reservoirs is obvious.

2.3 | The water reservoir and the surrounding structures

The dimensions of the studied reservoir can be estimated to be 10 m to 12 m in diameter and ca. 4 m to 5 m in depth, resulting in a water capacity of 300 m^3 to 600 m^3. The internal perimeter of the reservoir was stabilized by uncut stones that prevented collapse of side sediment when the installation was filled with water (Evenari et al., 1982). The sediment that was removed when digging the reservoir was dumped around it, forming a spoil pile (Figure 2). Upslope, two small channels were constructed from field stones, to lead runoff water into the reservoir (Figure 2c). Surface water contained sediment, which originated from the catchment area and was transported to the reservoir. To reduce sedimentation within the installation, sometimes small basins were installed at the end of the channels, before entering the reservoir, to reduce the flow velocity of the water, resulting in sediment deposition of the coarser fraction. However, for the studied installation, no sedimentation basins were observed and possibly, most of the sediments from the reservoir's catchment were deposited within it. To maintain the reservoir, removal of this sediment was needed from time to time, adding to the volume of the spoil pile surrounding it.

Two ancient sites are located in the vicinity of the reservoir (Figure 1). The Iron IIA site of Atar Haroa is situated about 500 m to its west. This site consists an enclosed compound, pillared houses, and a threshing floor. Agricultural terraces in the wadi are known next to it (Cohen, 1970; Shahack-Gross, Boaretto, Cabanes, Katz, & Finkelstein, 2014; Shahack-Gross & Finkelstein, 2008). The construction of the enclosed compound and pillared houses were radiocarbon-dated to the late 10th and mainly 9th century B.C.E. (Boaretto et al., 2010). Stratigraphic correlation indicates that the threshing floor was constructed and used much later than the Iron Age settlement (probably sub-modern; Shahack-Gross & Finkelstein, 2008). The agricultural terraces in the wadi were not numerically dated, but other studies have shown that the vast majority of these terraces in the Negev Highlands date to the Late Roman (2nd–3rd centuries C.E.), Byzantine (4rd–6th centuries C.E.), and Early Islamic (7th–9th centuries C.E.) periods (Avni et al. 2013). Investigation of the micro-remains from Atar Haroa indicates no cereal cultivation, whereas livestock herding was based on local shrubs (Shahack-Gross et al., 2014).

The second site is a square courtyard structure, ca. 23 m × 23 m in size, described as a "fortress." The structure, dated to the Persian Period (5th–4th centuries B.C.E.), is located above the studied reservoir on the top of the elongated hill, only ca. 50 m away (Cohen & Cohen-Amin, 2004; Figure 1).

3 | SAMPLING STRATEGY AND METHODS

To establish the age of construction, utilization, and end of use of the water reservoir, sediment accumulations from these three phases were investigated. For this purpose, a trench (Figures 2 & 3a) was dug



FIGURE 3 Photographs showing (a) the trench, looking from the center of the reservoir in the direction of the wadi (southwards). In the front, the stones from the lining of the inner side of the reservoir are visible. The deep part of the trench is lower than the nearby wadi surface. (b) The southern, deepest, part of the trench through the spoil pile (section HC-1), showing the massive lower part and inclined, laminated upper part of the sediment profile. (c) The middle part of the trench through the spoil pile, section HC-3. Note the massive appearance of sediment in the bottom, covered by loose sediments at the top. (d) The northern part of the trench, within the reservoir, section HC-2. The massive appearance of the grey bottom sediment overlain by grey and yellow laminated beds is displayed. The positions of OSL samples in section HC-2 (d) and HC-3 (c) are indicated by the black caps of the sample tubes. [Color figure can be viewed at wileyonlinelibrary.com]

from the center of the reservoir in an outward direction, through the spoil pile. Three different parts of the trench were sampled for OSL dating and micromorphology analysis. Sections HC-1 and HC-3 represent the spoil pile, whereas section HC-2 represents the fill within the reservoir.

The southern part of the trench (section HC-1) is situated in the outer edge of the spoil pile and is mainly composed of debris from the reservoir's construction and maintenance (Figures 3 & 4). Trenching stopped when large rounded boulders mixed with gravel and finer sediment were encountered at a topographic level below the current nearby wadi surface (Figure 2b). This indicated that the trenching reached ancient wadi alluvium. Although a clear paleosurface could not be observed, it is assumed that the lowermost part of this section

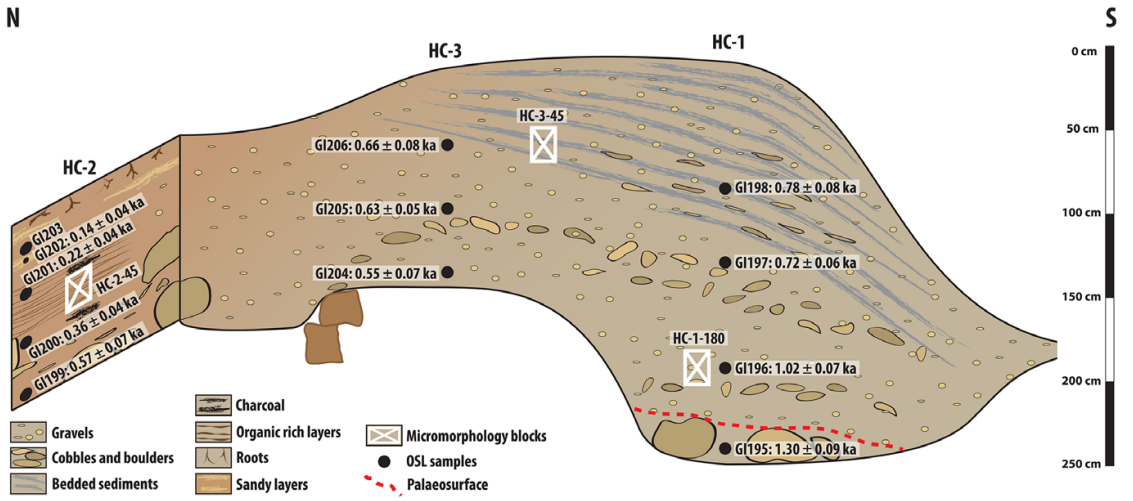


FIGURE 4 Composite schematic drawing of the eastern section in the trench, from the center of the reservoir (HC-2) through the spoil pile (HC-3 & HC-1). OSL samples with their ages and blocks for micromorphological analyses are marked. The dashed red line indicates the approximate transition from alluvial wadi deposits to the marly debris from the construction of the reservoir. Note the hill-like appearance of the massive and slightly inclined bottom suite of sediments, and the steeper inclination of the finely bedded sediments closer to the spoil pile's edge. [Color figure can be viewed at wileyonlinelibrary.com]

can serve as control for the latest time before reservoir construction took place. The lowermost part of section HC-1 consists of cobbles and boulders with a diameter up to 20 cm, embedded in fine-grained material. The material shows no layering and the stones have no specific orientation. This unit — the wadi alluvium — is represented by OSL sample GI195 (Figure 4). The sediments above include smaller and flatter cobble-sized stones having preferred orientation within compacted silty sediments (Figure 4). This massive sediment has a general hill-like appearance, representing the spoil of reservoir construction. The approximate position of the contact between the wadi alluvium and this hill-like deposit is marked by a dashed red line in Figure 4. From the lower part of this hill-like deposit, OSL sample GI196 was taken, associated with micromorphology sample HC-1-180. Another OSL sample was collected at the bottom of HC-3 (GI204), identified to belong stratigraphically to the same hill-like deposit but at a slightly higher level.

In the middle of section HC-1, a second layer of stones of variable sizes (up to 15 cm) may mark another phase of construction. Sample GI197 from section HC-1 and sample GI205 from section HC-3 were collected above the stony layer, still within rather massive sediment having some north-to-south-inclined layering of the fine-grained sediments. The orientation of the stones generally follows this layering.

Above the massive sediments with gentle north–south inclination, there is a suite of finely bedded, loose sediments having a steeper north–south inclination (Figure 4). It is assumed that the steeper and finer bedding, together with the finer-grained sediment and smaller gravel, represents spoil of sediment removed from within the reservoir as a succession of several cleanup maintenance procedures. Samples GI198 from section HC-1 and GI206 from section HC-3 were taken from the bottom of this suite of bedded sediments, associated with micromorphology sample HC-3-45.

Stones of the internal wall, which stabilized the reservoir, were found at the bottom of section HC-3. Moving into the reservoir, section HC-2 is composed of fine-grained fill with graded bedding. Cobbles and boulders comparable in size and shape to the stones in the bottom of section HC-1 have been found as well. These boulders possibly represent the collapsed lining stones as well as boulders from the slope above the reservoir. The bottom of the reservoir was probably not reached in section HC-2, that is, samples are expected to indicate post-abandonment or declined use (without maintenance) of the installation. The lower part of section HC-2 is unstratified, composed of loamy sediments with gravels (<4 cm) and a few stones with diameters up to 25 cm. OSL samples GI199 and GI200 come from the lowest part of this section. The middle part of section HC-2 is characterized by fine alternating laminations of light (yellowish) and dark (greyish) sediments with a few lenses of coarse sand and black-colored organic-rich layers and patches. This part is represented by OSL sample GI201 and micromorphology sample HC-2-45. The upper part of the section is unstratified and disturbed by roots of recent vegetation. A few coarse sand lenses occur as well, one of which was sampled for OSL dating (GI202). The uppermost OSL sample, GI203, was taken from a mostly undisturbed area near the surface. Samples GI199 to GI203 represent the continuous filling of the reservoir after it ceased to be maintained.

3.1 | OSL

3.1.1 | Sample preparation and instrumental setup

The OSL samples were collected during daytime, using steel cylinders with a diameter of 4.5 cm. To determine the equivalent dose (D_e), the coarse-grain (90–200 μm) quartz fraction was prepared. In the first step, the sediment was removed from the cylinders, whereas

the bleached material at both ends of the cylinders was discarded. The sediment was wet-sieved to separate the grain-size fractions, followed by treatment with 10% HCl and 10% H_2O_2 to dissolve carbonates and oxidize organic matter. To obtain the quartz fraction, lithium-heteropolytungstate (2.63 and 2.68 g/cm^3) was used for density separations.

Next, the quartz extract was etched in 40% hydrofluoric acid (HF) for 80 min to remove the α-irradiated outer layer of the grains and to eliminate remaining feldspar contamination. In the final step, the coarse-grain quartz fraction was washed for 30 min in 10% HCl and re-sieved (63 μm) to remove small residues and remaining feldspar fragments. All preparation steps were performed under subdued amber-colored light centered on 590 ± 10 nm.

The OSL measurements were executed on a Lexsyg Standard reader (Lomax, Kreutzer, & Fuchs, 2014). For stimulation, the reader was operated with green LEDs (525 ± 25 nm), whereas for signal detection, a Hamamatsu H7360 photomultiplier combined with a 5 mm Semrock HC377/50 filter and a 3 mm Schott BG3 filter was applied. This combination restricts the detection window to ca. 350 nm to 400 nm, thus is centered on the main OSL emission of quartz (Huntley, Godfrey-Smith, & Haskell, 1991; Lomax, Mittelstraß, Kreutzer, & Fuchs, 2015). Stimulation with infrared (IR) laser diodes (850 ± 3 nm) was used to check for the purity of the quartz extracts. Feldspar contamination was tested by visual inspection of the response to IR stimulation. For this test, signals were detected through a 3.5 mm Semrock HC414/46 interference filter in combination with a 3 mm Schott BG39 filter, which restricts the detection window to ca. 395 nm to 430 nm. Sample irradiation was performed with a calibrated ^{90}Y/^{90}Sr β-source (1.9 GBq), resulting in a dose rate for coarse-grain quartz on stainless steel cups of 0.125 ± 0.003 Gy/s (July 15, 2016).

3.1.2 | D_e estimation

For the determination of the D_e, a single-aliquot regenerative-dose (SAR) protocol after Murray and Wintle (2000) was applied. To define the dose-response curve, five or six regeneration cycles, including the zero dose and one repeated dose point, were used. The shine-down curves were measured for 50 s at elevated temperatures (125°C) after a preheat at 200°C (10 s) and a cut-heat at 180°C for the natural and regenerated signals. The preheat and cut-heat temperatures were chosen after preheat-plateau test (PHT) measurements and combined preheat-dose recovery tests (DRT). For the DRT the samples were bleached in the Lexsyg reader using the green LEDs and irradiated with a known β-dose close to the natural dose, followed by D_e determinations using a SAR protocol. For the PHT burial doses were also measured using the SAR protocol. Both tests were conducted at six different preheat temperature (180–280°C).

For D_e determination, the integral of the first 0.5 s of the quartz shine-down curves was used, after subtracting a background of 40 s to 50 s from the signal. Three millimeter aliquots were used for D_e determination of the coarse-grain fraction (ca. 200 grains; Fuchs & Wagner, 2003), except for samples GI203 and GI206 for which 1 mm and 2 mm aliquots were used, respectively, because of the lack of a sufficient amount of extracted quartz. In general, up to 30 aliquots were measured for each coarse grain sample to determine the D_e. After passing the rejection criteria of 10% for the recycling ratio, the test dose error and the recuperation value, the mean D_e of the aliquots was calculated using the central age model after Galbraith, Roberts, Laslett, Yoshide, and Olley (1999) for not significantly skewed samples, and the bootstrap minimum age model (Cunningham & Wallinga, 2012) for significantly skewed samples. The differentiation between skewed and un-skewed distributions is based on the comparison of the standardized values of skewness and their significance value (Bailey & Arnold, 2006). The age models were calculated with log-transformed D_e values for samples with D_e values >1 Gy (GI195, GI196, & GI198), whereas samples with resulting D_e values lower than 1 Gy (GI197, GI199–GI206) were calculated based on the un-logged D_e (Arnold, Roberts, Galbraith, & DeLong, 2009).

3.1.3 | Dose rate

Radionuclide concentrations were determined by thick source α-counting (U and Th) and ICP-OES (K). The cosmic radiation dose was calculated according to Prescott and Hutton (1994) using current burial depths for the samples from the spoil pile (GI195–GI198 & GI204–GI206), because the deposition of material ended several centuries ago, and using half the current burial depths for the samples within the reservoir (GI199–GI203) due to the relatively continuous accumulation until the present day. The measured concentrations were converted to dose rates using the conversion factors of Guérin, Mercier, and Adamiec (2011) and the β-attenuation factor of Mejdahl (1979).

3.1.4 | Water content

The construction of a water reservoir interferes with the natural water regime. Hence, it is necessary to pay particular attention to the water content in sediments and distinguish between the inner part of the reservoir and the spoil material surrounding the installation.

The water content of the OSL samples collected within the reservoir (HC-2: GI199–GI203) was set to 15 ± 7.5%. This value and its uncertainty represent the possible water content range, based on the porosity of loamy silt, the climate conditions, and the amount of water delivered by the channels from the adjacent slope. The water content values used for the OSL age calculation were checked by measuring the *in situ* water content of the samples, showing values between 10% and 15% (samples were collected during spring). The measured water content of the spoil pile sediments (HC-1: GI195–GI198 and HC-3: GI204–GI206) ranges between 1% and 3%. Whereas all sediment samples have similar properties, the difference in water content relates to poor drainage inside the reservoir and better drainage at the spoil pile. Additionally, in contrast to the reservoir, the spoil pile is not fed by water from the catchment. Based on this and the measurements of the actual water content, the water content used for OSL age calculation of the samples from the spoil pile was set to 6 ± 3%.

3.2 | Micromorphology

The monolithic sediment blocks were extracted using jackets of plaster of Paris (gypsum bandages). They were then dried at 55°C for three

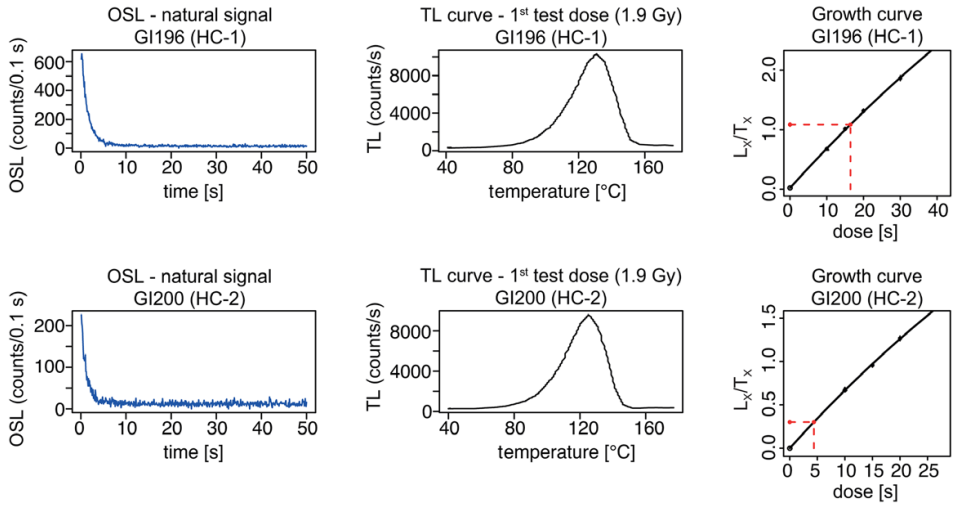


FIGURE 5 Luminescence properties of the sediments represented by samples GI196 (HC-1, construction debris) and GI200 (HC-2, within the reservoir). Shown are OSL shine-down curves of the natural signal, thermoluminescence (TL) curves of the first test dose cut-heat, and the growth curves. The graphs are created with the function plot_RLum() in R using the luminescence package (Kreutzer et al., 2017). [Color figure can be viewed at wileyonlinelibrary.com]

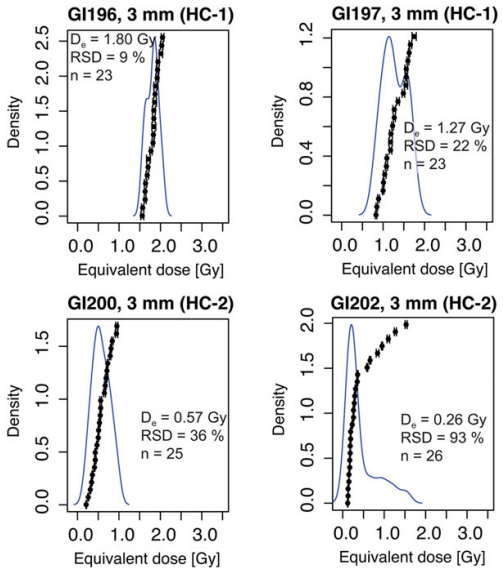


FIGURE 6 Kernel density estimation plot for representative samples (GI196, GI197, GI200, & GI202). For these samples, the accepted aliquots are shown in ascending order, with *n*, number of aliquots; RSD, relative standard deviation; D_e, equivalent dose and the aliquot diameter. The graphs are created with the function plot_KDE() in R using the luminescence package (Kreutzer et al., 2017). [Color figure can be viewed at wileyonlinelibrary.com]

days and impregnated by a 7:3 (v:v) mixture of polyester resin and acetone. A small amount of hardener (10 ml per 1 l of mixed resin) was added, without accelerator, in order to allow impregnation of small pores before consolidation. After several weeks, the blocks were cured at 55°C for 2 days, and cut to the desired thin section size (5 × 7 cm) using a slab saw. Two thin section-sized units were yielded from each block, covering the length of the original sample. The pre-cut units were sent for thin section preparation at Arizona Quality Thin Section Company. The prepared 30 μm thick thin sections were studied using a Nikon Eclipse 50i polarizing light microscope, and described using the conventional literature (Stoops, 2003).

4 | RESULTS

4.1 | OSL

The purity of the quartz extract and its suitability for OSL dating is demonstrated by the rapidly decaying OSL signal, combined with a prominent 110°C thermoluminescence (TL) peak (Figure 5) and negligible IRSL signal.

The D_e values were calculated by establishing growth curves with single exponential saturation functions. The resulting D_e distributions (Figure 6) of the two oldest samples (GI195 and GI196) are not significantly skewed (Bailey & Arnold, 2006). The relative standard deviation of the D_e distributions obtained from these samples (8% and 9%) and their overdispersion (7%) indicate relatively narrow distributions. These attributes are indicative of complete signal bleaching during the last process of sediment reworking and deposition, allowing the use of the central age model based on log-transformed D_e values. The D_e distribution of sample GI198, with a relative standard deviation of 21% and an overdispersion of 18%, is significantly right skewed. Thus, the D_e value was calculated by using the bootstrap minimum age model, also based on log-transformed D_e.

The remaining OSL samples collected from the spoil pile (GI197 & GI204–GI206) as well as the samples from within the reservoir (GI199–GI202) have relative standard deviations of 17 to 34 % (spoil

pile) and 36 to 99 % (reservoir) and overdispersions of 16 to 33 % (spoil pile) and 37 to 75 % (reservoir). In general, the overdispersion and relative standard deviations of the D_e distributions tend to increase with decreasing D_e values. Samples GI198, GI201, GI202, and GI204 are significantly skewed owing to a few outlying high D_e values. The occurrence of the outliers in the case of the spoil material is most likely caused by incomplete resetting of the luminescence signal during deposition, because the sediment was probably removed from the reservoir in large quantities causing an insufficient exposure to sunlight of a certain portion of grains. The outliers of the samples collected within the reservoir might be caused by post-depositional mixing due to bioturbation (Bateman et al., 2007). For these significantly skewed samples the D_e were calculated using the bootstrap minimum age model based on un-logged D_e values with a sigma b value of 0.23, which represents the average overdispersion of the normally distributed samples. The remaining samples (GI199, GI200, GI203, GI205, & GI206) showed no significant skewness in their distributions resulting in the application of the central age model based on un-logged D_e values. For sample GI203 no aliquot passed all rejection criteria, because of low OSL signal in combination with a small aliquot diameter (1 mm), resulting in the rejection of this sample.

The OSL ages were calculated based on the resulting D_e estimates and the parameters listed in Table 1. The resulting ages are listed in Table 2 and shown in Figure 4.

4.2 | Micromorphology

The sediment in the micromorphological thin sections from the monolithic block HC-1-180 collected in the deposit representing the reservoir construction spoil is composed of randomly oriented local sand- and gravel-sized marl fragments, within finer-grained calcitic-clay groundmass that is probably pulverized marl. The sediment is compact, massive, and does not include anthropogenic microartefacts or organic components (Figure 7a).

The sediment in the thin sections from block HC-2-45 collected from within the water reservoir includes laminated crusts that are internally graded (fining-up), characteristic of water-lain deposits (Figure 7b). In the field, organic matter was identified in pockets between the lamina. Micromorphological observation shows that the organic matter is the remains of burrowing, including soil fauna coprolites. The sediment includes vesicles and chambers, some of them with internal black organic coating, indicative of bioturbation. The presence of vertical cracks is interpreted to result from desiccation (Figure 7b). The burrowing activity disrupts the structure of the laminated sediments and must therefore be post-depositional.

The sediment from the finely bedded and steeply inclined unit (sample HC-3-45) does not appear laminated microscopically. It is composed of fine-grained calcitic-clay and occasional sand-to-gravel-sized marl fragments, arranged in an open (porous) structure (Figure 7c). Randomly oriented fragments bearing features similar to those observed within the installation, for example, graded bedding, are interpreted to be the remains of water-lain crusts, which formed within the reservoir and disaggregated when removed from the installation during cleanup activity.

5 | DISCUSSION

5.1 | Chronology of construction, use, and abandonment

The OSL samples show promising luminescence characteristics, which allowed age determination of the sediments associated with the water reservoir. With the support of the micromorphology analyses the ages can be correlated with the different modes of deposition of the sediments (Junge et al., 2016). Hence, it is possible to establish a chronostratigraphy of the reservoir and constrain ages of its construction, usage, and abandonment/disrepair (Figure 8).

As described above, the bottom part of section HC-1, composed of fine compacted sediment including boulders and cobbles with no preferred orientation, is identified as the alluvial deposits that pre-date the construction of the water reservoir. This deposit is represented by OSL sample GI195 that yields an age of 1.30 ± 0.09 ka. The D_e distribution of this sample is relatively narrow (relative standard deviation: 8%; overdispersion: 7%) and not significantly skewed, indicating complete removal of the OSL signal during sediment deposition. Thus, the yielded age reflects the last deposition of alluvium in the wadi before the water reservoir was constructed. This indicates a range between ca. 600 and 800 C.E., when the installation had not been constructed yet (Figure 8). One immediate conclusion is that the reservoir is not connected to the two nearby settlements — the Iron IIA site of Atar Haroa (10th–9th centuries B.C.E.) and the Persian period "fortress" (5th–4th centuries B.C.E.).

OSL sample GI196 is from the lowest part of the hill-like massive sediments with gently sloping stony layers that form the lower part of the spoil pile, interpreted as representing the construction of the reservoir. It yielded an age of 1.02 ± 0.07 ka (Figure 4). This age is younger than the age obtained in the compacted bottom alluvial deposit. Micromorphological examination of sediments associated with this sample shows that they are dominated by randomly oriented marl fragments, supporting the stratigraphic interpretation that this deposit reflects the spoil material due to reservoir construction. In addition, micromorphology shows no indication of post-depositional bioturbation in this unit, as the microstructure is compact and no organic components have been identified. This sample (GI196), representing the lowermost part of the spoil pile, is dated between 900 and 1,100 C.E. This allows to fix the date of construction of the reservoir between samples GI195 and GI196, at 600 to 1,100 C.E. (maximal range), or 800 to 900 C.E. (minimal range; Figure 8).

Sediments representing further construction in terms of deepening the reservoir and/or usage have been sampled further up the spoil pile's profile, still associated with massive but slightly bedded sediments, yielding the ages, 0.72 ± 0.06 ka, 0.55 ± 0.07 ka, and 0.63 ± 0.05 ka (samples GI197, GI204, and GI205, respectively). OSL samples GI198 and GI206 are associated with loose, finely bedded, and steeply inclined sediments. Micromorphology shows that this loosely packed material includes not only marl fragments, but also randomly oriented fragments of water-lain sediments — direct evidence for sediment originating from reservoir cleanup activities. The ages obtained from samples GI198 and GI206 are 0.78 ± 0.08 ka and 0.66 ± 0.08 ka.

TABLE 1 Sample ID, K-, Th-, and U-content, cosmic dose rate, and the resulting dose rate (Ḋ).

Sample ID	K [%]	Th [ppm]	U [ppm]	Cosmic dose rate [Gy/ka]	Ḋ [Gy/ka]
HC-1					
GI195	0.31 ± 0.02	2.33 ± 0.79	4.83 ± 0.25	0.16 ± 0.02	1.67 ± 0.10
GI196	0.33 ± 0.02	2.08 ± 0.79	5.18 ± 0.25	0.17 ± 0.02	1.77 ± 0.11
GI197	0.27 ± 0.01	2.99 ± 0.89	5.04 ± 0.28	0.19 ± 0.02	1.75 ± 0.11
GI198	0.28 ± 0.01	2.26 ± 0.89	5.78 ± 0.28	0.20 ± 0.02	1.91 ± 0.12
HC-2					
GI199	0.26 ± 0.01	1.92 ± 0.66	4.97 ± 0.21	0.21 ± 0.03	1.51 ± 0.14
GI200	0.32 ± 0.02	1.00 ± 0.71	5.37 ± 0.23	0.21 ± 0.03	1.59 ± 0.14
GI201	0.54 ± 0.03	3.96 ± 0.65	4.68 ± 0.21	0.22 ± 0.03	1.80 ± 0.16
GI202	0.45 ± 0.02	2.56 ± 0.80	5.79 ± 0.25	0.22 ± 0.03	1.88 ± 0.17
GI203	0.40 ± 0.02	2.04 ± 0.71	5.14 ± 0.22	0.22 ± 0.03	1.68 ± 0.15
HC-3					
GI204	0.20 ± 0.01	1.20 ± 0.61	4.96 ± 0.20	0.19 ± 0.02	1.55 ± 0.09
GI205	0.22 ± 0.01	1.49 ± 0.70	5.63 ± 0.21	0.20 ± 0.02	1.75 ± 0.10
GI206	0.34 ± 0.02	1.78 ± 0.74	5.74 ± 0.23	0.21 ± 0.03	1.91 ± 0.11

TABLE 2 Sample ID, sampling depth, equivalent dose (D_e), overdispersion, relative standard deviation, used age model, and the resulting OSL age.

Sample ID	Depth [cm]	D_e [Gy]	Overdispersion [%]	Relative standard deviation [%]	Age model	Age [ka]
HC-1						
GI195	228	2.17 ± 0.07	7	8	CAM	1.30 ± 0.09
GI196	180	1.80 ± 0.06	7	9	CAM	1.02 ± 0.07
GI197	117	1.27 ± 0.07	22	22	CAM	0.72 ± 0.06
GI198	73	1.49 ± 0.13	18	21	MAM	0.78 ± 0.08
HC-2						
GI199	105	0.87 ± 0.07	37	36	CAM	0.57 ± 0.07
GI200	74	0.57 ± 0.04	38	36	CAM	0.36 ± 0.04
GI201	45	0.40 ± 0.07	70	99	MAM	0.22 ± 0.04
GI202	25	0.26 ± 0.07	75	93	MAM	0.14 ± 0.04
GI203[a]	18					
HC-3						
GI204	121	0.86 ± 0.10	22	25	MAM	0.55 ± 0.07
GI205	83	1.09 ± 0.05	16	17	CAM	0.63 ± 0.05
GI206	45	1.26 ± 0.13	33	34	CAM	0.66 ± 0.08

CAM, central age model; MAM, minimum age model.
[a] All aliquots were rejected.

Taken together, the five samples in the middle and upper parts of the spoil pile, reflecting reservoir usage and maintenance operations with a possible deepening of the reservoir, span 1,100 to 1,500 C.E. Overall, use and maintenance of the water reservoir span several hundred years, between 900 to 1,500 C.E. (maximal range) or 1,100 to 1,400 (minimal range; possibilities calculated according to GI196 vs. GI204).

The ages obtained along section HC-1 are chronologically ordered, whereas those from section HC-3 are similar to one another within their errors. This may suggest that spoil of construction and maintenance debris may have shifted positions across the spoil pile after their deposition. Human trampling may have obliterated sequential activity surfaces resulting in the massive appearance of the sediments, whereas spoil of maintenance debris at the edge of the spoil pile preserved bedding as it was close to the steep edge where human traffic was milder.

The section studied within the water reservoir (HC-2) did probably not reach the bottom of the installation. The lowermost OSL sample of this section (GI199) dated back to 0.57 ± 0.07 ka, which is within the range of the later ages obtained in the spoil pile, associated with

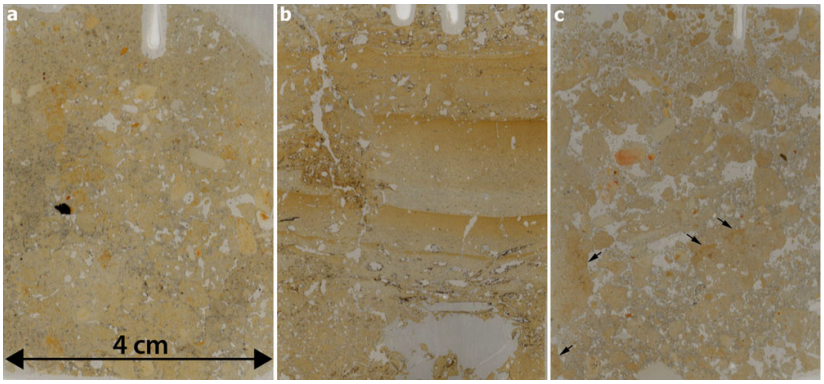


FIGURE 7 Flatbed scans of representative micromorphological thin sections. All scans are 4.1 × 5.7 cm. (a) Top part of HC-1-180 showing marl fragments within a compacted fine-grained deposit. Random orientations of the marl fragments indicate debris spoil. (b) Middle part of HC-2-45, within the reservoir, showing laminated crusts typified by graded bedding, chambers, and vesicles with black organic matter remains, some of them cross-cut crusts, indicating that bioturbation is later than the crust formation. (c) Top part of HC-3-45, from the finely bedded maintenance spoil. Note the porous nature of this deposit, with marl fragments and fragments of water-lain crusts (arrows) positioned at various orientations. [Color figure can be viewed at wileyonlinelibrary.com]

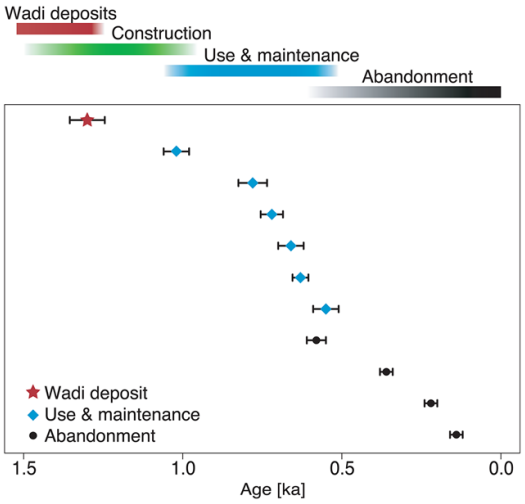


FIGURE 8 Summary of age range of the OSL samples, indicating pre-construction wadi deposits, construction, use, maintenance, and probable abandonment of the reservoir. [Color figure can be viewed at wileyonlinelibrary.com]

reservoir maintenance. Yet, the age of the last maintenance of the reservoir does not indicate abandonment, because even without removing the sediment refill, the installation can be used to store (lower amounts of) water. Therefore, the time span between the last maintenance and actual abandonment cannot be securely determined.

The 110 cm thick sediment accumulation within the reservoir took place during the last 600 years (samples GI199–GI202; Figure 4). The lower part of section HC-2 is characterized by the occurrence of cobbles and boulders, originating either from the collapsed walls of the reservoir or from debris moved into it from the slope. In the middle part of the section a distinctive, fine lamination of lighter and darker sediments, as well as characteristics of water-lain sediments are recognized by micromophological analyses, indicating gentle, episodic accumulation of sediments related to rain events. The upper part of section HC-2 consists of unstratified sediment and several sandy lenses and layers, which may indicate accumulation due to heavy precipitation events. Despite bioturbation along the section, OSL age determination of sample GI202 (0.14 ± 0.04 ka) allowed the nearly complete dating of the refill process during the last two centuries, establishing a 600 years chronostratigraphy of the sediment accumulation within the reservoir.

Organic matter found in section HC-2 was not used for radiocarbon dating. According to micromorphological observations, the origin of this organic material is from modern burrowing activity. Radiocarbon dating of this material would result in modern ages throughout the 110 cm thick accumulation within the reservoir, reflecting the age of the present vegetation, whereas the OSL ages represent the time of deposition of the sediments.

5.2 | Archaeological and historical implications

The open, stone-lined water reservoirs in the Negev Highlands have traditionally been associated with the wave of activity in the region in the Iron Age IIA (e.g., Cohen & Cohen-Amin, 2004; Evenari et al., 1958; Haiman, 1991; Lender, 1990). This settlement phase is now dated to the late 10th and mainly 9th century B.C.E. (Boaretto et al., 2010). The attribution of stone-lined open reservoirs to the Iron Age IIA was based on their proximity to Iron Age enclosed settlements such as Atar Haroa, and on the assumption that the water installations in the Negev represent a linear technological development from less (open reservoirs) to more sophisticated (rock-cut cisterns) solutions. The results of the present work on the water reservoir near Atar Haroa negate both assumptions. Based on OSL age constraints, the reservoir was dug and lined with stones between 600 to 1,100 C.E. (maximal range) or 800 to 900 C.E. (minimal range) — about 1,500 years later

than the nearby Iron Age site and about 1,000 years later than the Persian period "fortress."

In historical terms the construction of the studied reservoir took place during the strong settlement activity in the Negev Highlands in the Byzantine and Early Islamic periods (Avni, 1996; Rubin, 1990) or after the decline of this settlement system. The main period of use of this reservoir can be estimated between 900 and 1,500 C.E. (maximal range) or 1,100 to 1,400 C.E. (minimal range).

A stone-lined open reservoir with a volume of 300 m^3 to 600 m^3 can be used to water either herds or a restricted-in-size fruit plot (for the latter see, e.g., Rubin, 1990). In the case of the studied reservoir no evidence for such a plot (fences and a farmhouse) exists, so it is evident that the installation was used in order to water herds. This means that even if the reservoir was dug still in the period of prosperity in the Negev, which included strong agricultural activity, it must have served herders who were active out of the main large settlements (for pastoralism in this period, see Avni, 1996; Rosen, 1987a).

The date of decline and termination of the Byzantine–Early Islamic settlement system in the Negev Highlands is disputed — the 7th century C.E. (with the Arab conquest — recently Tepper, Erickson-Gini, Farhi, & Bar-Oz, 2018), a while later in the 8th century (Haiman, 1995), or still later in the 9th century (Avni, 2008). A recent OSL dating study of terraces in the region seems to point to the 10th or 11th century C.E. as providing the latest evidence for terrace agriculture in the region (Avni et al., 2012). Whether the studied reservoir was built before or after the end of permanent settlement activity in the region, the results of this work, though based on a single reservoir, indicate that presence of pastoral nomads in the region continued well after the latest possible date of termination of the Negev settlement system. It would be tempting to associate the decline of the Negev agriculture with the dry-period event in the Near East in the 11th century C.E. (Avni et al., 2012; for the textual data, see Ellenblum, 2012). The current study shows that had this been the case, pastoral subsistence — to differ from agriculture — continued for centuries after this datum.

The results of this work have broader archaeological and historical implications:

1. Until recent years the nature of settlement oscillations in the Negev Highlands has been debated, mainly regarding periods with no evidence for settlement activity (Finkelstein, 1995; Rosen, 1987b). Almost no sites representing most of the time range of activity in the studied reservoir are known in the Negev Highlands, meaning that pastoral nomads who did not leave behind permanent habitation remains were active here during this time span. Indeed, evidence has accumulated that pastoral nomads were also present in the Negev Highlands in other periods with no evidence for permanent settlement activity. This is also demonstrated in dung remains in shelters for herds (Rosen et al., 2005) and in radiocarbon age determinations, which fall in periods with no substantial remains (Avner & Carmi, 2001). It seems that the exceptions (rather than the rule) are periods in which the groups who lived in the region left significant settlement remains (for explanation of the subsistence economy of these periods, see, e.g., Shahack-Gross & Finkelstein, 2015).
2. More evidence is needed in order to determine whether the entire phenomenon of open water reservoirs in the Negev Highlands dates as late as the studied installation. If this is the case, and assuming that the rock-cut subterranean cisterns indeed date to the Roman—Byzantine periods, the inhabitants of the Early Bronze, Intermediate Bronze, and Iron IIA sites in the region managed to get their water needs from a small number of springs and wells, sometime located far from the sites, supplemented by seasonal water accumulation in natural bedrock depressions in the region's wadi beds.
3. Our results raise the possibility that the theory regarding the development of water installations in the Negev Highlands should be reconsidered: The elaborate rock-cut cisterns were dug in the Roman–Byzantine and possibly at the beginning of Early Islamic periods by (at least local) central authorities. In the centuries following the decline of permanent settlement activity in the region, and with possible expansion of pastoral nomadism, local groups, who were aware of the existence of cisterns (and probably used water that continued to accumulate in them) added in fact less "sophisticated" open water reservoirs.

6 | CONCLUSION

The study presented here demonstrates that sediments associated with water reservoirs in the Negev Highlands are suitable for OSL dating. The coarse-grain quartz fraction showed promising luminescence properties allowing a reliable age determination. Correlation of the resulting OSL ages with the different modes of sediment deposition in the spoil pile associated with the reservoir and inside the reservoir, supported by micromorphology, allowed the construction of the structure to be dated between the Late Byzantine and Early Islamic periods and usage in medieval times. This implies not only that the water reservoir next to Atar Haroa is not related to the Iron Age or Persian sites in its proximity, but that it was primarily utilized by pastoral nomads during medieval times, when there is no evidence for permanent settlements in the region. Open stone-lined reservoirs could have been constructed over many centuries; data for more reservoirs are necessary in order to provide a definite answer regarding the history of this phenomenon.

ACKNOWLEDGMENTS

This research was supported by a Grant (No. I-1244-107.4/2014 to R.S.-G. and M.F. as principal investigators and I.F. as coinvestigator) from the GIF, the German-Israeli Foundation for Scientific Research and Development. We would like to thank Manfred Fischer from the Bayreuth University for U and Th measurements. The anonymous reviewers and editors are thanked for the very useful and constructive comments.

ORCID

Andrea Junge http://orcid.org/0000-0003-4779-1199

Ruth Shahack-Gross http://orcid.org/0000-0001-8085-9381

REFERENCES

Arnold, L. J., Roberts, R. G., Galbraith, R. F., & DeLong, S. B. (2009). A revised burial dose estimation procedure for optical dating of young and modern-age sediments. *Quaternary Geochronology*, *4*, 306–325.

Avner, U., & Carmi, I. (2001). Settlement patterns in the Southern Levant Deserts during the 6th-3rd millennia BC: A revision based on ^{14}C dating. *Radiocarbon*, *43*, 1203–1216.

Avni, G. (1996). *Nomads, farmers and town dwellers: Pastoralist-sedentism interaction in the Negev Highlands, sixth-eighth centuries CE*. Jerusalem, Israel: Israel Antiquities Authority.

Avni, G. (2008). The Byzantine-Islamic transition in the Negev: An archaeological perspective. *Jerusalem Studies in Arabic and Islam*, *35*, 1–26.

Avni, Y., Porat, N., & Avni, G. (2012). Pre-farming environment and OSL chronology in the Negev Highlands, Israel. *Journal of Arid Environments*, *86*, 12–27.

Avni, G., Porat, N., & Avni, Y. (2013). Byzantine—Early Islamic agricultural systems in the Negev Highlands: Stages of development as interpreted through OSL dating. *Journal of Field Archaeology*, *38*(4), 332–346.

Avni, Y., Porat, N., Plakht, J., & Avni, G. (2006). Geomorphic changes leading to natural desertification versus anthropogenic land conservation in an arid environment, the Negev Highlands, Israel. *Geomorphology*, *82*(3–4), 177–200.

Avni, Y., & Weiler, N. (2013). *Geological map of Israel 1:50,000: Sede Boqer sheet 18-IV*. Jerusalem, Israel: Ministry of Energy and Water Resources, Earth and Marine Research Administration, Geological Survey.

Bailey, R. M., & Arnold, L. J. (2006). Statistical modelling of single grain quartz D_e distributions and an assessment of procedures for estimating burial dose. *Quaternary Science Reviews*, *25*(19–20), 2475–2502.

Bar-Matthews, M., & Ayalon, A. (2004). Speleothems as palaeoclimate indicators, a case study from Soreq Cave located in the eastern Mediterranean region, Israel. In R. W. Battarbee, F. Gasse, & C. E. Stickley (Eds.), *Past climate variability through Europe and Africa* (pp. 363–391). Dordrecht, the Netherlands: Springer.

Bar-Matthews, M., Ayalon, A., Gilmour, M., Matthews, A., & Hawkesworth, C. J. (2003). Sea–land oxygen isotopic relationships from planktonic Foraminifera and speleothems in the Eastern Mediterranean region and their implication for paleorainfall during interglacial intervals. *Geochimica et Cosmochimica Acta*, *67*(17), 3181–3199.

Bateman, M. D., Boulter, C. H., Carr, A. S., Frederick, C. D., Peter, D., & Wilder, M. (2007). Detecting post-depositional sediment disturbance in sandy deposits using optical luminescence. *Quaternary Geochronology*, *2*, 57–64.

Boaretto, E., Finkelstein, I., & Shahack-Gross, R. (2010). Radiocarbon results from the Iron IIA site of Atar Haroa in the Negev Highlands and their archaeological and historical implications. *Radiocarbon*, *52*, 1–12.

Bookman, R., Enzel, Y., Agnon, A., & Stein, M. (2004). Late Holocene lake levels of the Dead Sea. *Bulletin of the Geological Society of America*, *116*, 555–571.

Bruins, H. J. (1986). *Desert environment and agriculture in the Central Negev and Kadesh Barnea during historical times* (Published PhD dissertation). University of Wageningen, Wageningen, the Netherlands; Stichting Midbar Foundation, Nijkerk, the Netherlands.

Bruins, H. J. (2012). Ancient desert agriculture in the Negev and climate-zone boundary changes during average, wet and drought years. *Journal of Arid Environments*, *86*, 28–42.

Cohen, R. (1970). Atar Haroa. *Atiqot*, *6*, 6–24 (in Hebrew).

Cohen, R., & Cohen-Amin, R. (2004). *Ancient settlement of the Negev Highlands: The Iron Age and the Persian period* (Vol. *II*, in Hebrew). Jerusalem, Israel: Israel Antiquities Authority.

Crouvi, O., Amit, R., Enzel, Y., Porat, N., & Sandler, A. (2008). Sand dunes as a major proximal dust source for Late Pleistocene loess in the Negev Desert, Israel. *Quaternary Research*, *70*(2), 275–282.

Cunningham, A. C., & Wallinga, J. (2012). Realizing the potential of fluvial archives using robust OSL chronologies. *Quaternary Geochronology*, *12*, 98–106.

Ellenblum, R. (2012). *The collapse of the Eastern Mediterranean: Climate change and the decline of the East, 950–1072*. Cambridge, England: Cambridge University Press.

Evenari, M., Aharoni, Y., Shanan, L., & Tadmor, N. H. (1958). The ancient desert agriculture of the Negev: III. Early beginnings. *Israel Exploration Journal*, *8*(4), 231–268.

Evenari, M., Shanan, L., & Tadmor, N. (1982). *The Negev: The challenge of a desert* (2nd ed.). Cambridge, MA: Harvard University Press.

Finkelstein, I. (1995). *Living on the fringe: The archaeology and history of the Negev, Sinai and neighboring regions in the Bronze and Iron Ages*. Sheffield, England: Sheffield Academic Press.

Finkelstein, I., & Piasetzky, E. (2010). Radiocarbon dating the Iron Age in the Levant: A Bayesian model for six ceramic phases and six transitions. *Antiquity*, *84*(324), 374–385.

Finné, M., Holmgren, K., Sundqvist, H. S., Weiberg, E., & Lindblom, M. (2011). Climate in the eastern Mediterranean, and adjacent regions, during the past 6000 years—A review. *Journal of Archaeological Science*, *38*(12), 3153–3173.

Fuchs, M., & Wagner, G. A. (2003). Recognition of insufficient bleaching by small aliquots of quartz for reconstructing soil erosion in Greece. *Quaternary Science Reviews*, *22*(10–13), 1161–1167.

Galbraith, R. F., Roberts, R. G., Laslett, G. M., Yoshide, H., & Olley, J. M. (1999). Optical dating of single and multiple grains of quartz from Jinmium Rock Shelter, Northern Australia: Part I, experimental design and statistical models. *Archaeometry*, *41*(2), 339–364.

Goldreich, Y. (2003). *The climate of Israel: Observation, research and application*. New York, NY: Kluwer Academic/Plenum Publishers.

Guérin, G., Mercier, N., & Adamiec, G. (2011). Dose-rate conversion factors: Update. *Ancient TL*, *29*, 5–8.

Haiman, M. (1991). *Archaeological survey of Israel, map of Mizpe Ramon Southwest (200)*. Jerusalem, Israel: Israel Antiquities Authority.

Haiman, M. (1995). Agriculture and nomad-state relations in the Byzantine and Early Islamic periods. *Bulletin of the American Schools of Oriental Research*, *297*, 29–53.

Heim, C., Nowaczyk, N. R., Negendank, J. F. W., Leroy, S. A. G., & Ben-Avraham, Z. (1997). Near East desertification: Evidence from the Dead Sea. *Naturwissenschaften*, *84*, 398–401.

Huntley, D. J., Godfrey-Smith, D. I., & Haskell, E. H. (1991). Light-induced emission spectra from some quartz and feldspars. *International Journal of Radiation Applications and Instrumentation. Part D. Nuclear Tracks and Radiation Measurements*, *18*(1–2), 127–131.

Itzhaki, Y. (1971). The geological history of the Negev. In M. Evenari, L. Shanan, & N. H. Tadmor (Eds.), *The Negev, the challenge of a desert*. Cambridge, MA: Harvard University Press.

Junge, A., Lomax, J., Shahack-Gross, R., Dunseth, Z. C., Finkelstein, I., & Fuchs, M. (2016). OSL age determination of archaeological structures using trapped aeolian sediments: A case study from the Negev Highlands, Israel. *Geoarchaeology*, *31*, 550–563.

Kafle, H. K., & Bruins, H. J. (2009). Climatic trends in Israel 1970–2002: Warmer and increasing aridity inland. *Climatic Change*, *96*(1–2), 63–77.

Kagan, E. J., Langgut, D., Boaretto, E., Neumann, H. F., & Stein, M. (2015). Dead Sea levels during the Bronze and Iron ages. *Radiocarbon*, *57*(2), 237–252.

Kidron, G. J. (1999). Altitude dependent dew and fog in the Negev Desert, Israel. *Agricultural and Forest Meteorology*, *96*(1–3), 1–8.

Kraushaar, S., Ollesch, G., Siebert, C., Vogel, H.-J., & Fuchs, M. (2015). Long-term sediment export estimates from Northern Jordan using Roman cisterns as sediment traps. *Geoarchaeology*, *30*, 369–378.

Kreutzer, S., Dietze, M., Burow, C., Fuchs, M. C., Schmidt, C., Fischer, M., & Friedrich, J. (2017). *Luminescence: Comprehensive luminescence dating data analysis. R package version 0.7.3*. Retrieved from https://CRAN.R-project.org/package=Luminescence.

Langgut, D., Neumann, F. H., Stein, M., Wagner, A., Kagan, E. J., Boaretto, E., & Finkelstein, I. (2014). Dead Sea pollen record and history of human activity in the Judean Highlands (Israel) from the intermediate Bronze into the Iron Ages (~2500–500 BCE). *Palynology*, *38*, 1–23.

Lender, Y. (1990). *Archaeological survey of Israel, map of Har Nafha (196)*. Jerusalem, Israel: Israel Antiquities Authority.

Lichtenberger, A., Lindroos, A., Raja, R., & Heinemeier, J. (2015). Radiocarbon analysis of mortar from Roman and Byzantine water management installations in the Northwest Quarter of Jerash, Jordan. *JASREP*, *2*, 114–127.

Litt, T., Ohlwein, C., Neumann, F. H., Hense, A., & Stein, M. (2012). Holocene climate variability in the Levant from the Dead Sea pollen record. *Quaternary Science Reviews*, *49*, 95–105.

Lomax, J., Kreutzer, S., & Fuchs, M. (2014). Performance tests using the Lexsyg luminescence reader. *Geochronometria*, *41*(4), 327–333.

Lomax, J., Mittelstraß, D., Kreutzer, S., & Fuchs, M. (2015). OSL, TL and IRSL emission spectra of sedimentary quartz and feldspar samples. *Radiation Measurements*, *81*, 251–256.

Mejdahl, V. (1979). Thermoluminescence dating: Beta-dose attenuation in quartz grains. *Archaeometry*, *21*, 61–72.

Migowski, C., Stein, M., Prasad, S., Negendank, J. F., & Agnon, A. (2006). Holocene climate variability and cultural evolution in the Near East from the Dead Sea sedimentary record. *Quaternary Research*, *66*(3), 421–431.

Murray, A. S., & Wintle, A. G. (2000). Luminescence dating of quartz using an improved single-aliquot regenerative-dose protocol. *Radiation Measurements*, *32*(1), 57–73.

Neumann, F. H., Kagan, E. J., Leroy, S. A. G., & Baruch, U. (2010). Vegetation history and climate fluctuations on a transect along the Dead Sea west shore and their impact on past societies over the last 3500 years. *Journal of Arid Environments*, *74*, 756–764.

Orland, I. J., Bar-Matthews, M., Kita, N. T., Ayalon, A., Matthews, A., & Valley, J. W. (2009). Climate deterioration in the Eastern Mediterranean as revealed by ion microprobe analysis of a speleothem that grew from 2.2 to 0.9 ka in Soreq Cave, Israel. *Quaternary Research*, *71*, 27–35.

Prescott, J. R., & Hutton, J. T. (1994). Cosmic ray contributions to dose rates for luminescence and ESR dating: Large depths and long-term time variations. *Radiation Measurements*, *23*(2-3), 497–500.

Rosen, S. A. (1987a). Byzantine nomadism in the Negev: Results from the emergency survey. *Journal of Field Archaeology*, *14*, 29–42.

Rosen, S. A. (1987b). Demographic trends in the Negev Highlands: Preliminary results of the emergency survey. *Bulletin of the American Schools of Oriental Research*, *266*, 45–58.

Rosen, S. A., Savinetsky, A. B., Plakht, Y., Kisseleva, N. K., Khassanov, B. F., Pereladov, A. M., & Haiman, M. (2005). Dung in the desert: Preliminary results of the Negev Holocene ecology project. *Current Anthropology*, *46*, 317–327.

Roskin, J., Tsoar, H., Porat, N., & Blumberg, D. G. (2011). Palaeoclimate interpretations of Late Pleistocene vegetated linear dune mobilization episodes: Evidence from the northwestern Negev dunefield, Israel. *Quaternary Science Reviews*, *30*(23–24), 3364–3380.

Rubin, R. (1988). Water conservation methods in Israel's Negev desert in late antiquity. *Journal of Historical Geography*, *14*, 229–244.

Rubin, R. (1990). *The Negev as a settled land: Urbanization and settlement in the desert in the Byzantine period*. Jerusalem, Israel: Yad Izhak Ben-Zvi.

Shahack-Gross, R., & Finkelstein, I. (2008). Subsistence practices in an arid environment: A geoarchaeological investigation in an Iron Age site, the Negev Highlands, Israel. *Journal of Archaeological Science*, *35*, 965–982.

Shahack-Gross, R., Boaretto, E., Cabanes, D., Katz, O., & Finkelstein, I. (2014). Subsistence economy in the Negev Highlands: The Iron Age and the Byzantine/Early Islamic period. *Levant*, *46*, 98–117.

Shahack-Gross, R., & Finkelstein, I. (2015). The Settlement Oscillations in the Negev Highlands Revisited: The Impact of Micro-archaeological Methods. *Radiocarbon*, *57*, 253–264.

Shanan, L. (2000). Runoff, erosion, and the sustainability of ancient irrigation systems in the Central Negev Desert. In M. A. Hassan & O. Slaymaker (Eds.), *The hydrology-geomorphology interface: Rainfall, floods, sedimentation, land use* (pp. 75–106). Jerusalem, Israel: IAHS Publications.

Stoops, G. (2003). *Guidelines for analysis and description of soil and regolith thin sections*. Madison, WI: Soil Science Society of America.

Survey of Israel. (2007). *Mapping and GIS*. Retrieved from https://www.govmap.gov.il

Tepper, Y., Erickson-Gini, T., Farhi, Y., & Bar Oz, G. (2018). Probing the Byzantine/Early Islamic transition in the Negev: the renewed Shivta excavations, 2015–2016. *Tel Aviv*, *45*, 120–152.

How to cite this article: Junge A, Lomax J, Shahack-Gross R, Finkelstein I, Fuchs M. Chronology of an ancient water reservoir and the history of human activity in the Negev Highlands, Israel. *Geoarchaeology*. 2018;, 1–13. https://doi.org/10.1002/gea.21682

Second Study

Construction and use of rock-cut cisterns: a chronological OSL approach in the arid Negev Highlands, Israel

Andrea Junge, Zachary C. Dunseth, Ruth Shahack-Gross,
Israel Finkelstein, & Markus Fuchs

Archaeological and Anthropological Sciences, 13, Article number 150, 2021

Manuscript Received: 1^{st} February 2021
Manuscript Accepted: 20^{th} May 2021
Published: 17^{th} August 2021

Archaeological and Anthropological Sciences (2021) 13: 150
https://doi.org/10.1007/s12520-021-01366-5

ORIGINAL PAPER

Construction and use of rock-cut cisterns: a chronological OSL approach in the arid Negev Highlands, Israel

Andrea Junge[1] · Zachary C. Dunseth[2] · Ruth Shahack-Gross[3] · Israel Finkelstein[4] · Markus Fuchs[1]

Received: 1 February 2021 / Accepted: 20 May 2021 / Published online: 17 August 2021
© The Author(s) 2021

Abstract
The Negev Highlands (Israel) are characterized by a rich settlement history over the last millennia. To sustain life in this arid environment, measures to collect and store water were introduced. Two types of installations to collect and store runoff water were built in the region: open reservoirs, and more elaborate subterranean rock-cut cisterns. This article focuses on the latter. Based on a few inscriptions found in rock-cut cisterns, it is assumed that the majority were constructed in the Hellenistic (Nabatean) to Byzantine period. To evaluate this age assessment, this study was carried out at the Borot Hazaz cisterns system, using optically stimulated luminescence (OSL) dating together with micromorphological analyses. Both were applied to sediments that were relocated during the cistern's construction and usage and after the maintenance activities ended. Despite unfavourable conditions for resetting the OSL signal, including fluvial transport over short distances and sediment deposition by humans in large quantities, it was possible to reconstruct the life cycle of the cistern system. The present study places the construction of the system during the late Roman to Byzantine period, with utilization and long-term maintenance during the following centuries. Maintenance ceased at the Borot Hazaz cistern system gradually over the course of the last 500 years.

Keywords Arid environment · Water harvesting · Optically stimulated luminescence · Byzantine Period · Early Islamic Period

Introduction

The arid Negev Highlands in southern Israel feature stone-built archaeological evidence for human activity in several periods—the Early Bronze and Intermediate Bronze Ages (ca. 3500–2000 BCE), the late Iron I–Iron IIA (ca. 1000–800 BCE) and the Hellenistic-Roman-Byzantine and Early Islamic periods (ca. 200 BCE–800 CE, although in this phase both the beginning and end are disputed). Stable water sources in this region are few and their yield is rather low. Hence, during certain periods of strong human activity, hundreds of open-water reservoirs and subterranean cisterns (Fig. 1) were constructed to collect runoff water during the scarce rain events (Evenari et al. 1982; Rubin 1988).

The simpler open reservoirs (Fig. 1a) are man-made basins located along footslopes dug into soft sediments and lined with stones in order to stabilize them (Evenari et al. 1958; Rubin 1988). They have no protective roof, leading to contamination and significant water loss due to evaporation. The permeable soft sediments result in water loss through infiltration. The subterranean cisterns (Fig. 1b) are less vulnerable to pollutants, and the protective roof limits evaporation even during the hot and dry summer months. These installations were usually hewn into less-permeable solid chalk formations, and occasionally lined with plaster (Evenari et al. 1958).

In terms of construction and maintenance, the two types of water storage systems are similar. During construction,

Ruth Shahack-Gross, Israel Finkelstein, Markus Fuchs are Project directors

✉ Andrea Junge
andrea.junge@geogr.uni-giessen.de

[1] Department of Geography, Justus Liebig University Giessen, Senckenberstr. 1, 35390 Giessen, Germany

[2] Joukowsky Institute for Archaeology and the Ancient World, Brown University, Providence, RI, USA

[3] Department of Maritime Civilizations, Charney School of Marine Sciences, Recanati Institute of Maritime Studies, University of Haifa, Haifa, Israel

[4] Institute of Archaeology, Tel Aviv University, Tel Aviv, Israel



Fig. 1 Photographs of **a** the open water reservoir of Bor Hemet (16–18 m wide) and **b** cistern III of the Borot Hazaz system. Both have been maintained recently for tourism.

the excavated material (sediment or chalk) was deposited on a spoil pile close to the installation. To increase their water catchment area, dams and channels were built on the adjacent slopes to direct the surface runoff into the cistern or reservoir (Figs. 2 and 3). However, surface runoff also fed the water storage systems with sediments eroded from the catchment. While the systems were in use, these sediments needed to be occasionally removed from the installations, and were deposited on the adjacent spoil piles. With the cessation of maintenance, the reservoirs and cisterns were rapidly refilled by sediments.

While the construction and operating principles of open-water reservoirs and subterranean cisterns are similar, the chronology of the two types of installations, and the relationship between them, is not clear. Open reservoirs are traditionally dated to the Iron Age based on their proximity to sites from this period (e.g., Cohen & Cohen-Amin 2004; Evenari et al. 1958; Haiman 1991; Lender 1990). A recent study by Ore et al. (2020) showed a spatial correlation between open reservoirs and Early Bronze Age and/or Intermediate Bronze Age sites. Based on this circumstantial evidence, the authors placed the construction of open reservoirs predominantly during these periods. Focusing on sites with chronometric data, Junge et al. (2018) used optically stimulated luminescence (OSL) to determine the age of an open reservoir near the site of Atar Haroa and present a detailed history of the reservoir. Micromorphology was used to identify different modes of deposition, and consequently support the interpretation of the OSL ages. This research indicated the open reservoir was constructed in the eighth–eleventh century CE (the Early Islamic period), and continued to be utilized and maintained until the fifteenth century CE (medieval period), and subsequently infilled with sediment due to cessation of maintenance. These results showed that while the habitation site of Atar Haroa dates to the Iron Age IIA (mainly ninth century BCE; Boaretto et al. 2010), the reservoir next to it is not contemporaneous, highlighting the difficulty in determining ages of spatially close yet disconnected archaeological features.

In contrast to open-water reservoirs, the construction of rock-cut cisterns in the Negev Highlands is traditionally constrained between 200 BCE and 640 CE based on Nabatean and Byzantine inscriptions discovered on the walls of several of these installations (Rubin 1988). Tepper et al. (2020) attempted to use OSL dating to determine the age of a rock-cut cistern that is part of an agricultural system near the ancient (mainly Byzantine) village of Shivta. The spoil pile related to it was dated to the sixteenth century CE, and was interpreted as representing the maintenance of the cistern. In comparison, the shallow sediment accumulation within the cistern was dated to 60 ± 10 years old, representing the time after the last cleaning of the cistern. No spoil pile containing construction material was included in this study, and therefore the cistern's construction could not be determined by numerical dating.

To evaluate the archaeological age of the subterranean cisterns based on typology, inscriptions and artefacts, it is necessary to apply numerical dating on sediments that are not only associated with the construction of cisterns, but also with the utilization and maintenance of these installations. In the current study, OSL dating was used at the elaborate system of cisterns known as Borot Hazaz, located ca. 5 km to the northeast of Kibbutz Sede Boqer (Fig. 2). The study aims to determine sediment deposition of the following stages: (1) construction (rock-cutting), (2) maintenance and (3) cessation of maintenance of the cisterns.

To support the interpretation of the OSL results and to identify the mode of sediment deposition, detailed micromorphological analyses were conducted in tandem. A complete chronological life cycle of the Borot Hazaz cisterns is presented for the first time, and the methodological approach can be used as a general blueprint for establishing cistern chronologies.

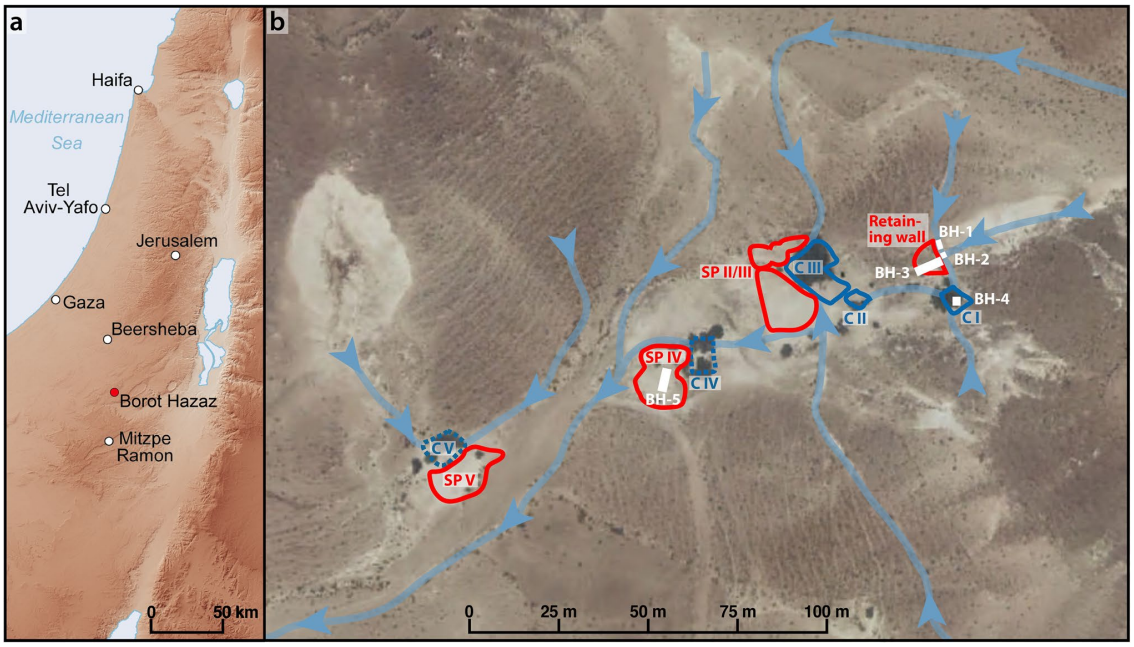


Fig. 2 **a** Map of the southern Levant with the location of the Borot Hazaz cistern system marked in comparison to modern cities, and **b** satellite image of the study area (Survey of Israel 2007). The position and layout of the cisterns are marked in dark blue (dotted lines indicate that the size of the cistern cannot be estimated due to complete infilling) and the locations of the spoil piles are marked in red. The light blue lines show the channels that conduct the water from the slopes to the cisterns, and from one overflowing cistern to the next. When the cisterns are completely filled, water exits the system following the wadi's depression line out of the system to the southwest. The arrows indicate the direction of water flow. The white boxes indicate the location of the excavated trenches.

The study area

The arid Negev Highlands are situated in the south of modern Israel, with elevations ranging between 600 m a.s.l. in the northeast and 1000 m a.s.l. in the southwest (Fig. 2a). The rolling-hill topography was formed following the uplift of the highlands and faulting processes of the Dead Sea Rift during the Late Miocene to the Early Pleistocene, resulting in a series of northeast-to-southwest-oriented anticlines and synclines (Avni et al. 2006; Itzhaki 1971). The bedrock mainly consists of Cretaceous and Eocene marine carbonates (primarily limestone, dolomite, chalk, chert and marl), traversed by wadis, which are the result of erosion processes during the Plio-Pleistocene (Avni & Weiler 2013; Bruins 1986; Starinsky et al. 2010). Aeolian sediments primarily from the Sinai and the Sahara accumulated across the Negev Highlands during the Late Pleistocene and Early Holocene (Avni et al. 2012, 2006; Crouvi et al. 2008; Roskin et al. 2011). Following this, the formation of thick alluvial deposits in the wadis was caused by erosion of aeolian fines and mixing with local sediments (Avni et al. 2013; Bowman et al. 1986; Faershtein et al. 2016). These sediments are found redeposited as the accumulations within the cisterns and channels, as well as in the maintenance accumulations on the spoil piles.

The present-day climate in the study area is characterized by mean annual air temperature between 17 and 19 °C (with temperatures in the summers up to 40 °C, and winters down 0 °C) and annual precipitation between 80 and 150 mm (Kafle & Bruins 2009). Most rainfall occurs during the winter months, roughly between October and April (Avni et al. 2006; Goldreich 2003), with strong year-to-year variations (Bruins 2012; Evenari et al. 1982; Shanan 2000). Fog and dew add to the annual precipitation an equivalent of 10 mm for each 100-m increase in elevation (Kidron 1999).

In the study area, the climate of the last 2000 years is characterized by lower precipitation at the beginning of the first millennium CE compared to the following centuries and the modern climate (Bar-Matthews & Ayalon 2004; Orland et al. 2009; Bookman et al. 2004; Neumann et al. 2010). Bar-Matthews et al. (2003) reconstructed drier conditions during most of the last two millennia, while Neumann et al. (2010) and Bookman et al. (2004) postulated strong oscillations in precipitation following an initial reduction at the beginning of the first millennium CE. Orland et al. (2009) described a second decrease in rainfall at about 400 CE,

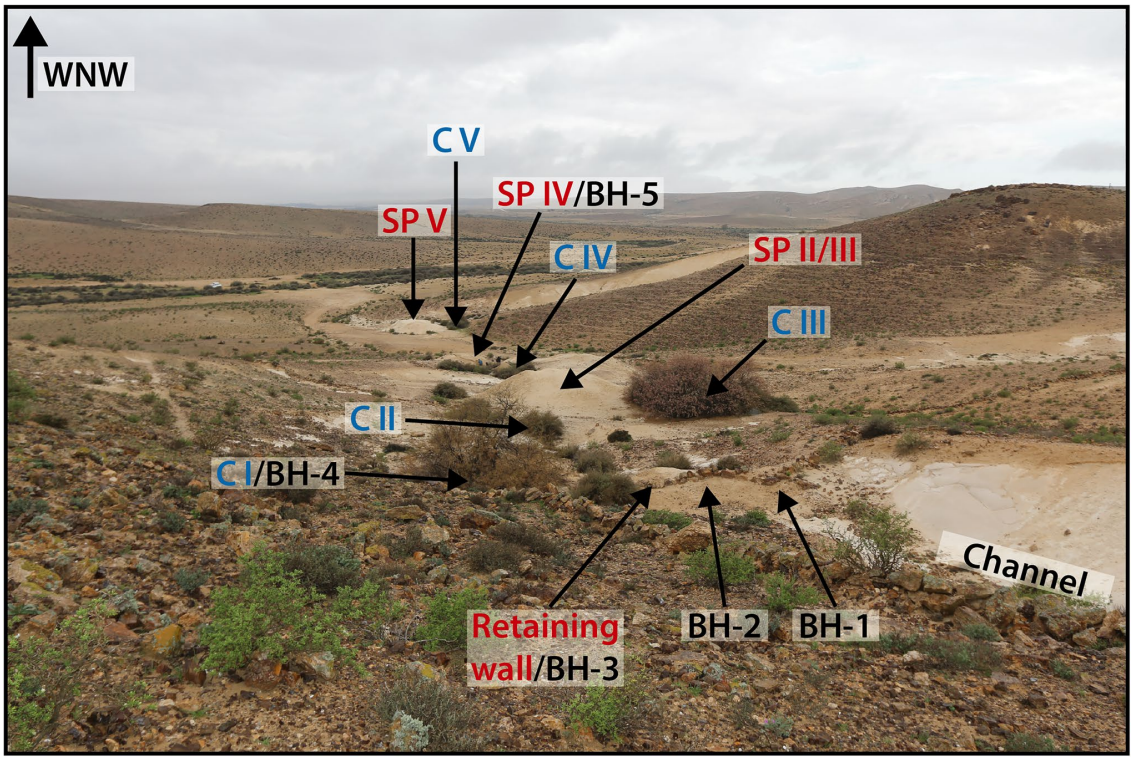


Fig. 3 Overview photograph of the Borot Hazaz cistern system. The location of the cisterns (C) I–IV are marked in blue, the spoil piles (SP) II-IV and the retaining wall of cistern I in red, and the excavated trenches BH-1 to BH-5 are marked in black.

possibly followed by further variations, which follows other palaeoclimate reconstructions presenting similar arid events between 500 and 1600 CE (Heim et al. 1997), or between 500 and 1200 CE (Migowski et al. 2006).

Although these climate reconstructions do not show a congruent picture of the changes in precipitation over the last 2000 years, they generally indicate drier or similar conditions compared to today's precipitation regime in the study area.

The cisterns system

The installations studied here belong to the water harvesting system of Borot Hazaz (cisterns), located in the northern part of the Negev Highlands (Fig. 2a) within a small wadi that drains from the northeast to southwest into Nahal Hazaz (Fig. 2b). During sufficiently strong precipitation events, the adjoining slopes to the north, east and southeast feed the cisterns with surface runoff. The system consists of five subterranean cisterns of different sizes, several channels that lead surface runoff from the slopes into the cisterns, and spoil piles with sediments from the construction and maintenance of the installations. The cisterns were dug into the soft chalk of the Menuha Formation (Avni & Weiler 2013). The arrangement of the cisterns follows the direction of the wadi from cistern I in the northeast to cistern V in the southwest (Figs. 2b and 3).

The cisterns are rectangular in shape and show no evidence for plastering, which was done in some cisterns to reduce the permeability of the chalk they are cut into. Due to its large size of ca. 15 m by 9 m, cistern III has two roof-supporting rock-cut pillars aimed to stabilize the overlying bedrock. Because cisterns I and II are only ca. 3 by 4 m, pillars did not appear to be necessary to support the roof in antiquity, although parts of the roof of cistern I have since collapsed. Cisterns IV and V are completely filled with sediments, and consequently, determining their size and shape is impossible without excavation. Since none of the cisterns was completely excavated during this study, their water capacity can only be approximated and ranges in the order of dozens of cubic metres to several hundred cubic metres.

The Borot Hazaz cistern system is described by Cohen (1981) but no excavations or detailed analyses were

conducted at that time. According to a local farmer, the largest cistern in the system (cistern III) was cleaned in the 1960s by members of a nearby kibbutz to water their flocks.

Sampling strategy

The investigations focused on cistern I along with its channel, retaining wall and its sediment fill, as well as on the spoil pile of cistern IV (Figs. 2b and 3). The time of construction, utilization and cessation of maintenance of these cisterns was determined by OSL dating of the different components of the system, while micromorphological analyses were used to identify the different modes of sediment deposition. The infill of cistern I was selected for excavation since no recent use or disturbance was visible on the surface, and because it was easily accessible.

The channel of cistern I: trench BH-1 and BH-2

The sediment accumulation in the channel leading water into cistern I was excavated and sampled in two locations (Figs. 2b and 3, BH-1 and BH-2). The base of both trenches was the chalk bedrock of the Menuha Formation (Fig. 4). The sediments exposed in these trenches were composed of layered fluvial fines and stony debris of up to 10 cm in diameter. Evidently, sedimentation within the channel took place after the last channel cleaning. To evaluate when maintenance and cleaning activities ceased, two OSL samples were taken from the section in the western trench (BH-1, Fig. 4b) and three OSL samples from the section in the eastern trench (BH-2, Fig. 4a). The samples at the base of both sections date the onset of the final sediment accumulation within the channel. The sampling of the overlying sediments was carried out to gather information about the development of sediment accumulation in the channel.

The retaining wall of cistern I: trench BH-3

A retaining wall was constructed to redirect surface runoff from the channels into cistern I (Figs. 2 and 3). It is assumed that the cistern could only be used while the retaining wall existed; otherwise, only a fraction of the available surface runoff would reach the cistern. Thus, by dating the construction of the retaining wall, a temporal connection to the cistern's construction can be established. The retaining wall was cut at some point by water overflowing from the cistern. This existing cut was trenched from the channel-facing part of the retaining wall to its lower limit (Fig. 5, BH-3). The bottom of the trench was defined by bedrock and

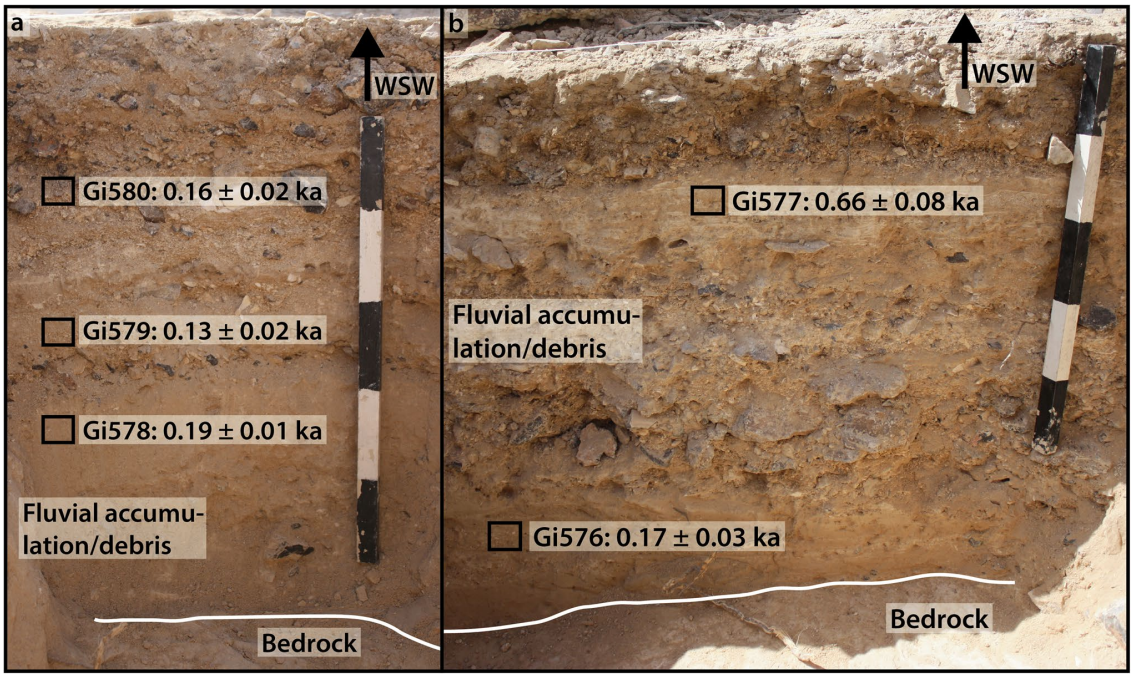


Fig. 4 Trench BH-2 (**a**) and BH-1 (**b**) showing the sediment accumulation and bedrock within the channel leading towards cistern I. Location of the OSL samples are marked by black boxes and labelled and the ages are presented. One unit of the scale bar equals 10 cm.

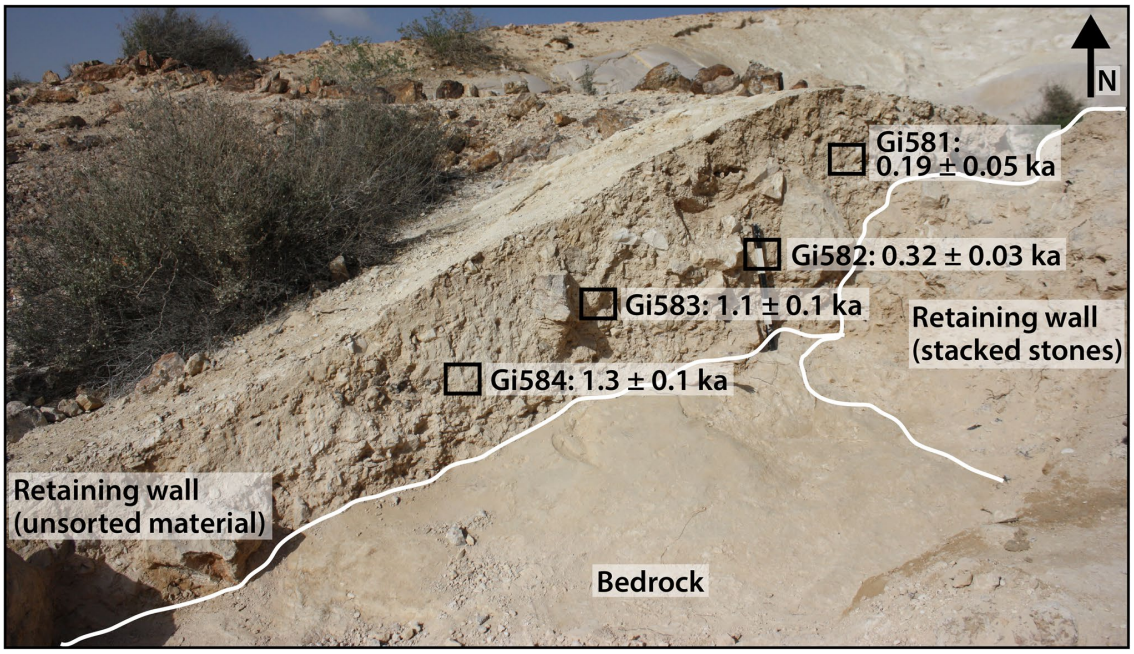


Fig. 5 Trench BH-3 cuts through the retaining wall of cistern I. Location of the OSL samples are marked by black boxes, the samples are labelled and ages presented.

the channel-facing end of the retaining wall was constructed of flat limestone slabs. On top of the stacked stones, and in the centre and lower end of the trench, sediments and stones were exposed, likely deposited to stabilize the feature. This deposit showed no layering or orientation, and consequently only one depositional event can be identified by stratigraphic evidence. To determine if more than one event was exposed, and to constrain the time of construction and possible maintenance event(s), four OSL samples were taken across the exposed section (Fig. 5).

Filling of cistern I: trench BH-4

The sediments within cistern I (Figs. 2b and 3) were interpreted as the accumulation after the last cleaning of the installation. They were composed of fluvial fines with vague layering (Fig. 6, BH-4). The trench was cut 2 m deep without reaching bedrock. The accumulation was mixed with plastic and metal trash. Three OSL samples were taken, but only the lowermost sample was prepared and measured to check the reliability of the OSL dating approach for the cistern filling, as it could be correlated with a (pre)modern enamelled metal bucket found next to the OSL sampling location. At the same depth, a micromorphology sample was taken in order to identify the mode of sediment deposition at the bottom of the trench.

The interpretation of OSL ages from cistern I is limited, because the contemporaneity of the construction of the cistern and the retaining wall is only assumed, and a spoil pile with a clear succession of construction and maintenance material was not available to sample. Therefore, the spoil pile of cistern IV (Figs. 2 and 3) of the system was added to the study.

The spoil pile of cistern IV: trench BH-5

The spoil pile of cistern IV (Figs. 2 and 3) was cut in the past by water overflow from the cistern. A four-step trench was excavated in the original centre of the spoil pile (BH-5, Fig. 7) to expose the complete stratigraphy, as well as conserve the spoil pile. The lowermost and the uppermost steps were sampled and studied in detail. At the bottom of the lower step, the chalk bedrock was exposed, overlain by unsorted alluvial sediments that accumulated before cistern IV was constructed. Above this palaeosurface, construction and maintenance material were deposited. The top step of the trench was composed of three layers of construction and maintenance material. Both steps were sampled in triplicate for OSL dating to constrain pre-construction, construction and maintenance over time. One micromorphology block encompassing the contact between the pre-construction and construction

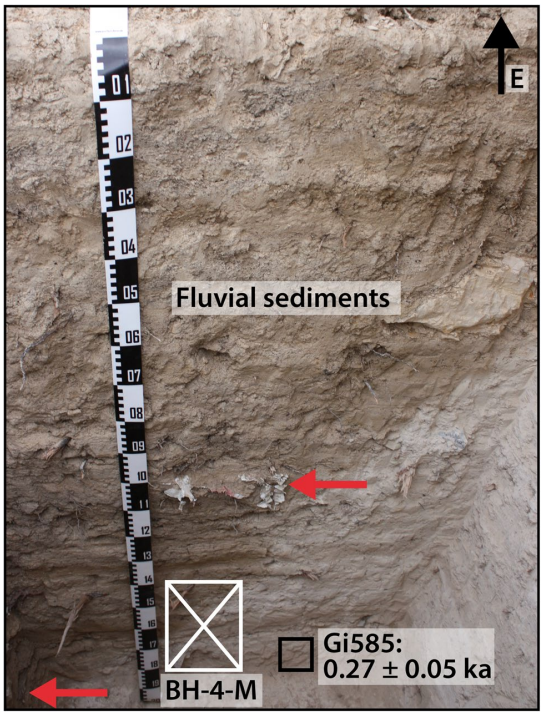


Fig. 6 Trench BH-4, situated within cistern I. Location of the OSL sample is marked by a black box, the sample number is labelled and the age presented. A micromorphology sample (BH-4-M, white box) was taken from the bottom of the eastern section. The upper arrow points at a plastic item and the lower arrow points at an enamelled metal bucket. The small graduation on the left side of the scale bar equals 1 cm, the units on the right represent 10 cm.

deposits was collected to confirm the presumed modes of deposition.

Methods

Optically stimulated luminescence dating

The majority of OSL samples were collected at night by thoroughly cleaning the sections before OSL sampling and filling the sample material directly into light-proof bags. Two of the analysed OSL samples (Gi577 and Gi585) were sampled during daytime using steel cylinders with a diameter of 5.6 cm. To determine the equivalent dose (D_e), the coarse-grain (90–200 µm) quartz fraction was prepared. First, sediment was removed from the bags or cylinders, and in the latter case the bleached material at both ends of the cylinders was discarded. The sediment was wet-sieved to separate the grain-size fractions, followed by treatment with 10% HCl and 10% H_2O_2 to dissolve carbonates and oxidize organic matter. To obtain the quartz fraction, lithium-heteropolytungstate (2.63 and 2.68 g/cm^3) was used for density separations. Next, the quartz extract was etched in 40% hydrofluoric acid (HF) for 80 min to remove the α-irradiated outer rim of the grains and to eliminate any remaining feldspar contamination. Finally, the coarse-grain quartz fraction was washed for 30 min in 10% HCl and re-sieved (63 µm) to remove small residues and remaining feldspar fragments. All sample preparation was performed under subdued amber-coloured light centred on a wavelength of 590 ± 10 nm.

The OSL measurements were executed on a Lexsyg Standard reader (Lomax et al. 2014). For stimulation, the reader was operated with green LEDs (525 ± 25 nm), whereas for signal detection, a Hamamatsu H7360 photomultiplier combined with a 5-mm Semrock HC377/50 filter and a 3-mm Schott BG3 filter was applied. This combination restricts the detection window to ca. 350–400 nm, thus is centred on the main OSL emission of quartz (Huntley et al. 1991; Lomax et al. 2015). Stimulation with infrared (IR) laser diodes (850 ± 3 nm) was used to check for the purity of the quartz extracts. Feldspar contamination was tested by applying the OSL IR depletion ratio (Duller 2003). For this test, IR signals were detected through a 3.5-mm Semrock HC414/46 interference filter in combination with a 3-mm Schott BG39 filter, which restricts the detection window to ca. 395–430 nm. Sample irradiation was performed with a calibrated 90Y/90Sr β-source (1.8 GBq), resulting in a dose rate for coarse-grain quartz on stainless steel cups of 0.119 ± 0.003 Gy/s (February 2019).

For the determination of D_e, a single-aliquot regenerative-dose (SAR) protocol was applied (after Murray and Wintle 2000, 2003). To define the dose–response curve, five or six regeneration cycles, including the zero dose and one repeated dose point, were used. The shine-down curves were measured for 50 s at elevated temperatures (125 °C) after a preheat at 180 °C (10 s) and a cut-heat at 160 °C for the natural and regenerated signals. The preheat and cut-heat temperatures were chosen after combined preheat-dose recovery tests (DRT, Fig. 8a) and preheat-plateau test (PHT, Fig. 8b) for the two samples representing construction (Gi592) and maintenance (Gi593) material. For the DRT, the samples were bleached in the Lexsyg reader using the green LEDs and irradiated with a known β-dose close to the natural dose, followed by D_e determinations using a SAR protocol. For the PHT, burial doses were also measured using the SAR protocol. Both tests were conducted at six different preheat temperatures (180–280 °C) with a cut-heat temperature 20 °C below the preheat temperature, but with a maximum at 220 °C. The tests were conducted on three fresh aliquots per temperature combination for each sample. The selection of the preheat (180 °C) and cut-heat (160 °C) temperatures used in this study is based on the successful replication of the known given dose within the 10% error range at 180 °C for

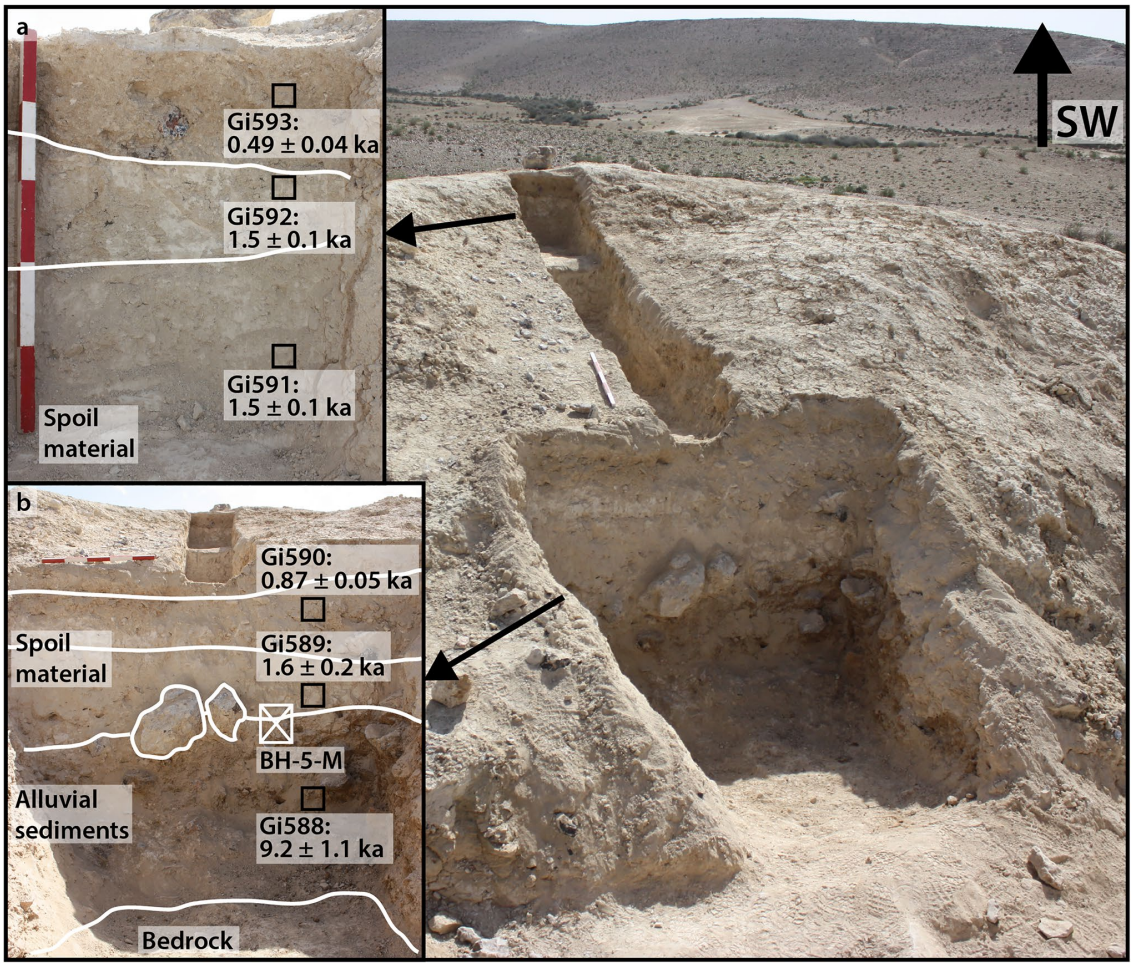


Fig. 7 Stepped trench BH-5 was cut into the spoil pile of cistern IV. The upper (a) and lower (b) steps of the trench were sampled and studied in detail. Location of the OSL samples are marked by black boxes, the samples are labelled and the ages presented. A micromorphology sample (BH-5-M, white box) included the contact between the natural alluvial deposits and cistern construction material. One unit of the scale bar equals 10 cm.

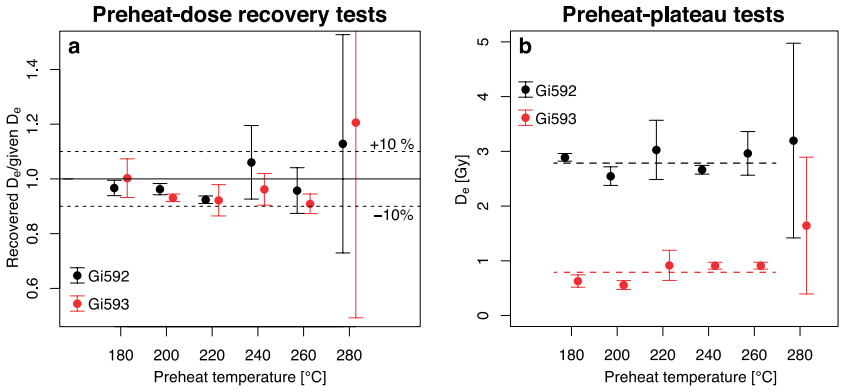


Fig. 8 Results of the dose recovery tests (**a**) and preheat plateau tests (**b**) of samples Gi592 representing the sampled construction material and Gi593 representing the maintenance and refill material at this site. For each temperature combination, the average of three measured aliquots were calculated and displayed. The given doses for the dose recovery tests were 0.9 Gy for sample Gi592 and 3.0 Gy for Gi593.

both samples using the DRT (Fig. 8a). The PHT supports this outcome by showing a preheat plateau covering the preheat temperatures from 180 to 260 °C (Fig. 8b).

For D_e calculation, the integral of the first 0.5 s of the quartz shine-down curves was used, after subtracting a background of 40 to 50 s from the signal. One- to 4-mm aliquots (30 to 500 grains; Burow 2020; Fuchs & Wagner 2003) were used for D_e determination of the coarse-grain fraction, depending on the amount of quartz material extracted and the strength of the OSL signal. In general, up to 60 aliquots were measured for each coarse-grain sample to determine the D_e. After passing the rejection criteria of 10% for the recycling ratio, the test dose error, the recuperation value and the OSL IR depletion ratio, and 15% for the palaeodose error, the mean D_e of the aliquots was calculated using the central age model after Galbraith et al. (1999) for not significantly skewed samples, and the bootstrap minimum age model (Cunningham & Wallinga 2012) for significantly skewed samples. The differentiation between skewed and un-skewed distributions is based on the comparison of the standardized values of skewness and their significance value (Bailey & Arnold 2006). The age models were calculated with log-transformed D_e values for samples with D_e values > 1 Gy (Gi584, Gi588, Gi591 and Gi592), whereas samples with measured D_e values ≤ 1 Gy (Gi576–Gi583, Gi585, Gi589, Gi590 and Gi593) were calculated based on the unlogged D_e (Arnold et al. 2009).

Radionuclide concentrations were determined by thick source α-counting (U and Th) and ICP-OES (K). To account for heterogeneous dose rate environments at the OSL sampling locations, dose rate samples were collected from the 30 cm surrounding the OSL sample, gathering material that represented the different sediments, stones and bedrock in the surroundings. The cosmic radiation dose was calculated according to Prescott and Hutton (1994). To estimate the change in attenuation of the cosmic dose rate over time, it is distinguished between a prompt and a gradual sediment accumulation: using current burial depths for the samples from the retaining wall (BH-3: Gi581–Gi584) and the spoil pile (BH-5: Gi588–Gi593), because the deposition interval of the material was relatively short and ended several centuries ago, and using half the current burial depths for the samples within the cistern (BH-4: Gi585) and within the channel (BH-1 and BH-2: Gi576–Gi580), because a relatively gradual accumulation continuing until the present day is assumed. The measured concentrations were converted to dose rates using the conversion factors of Guérin et al. (2011) and the β-attenuation factor of Mejdahl (1979). The age calculation was performed using DRAC v1.2 (Dose Rate and Age Calculator) by Durcan et al. (2015).

The water content for dose rate calculation was selected depending on which part of the cistern system the sample was collected from. The water content of the OSL sample collected within cistern I (BH-4: Gi585) was set to $15 \pm 7.5\%$. This value and its uncertainty represent the possible water content range based on the porosity of the loamy silt, the climatic conditions and the amount of water delivered by the channels from the adjacent slopes. The flood frequency in the channel is comparable to the situation inside of the cistern. However, unlike the cistern, the channel is not constructed to hold the water over longer periods of time. Taking this into account, the water content for the channel samples (BH-1 and BH-2: Gi576–Gi580) was set to $10 \pm 5\%$. For the retaining wall and spoil pile samples, a lower water content of $6 \pm 3\%$ is assumed because these structures are not fed by surface runoff from adjoining slopes, and they are better drained than both the cistern and the channel (Table 1). The actual measured water contents of the sediments after sampling confirmed the water content values utilized for the dose rate calculation. However, the water contents and their errors utilized were not solely based on the measured values, because they only represent the current hydrological conditions.

Micromorphology

The monolithic sediment blocks were extracted using plaster of Paris (gypsum) bandages. They were then dried at 50 °C for 3 days and impregnated by a 7:3 (v:v) mixture of polyester resin and acetone. A small amount of hardener (10 ml per 1 l of mixed resin) was added, without accelerator, in order to assure penetration of the resin into small pores before consolidation. After several weeks, the blocks were cured at 50 °C for 2 days and cut to the desired thin section size (5×7 cm) using a slab saw. Two thin sections, prepared by Quality Thin Sections (Arizona, USA), were yielded from each block, covering the length of the original sample. The final 30-µm thin sections were studied using a Nikon Eclipse 50i polarizing light microscope, in plane-polarized light (PPL) and crossed-polarized light (XPL) under various magnifications, and described using the conventional literature (Stoops 2003).

Results

Optically stimulated luminescence

As already shown in OSL dating studies at other archaeological sites in the Negev Highlands (e.g., Porat et al. 2006; Junge et al. 2016, 2018; Dunseth et al. 2017), the coarse-grained quartz is highly suitable for OSL dating. The quartz extract is characterized by a rapidly decaying OSL signal (Fig. 9) implying a prominent fast component of the OSL signal, resulting in bleaching even during short sunlight exposure (Bailey et al. 1997). A distinctive

Table 1 Sample ID, K-, Th- and U-content, cosmic dose rate, water content and the resulting dose rate (Ḋ).

Sample ID	K [%]	Th [ppm]	U [ppm]	Cosmic dose rate [Gy/ka]	Water content [%]	Ḋ [Gy/ka]
BH-1						
Gi576	0.43 ± 0.02	2.29 ± 0.63	5.15 ± 0.20	0.23 ± 0.02	10 ± 5	1.81 ± 0.08
Gi577	0.49 ± 0.03	1.51 ± 0.55	4.50 ± 0.18	0.28 ± 0.03	10 ± 5	1.66 ± 0.07
BH-2						
Gi578	0.34 ± 0.02	2.36 ± 0.78	6.66 ± 0.24	0.25 ± 0.03	10 ± 5	2.05 ± 0.09
Gi579	0.31 ± 0.02	1.30 ± 0.64	5.88 ± 0.20	0.26 ± 0.03	10 ± 5	1.79 ± 0.08
Gi580	0.24 ± 0.01	1.26 ± 0.49	6.17 ± 0.16	0.28 ± 0.03	10 ± 5	1.74 ± 0.07
BH-3						
Gi581	0.28 ± 0.01	1.28 ± 0.48	5.91 ± 0.15	0.23 ± 0.02	6 ± 3	1.85 ± 0.06
Gi582	0.31 ± 0.02	1.21 ± 0.46	5.74 ± 0.15	0.21 ± 0.02	6 ± 3	1.81 ± 0.06
Gi583	0.32 ± 0.02	1.67 ± 0.48	5.52 ± 0.15	0.23 ± 0.02	6 ± 3	1.82 ± 0.06
Gi584	0.36 ± 0.02	1.95 ± 0.57	4.87 ± 0.18	0.23 ± 0.02	6 ± 3	1.73 ± 0.06
BH-4						
Gi585	0.30 ± 0.02	2.00 ± 0.58	4.88 ± 0.18	0.20 ± 0.02	15 ± 7.5	1.52 ± 0.09
BH-5						
Gi588	0.91 ± 0.05	7.71 ± 0.82	3.52 ± 0.25	0.19 ± 0.02	6 ± 3	2.29 ± 0.09
Gi589	0.26 ± 0.01	3.64 ± 0.70	2.72 ± 0.22	0.20 ± 0.02	6 ± 3	1.26 ± 0.06
Gi590	0.30 ± 0.02	1.92 ± 0.65	4.52 ± 0.21	0.24 ± 0.02	6 ± 3	1.60 ± 0.06
Gi591	0.27 ± 0.01	1.35 ± 0.64	5.04 ± 0.21	0.23 ± 0.02	6 ± 3	1.64 ± 0.06
Gi592	0.26 ± 0.01	1.19 ± 0.64	5.35 ± 0.21	0.25 ± 0.03	6 ± 3	1.70 ± 0.07
Gi593	0.32 ± 0.02	2.33 ± 0.75	5.41 ± 0.24	0.28 ± 0.03	6 ± 3	1.79 ± 0.07

110 °C thermoluminescence (TL) peak and the absence of a considerable IRSL (infrared stimulated luminescence) signal highlight the purity of the quartz extract (Hütt et al. 1988; Aitken 1998). The OSL ages were calculated

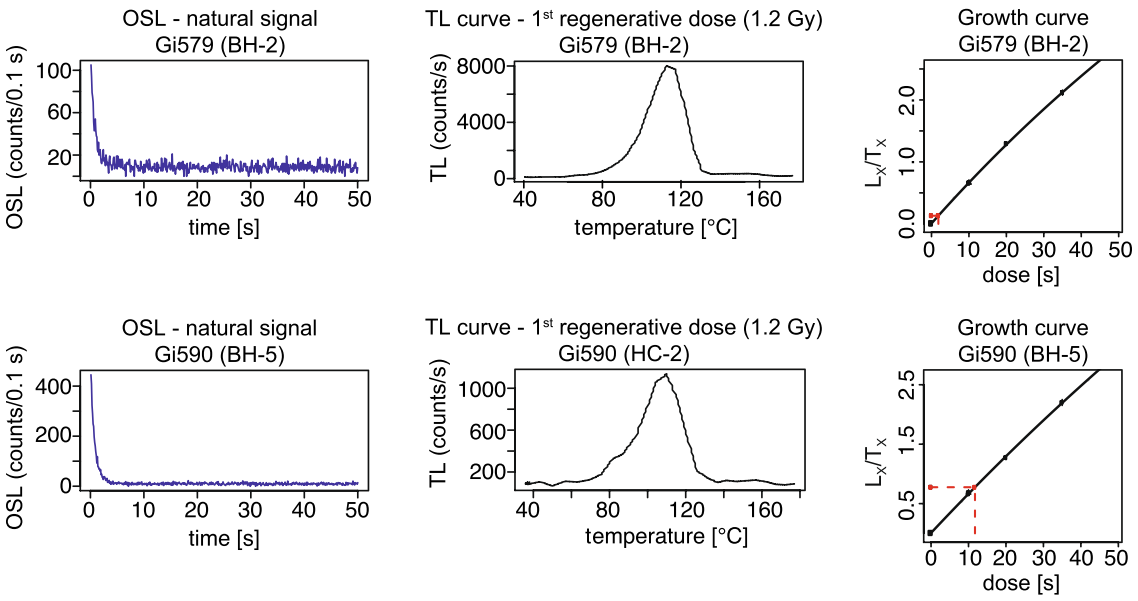


Fig. 9 Luminescence properties of the sediments represented by the samples Gi579 (BH-2) and Gi590 (BH-5). OSL shine-down curves of the natural signal, TL curves of the first regenerated dose preheat and the growth curves are shown. The graphs are created using the function plot_RLum() in the R luminescence package (Kreutzer et al. 2020).

based on the D_e estimates and the parameters listed in Tables 1 and 2. The resulting ages and their 1σ errors are listed in Table 2 and shown in Fig. 4 to 7.

The D_e values were calculated by establishing growth curves with single exponential saturation functions. Based on the resulting D_e distributions and their dispersion parameters (skewness and kurtosis), 11 out of 16 OSL samples were identified as incompletely bleached (Table 2), resulting in the application of the bootstrap minimum age model (Cunningham & Wallinga 2012). The minimum age model was executed with a sigma b value of 0.23, based on the average overdispersion of unskewed D_e values that were measured for the open-water reservoir at Atar Haroa in the Negev Highlands (Junge et al. 2018). The incompletely bleached samples are often characterized by some outliers with higher doses (e.g., Gi576, Fig. 10). The remaining five samples do not show evidence for insufficient bleaching, and consequently the central age model was used (Galbraith et al. 1999).

The occurrence of incomplete bleaching does not appear to be caused by a certain mode of deposition at this site, because samples considered to be incompletely bleached can be found in all the sections. This includes the fluvial sediment accumulation within the channel and the cistern fill, as well as the retaining wall and spoil pile sediments transported and deposited by humans. For the retaining wall and the spoil pile (BH-3 and BH-5), incomplete bleaching might occur because the sediments were shovelled and moved by humans in large quantities rapidly over a short distance. This can result in insufficient exposure to sunlight, causing residual OSL signals in a portion of the grains. However, fluvial transported sediments accumulated in the channel (BH-1 and BH-2) and cistern (BH-4) sometimes show evidence for incomplete bleaching, as well. In this case, the individual grains are more likely to be exposed to sunlight, but due to the small catchment size, the transport distances are relatively short, reducing the possibility of complete bleaching of all grains. Also, the high-energy rainfall events, typical for this arid environment, generate a high transport capacity resulting in carrying of large amounts of material in short periods of time, hampering the bleaching of the quartz grains. Additionally, the dominant carbonate lithology of the Negev Highlands often results in aggregates or carbonate coatings of the grains, and therefore reduces the likelihood of bleaching individual grains. Finally, one should also consider the possibility of post-depositional mixing by animal burrowing, where sediments from over- or underlying strata could be incorporated into the sampled layer.

The relative standard deviations (RSD) and overdispersions (OD) are fairly high, ranging between 11 to 93% and 9 to 90%, respectively. In general, OD and RSD tend to increase with decreasing D_e values, because the residual doses increase relatively to the dose accumulated since the last bleaching event. Hence, even the smallest residual doses due to incomplete bleaching or the incorporation of grains from other layers can cause wide distributions for low D_e values. For some of the samples from the studied site, the wide distributions are dominantly caused by outliers and can be associated with incomplete bleaching (Fuchs et al. 2007). Besides the high RSD, these samples are also characterized by skewed D_e distributions. But even some samples with un-skewed D_e distributions have higher OD and RSD values (e.g., Gi584: RSD = 32%, OD = 32%, Fig. 10) than expected for a well-bleached sample. An explanation for this might be a heterogeneous microdosimetry (Mayya et al. 2006). Microdosimetric effects can cause an increase of the RSD, especially with lower contents of U, Th and K, like in the case for the studied sediments (Table 1). The carbonatic nature of these deposits (see micromorphology section below) may amplify this effect.

Micromorphology

Sample BH-4-M was collected at the bottom of trench BH-4 within cistern I (Figs. 6 and 11). The lower 5 cm of the sample, reddish-brown in colour, is composed primarily of a micritic calcite groundmass that includes quartz grains (Fig. 11b–d). The microstructure is massive with occasional channels and chambers indicative of bioturbation. Fe/Mn-oxide stains and nodules are present, evidencing hydromorphic conditions. The next unit of sediments (6 cm thick; greyish with brownish patches) is characterized by a more open structure due to the inclusion of chalk gravel (Fig. 11a, e). Angular gravel probably originates from erosion of the cistern walls. Rounded chalk gravel occurs as well, probably originating from washed in debris. Finer components include calcite and quartz grains. The uppermost deposit (3 cm thick; greyish) is composed of rounded chalk gravel and finer grains (calcite and quartz sand), probably all originating from washed in debris.

Sample BH-5-M was collected from the spoil pile of cistern IV covering the transition between pre-construction and construction material in the lowermost step (Figs. 7 and 12). The lower 3–4 cm of the sample (Fig. 12b–d), yellowish-brown in colour, is composed of calcitic clay with abundant quartz silt and sand. The sediment is poorly sorted, including many snail shell fragments and rounded chert gravel. Its upper contact is uneven but sharp. This deposit is interpreted as the palaeosurface. The deposit overlying the palaeosurface (8–9 cm thick; light yellowish) is composed of angular chalk and chert gravel within a calcitic matrix (Fig. 12a, d). Snail shell fragments and quartz grains occur but in small quantities relative to the palaeosurface. This deposit is interpreted as resulting from cistern construction. Its contact with the overlying deposit is sharp. The latter deposit is a thin

Table 2 Sample ID, deposition mode, sampling depth, equivalent dose (D_e), number of measured aliquots, aliquot diameter, overdispersion, relative standard deviation, transformation for D_e calculation (logged or unlogged), used age models (*CAM* central age model, *MAM* minimum age model) and the resulting OSL age.

Sample ID	Section location/ deposition mode	Sampling depth [cm]	D_e [Gy]	Number of aliquots	Aliquot diameter [mm]	Overdis-persion [%]	Rel. standard deviation [%]	Logged or unlogged	Age model	Age [ka]	Age in calendar years
BH-1	Channel fill										
Gi576	Abandonment	70	0.31 ± 0.05	28	4	90	93	Unlogged	MAM	0.17 ± 0.03	1820–1880 CE
Gi577	Abandonment	20	1.09 ± 0.12	24	3	59	61	Unlogged	MAM	0.66 ± 0.08	1280–1440 CE
BH-2	Channel fill										
Gi578	Abandonment	45	0.38 ± 0.02	27	3	28	29	Unlogged	CAM	0.19 ± 0.01	1820–1840 CE
Gi579	Abandonment	33	0.23 ± 0.04	36	3	82	86	Unlogged	MAM	0.13 ± 0.02	1870–1910 CE
Gi580	Abandonment	17	0.27 ± 0.04	29	3	47	49	Unlogged	MAM	0.16 ± 0.02	1840–1880 CE
BH-3	Retaining wall										
Gi581	Maintenance	33	0.35 ± 0.09	28	4	65	67	Unlogged	MAM	0.19 ± 0.05	1780–1880 CE
Gi582	Maintenance	60	0.58 ± 0.05	29	4	63	65	Unlogged	MAM	0.32 ± 0.03	1670–1730 CE
Gi583	Construction	39	2.04 ± 0.15	31	2	38	39	Unlogged	CAM	1.1 ± 0.1	800–1000 CE
Gi584	Construction	41	2.17 ± 0.15	27	2	32	32	Logged	CAM	1.3 ± 0.1	600–800 CE
BH-4	Cistern fill										
Gi585	Abandonment	182	0.41 ± 0.07	25	4	65	66	Unlogged	MAM	0.27 ± 0.05	1700–1800 CE
BH-5	Spoil pile										
Gi588	Pre-construction	110	21.14 ± 2.49	36	1	37	40	Logged	MAM	9.2 ± 1.1	8300–6100 BCE
Gi589	Construction	70	2.00 ± 0.17	23	2	37	39	Unlogged	CAM	1.6 ± 0.2	200–600 CE
Gi590	Maintenance	30	1.39 ± 0.06	36	2	21	25	Unlogged	MAM	0.87 ± 0.05	1100–1200 CE
Gi591	Construction	41	2.43 ± 0.19	24	2	16	20	Logged	MAM	1.5 ± 0.1	400–600 CE
Gi592	Construction	21	2.43 ± 0.09	23	2	9	11	Logged	CAM	1.5 ± 0.1	400–600 CE
Gi593	Maintenance	8	0.87 ± 0.06	21	3	46	50	Unlogged	MAM	0.49 ± 0.04	1490–1570 CE

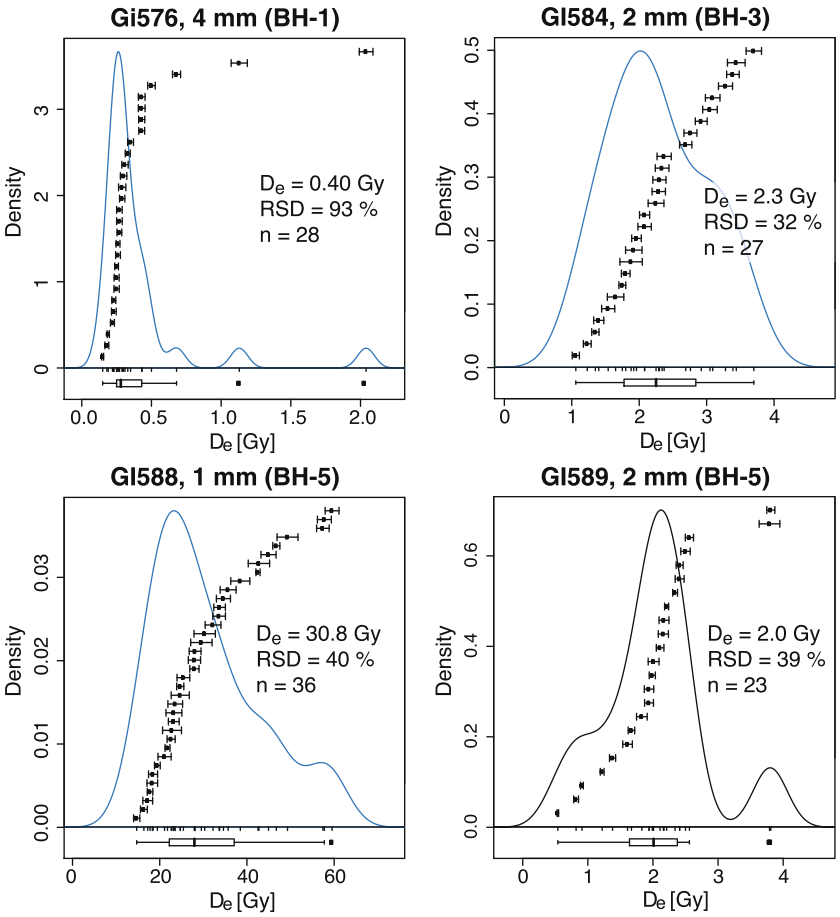


Fig. 10 Kernel density estimation plot for representative samples (Gi576, Gi584, Gi588 and Gi589). For these samples, the accepted aliquots are shown in ascending order, with n (number of aliquots), RSD (relative standard deviation), mean D_e (equivalent dose) and the aliquot diameter. The graphs were created with the function plot_KDE() in R using the luminescence package (Kreutzer et al. 2020).

(no more than 1 mm thick) greyish layer of 1–2 micritic calcite crusts that seems to indicate sheetwash (Fig. 12e). This deposit signifies exposure of the deposit below it for at least one winter. The deposit that overlies the crust(s) (2 cm thick) is mostly fine (i.e., no chert or chalk gravel) composed of calcitic clay, with a few snail shell fragments (Fig. 12f). Notably, it includes fragments of crusts, some of them oriented sub-vertically, which are typical for sediment accumulations removed from cisterns.

Discussion

To interpret the OSL results and therefore to reconstruct the cisterns system's history, micromorphological analyses, field stratigraphy and the bleaching abilities for different modes of deposition need to be taken into consideration. This is done separately for the spoil pile of cistern IV and the retaining wall, channel fill and cistern fill of cistern I.

The spoil pile (BH-5) of cistern IV

Above bedrock, four stratigraphic units can be distinguished macroscopically in the bottom step of trench BH-5 (Figs. 7b and 13). The lowermost sediment unit is about 45 cm thick and consists of yellowish-brown calcitic loam with many cobbles (dominantly flint, < 15 cm) and a few boulders. This unsorted alluvial deposit yields an OSL age of 9.2 ± 1.1 ka (Gi588). The deposition of the material during the Early Holocene and the sediment properties clearly marks this layer as natural deposition before the cistern was constructed. These sediments are sharply separated (Fig. 12b) from the overlying ca. 35-cm-thick light yellowish deposits composed of calcic fines with a few flint cobbles (up to 10 cm). Microscopically, it shows a distinctly different composition and microstructure with abundant angular chalk fragments typical of construction deposits (Fig. 12d). The OSL dating of this unit yields an age of 1.6 ± 0.2 ka (Gi589), indicating construction during the late-Roman or Byzantine period. Due to the absence of fine to medium quartz sand

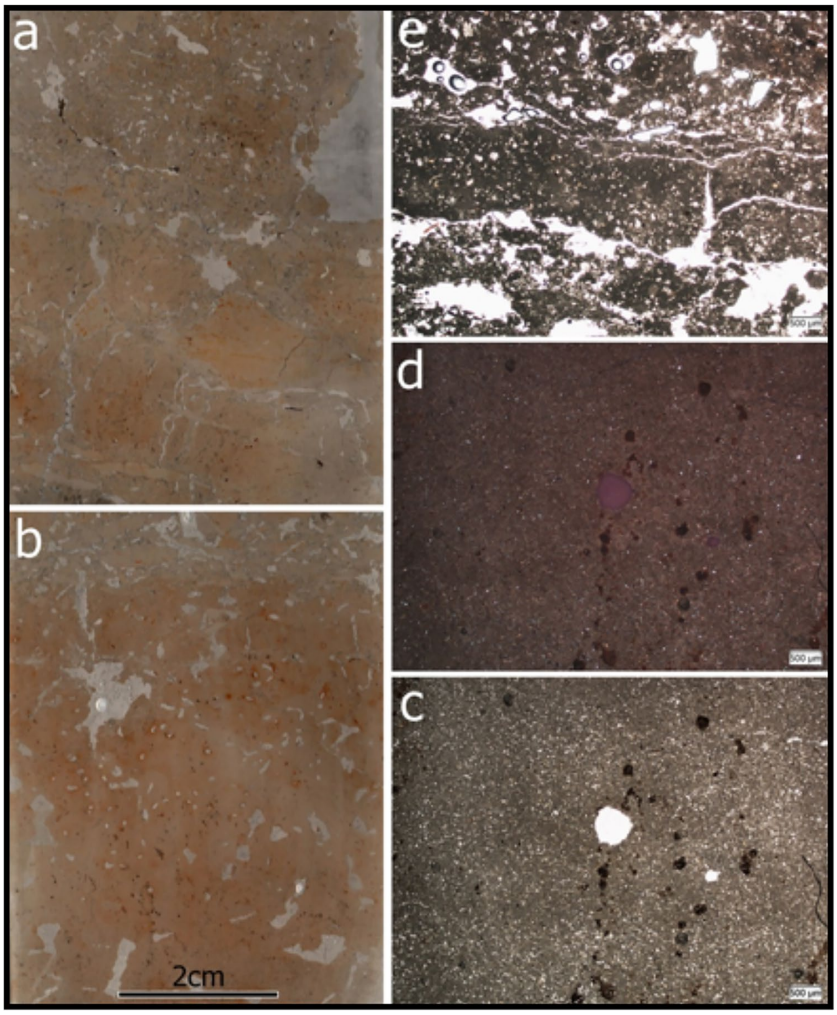


Fig. 11 Micromorphology of deposits within cistern I. **a** Flatbed scan of the thin section of the upper part of the block sample. **b** Flatbed scan of the thin section of the lower part of the block sample. **c** Microphotograph (PPL) of the lower reddish-brown layer. Note vesicles from bioturbation and dark Fe/Mn-oxide nodules from hydromorphic conditions within the cistern. **d** Same as c but under XPL. The fine whitish speckles are from quartz silt and fine sand. **e** Microphotograph of the upper mixed layer of the deposit. Note the open structure with a rectangular fragment of chalk (middle of the image) surrounded by disintegrated chalky matter. Scale bar in **c**–**e** is 500 µm.

in the chalk bedrock, it is assumed that quartz grains were incorporated into the construction deposit either by humans trampling over the spoil pile or by aeolian transport during the ongoing construction work. The D_e values of the OSL sample Gi589 show a slightly left-skewed distribution with several lower values (Fig. 10). The skewed distribution can be the result of the incorporation of grains with a lower OSL signal or two sample populations, due to separate deposition events. To minimize the risk of post-depositional incorporation of younger grains and to ensure that the sampled grains were incorporated during construction, the dated material was taken from the centre of the construction layer. Accordingly, it is more likely that the high amount of calcium carbonate of the sediment increased the attenuation of the ionizing radiation, especially for grains with a calcium carbonate crust, and the low dose rate ($\dot{D}$ in Table 1) of the sample caused microdosimetric effects, resulting in a slightly left-skewed distribution. Despite the occurrence of low D_e values, the distribution parameters (Bailey & Arnold 2006) of the sample led to the use of the CAM, putting no stronger emphasis on the low D_e values to prevent an age underestimation.

The upper part of the micromorphology block contains a ca. 1-mm-thick crust marking sheetwash within the construction layer (Fig. 12e). This indicates a time gap of at least one winter of exposure between the two depositions within this unit. The upper part of the micromorphological sample shows crust fragments with various orientations that are typical for sediment refill that was removed from cisterns during maintenance operation. This and the thin crust indicate that the construction of the cistern took place over the course of at least 1 year, with a partial refill of the cistern

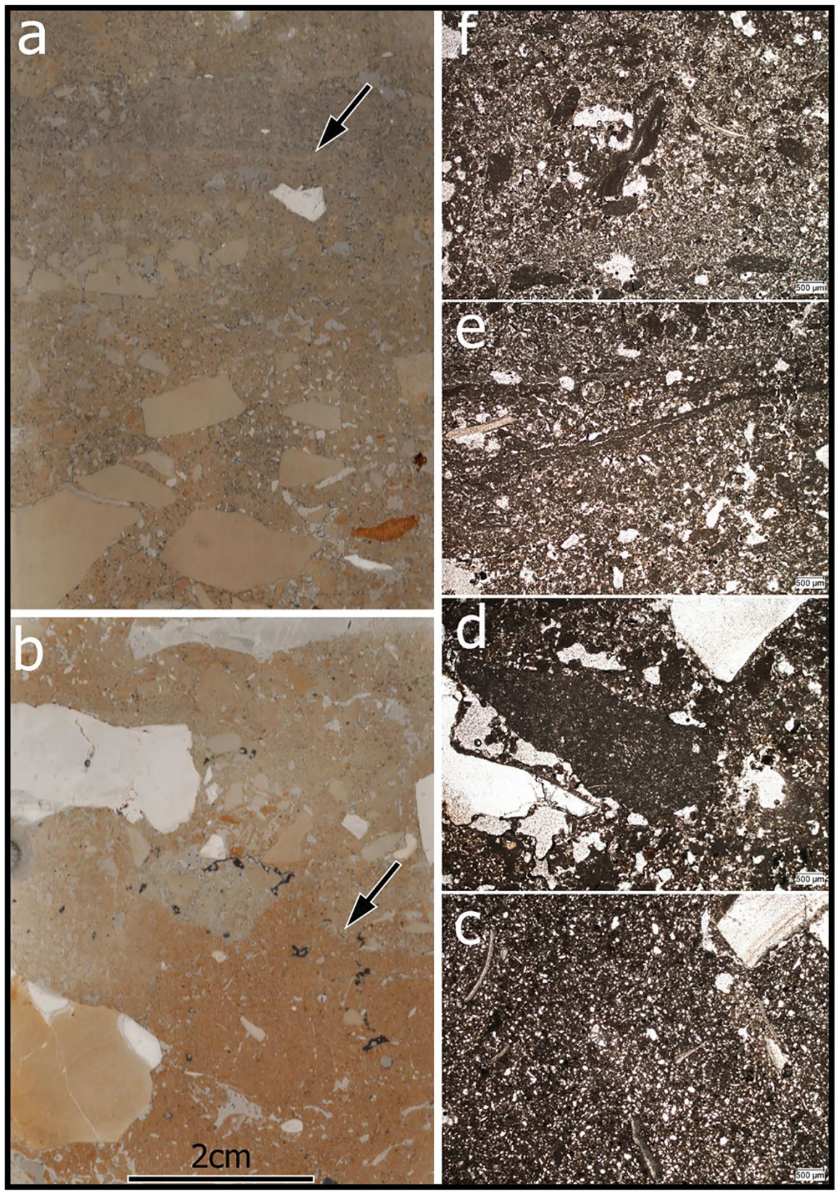


Fig. 12 Micromorphology of the spoil pile of cistern IV. **a** Flatbed scan of the thin section of the upper part of the block sample. The arrow indicates the location of in situ crusts (image **e**, see below). **b** Flatbed scan of the thin section of the lower part of the block sample. Arrow indicates the contact between the reddish-brown alluvial deposition and the construction material of the spoil pile. **c** Microphotograph (PPL) of the alluvium. Note abundant transparent rounded quartz particles as well as elongated snail shell fragments. **d** Microphotograph of the coarse fragments typical of the deposit consisting of construction debris. PPL. **e** Microphotograph (PPL) of the finer-grained deposit consisting of two sub-horizontal crusts indicating aerial exposure and sheetwash. **f** Microphotograph (PPL) of the fine-grained deposit consisting of sub-vertical elongated fragments of crusts resulting from cistern maintenance activities. Scale bar in **c**–**e** is 500 µm.

during this time. A temporal resolution of such short time spans is not possible with OSL dating.

The overlying unit in the upper centre of the lower step is characterized by light yellowish calcitic fines with many unoriented chalk cobbles and a few flint cobbles (up to 7 cm). The chalk cobbles indicate construction because they originate from the relocation of bedrock, while the majority of the flint gravels were washed from the slopes into the cistern and then removed in terms of cistern maintenance. The dating of sample Gi590 yields a time of deposition 0.87 ± 0.05 ka ago. The sedimentary properties of the material do not allow a definite distinction of the deposition mode: it is possible that the material was either deposited on top of the spoil pile during the initial construction in the late-Roman or Byzantine period and later washed or tramped down during the twelfth century, or the material was deposited in this location during cistern maintenance during the twelfth century. The thin top layer of the lower step is also composed of weakly compacted, light yellowish sandy silt, but carries only very few small cobbles (< 4 cm).

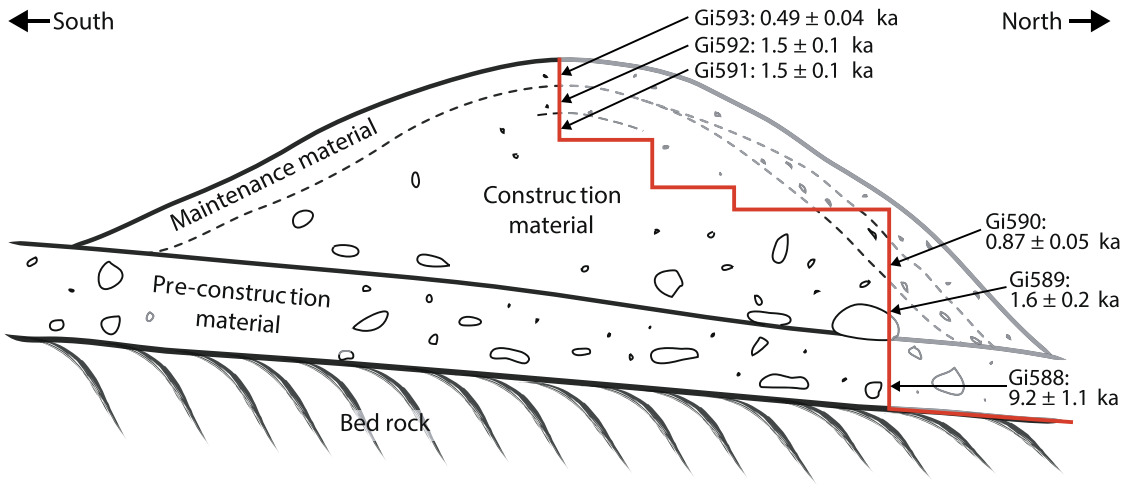


Fig. 13 Schematic section of spoil pile IV (the stepped trench is marked in red), displaying OSL ages and layers observed in the field.

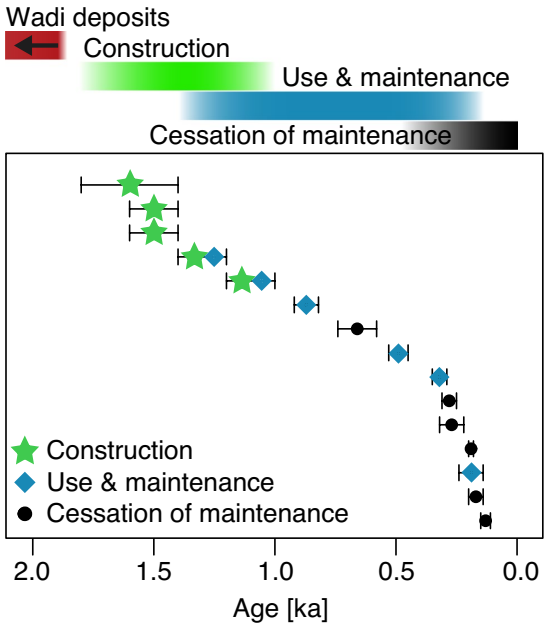


Fig. 14 Summary of the age ranges of the OSL samples ordered in accordance to their age, indicating construction (green), use and maintenance (blue), and the cessation of maintenance (black) of the cistern system. The position of the age of alluvial deposition is only implied, because of its high value. Two of the samples of the retaining wall could not be clearly identified as construction or maintenance; hence, they are marked as both in this graph (green star and diamond).

The material was not sampled for dating due to its proximity to the current surface and the lack of compaction, which risks mixing of the material from the surface with the upper part of the spoil pile.

The upper step of the BH-5 trench (Figs. 7a and 13) is composed of three macroscopically defined units, each 16–18 cm thick. The two lower deposits consist of yellowish fines with very few gravels and are assumed to be relocated bedrock material from the cistern's construction, because of its homogeneous composition and the light colour. The layer in the centre of this section is only distinguished from the lower unit by its slightly stronger compaction. The OSL dating of both units results in the similar age of 1.5 ± 0.1 ka (Gi591 and Gi592). Within their errors, these ages agree with sample Gi589 (1.6 ± 0.2 ka) in the lowest step of the spoil pile trench (Fig. 13), which strengthens the dating of the cistern's construction to the late-Roman to Byzantine period. The two slightly distinguishable layers might reflect the time gap within the construction that is reflected by unoriented fragments of crusts in the micromorphology sample from the lower step (BH-5-M). The consensus of the three samples can be used as an age control showing the reliability of the OSL dating at this site, and that the application of the MAM is able to correct incomplete bleaching (as used for sample Gi591). The uppermost layer of the spoil pile is a slightly compacted yellowish-brown sandy silt with some pebbles and very few stones (< 5 cm, flint). The OSL age of 0.49 ± 0.04 ka and the location on top of the spoil pile marks this unit as maintenance material—possibly the final cleaning of cistern IV.

To summarize, the OSL dating of the spoil pile allows the construction of cistern IV to be constrained to the third to

sixth century CE, during the late Roman or Byzantine periods. One phase of the cistern's maintenance likely occurred during the twelfth century CE, while this age could also reflect a post-depositional transport of construction material from the upper part of the spoil pile. The latest use in terms of maintenance material dates to ca. 1500 CE and marks the earliest possible date for the beginning of the final infill and the subsequent end of cistern IV maintenance.

The retaining wall (BH-3) of cistern I

Trench BH-3 (Fig. 5) exposed material deposited in order to construct and possibly reinforce the retaining wall diverting water into cistern I. The channel-facing side of the retaining wall is constructed of flat stones. On top of the piled stones, and in the centre and lower end of the retaining wall, yellowish sandy silt, many cobbles in different sizes and some boulders (up to 50 cm) accumulated. No layering or changes in the sediment composition throughout the trench could be identified. The two lower samples Gi584 and Gi583 yield ages of 1.3 ± 0.1 ka and 1.1 ± 0.1 ka, respectively (late Byzantine and early Islamic periods), and therefore are the same within their 2σ errors. To interpret these ages, it is essential to understand that only a limited amount of water would reach the cistern without the retaining wall. Consequently, it is assumed that the retaining wall was constructed contemporaneously with the cistern or shortly thereafter. However, the stacked stone pile can be interpreted as the initial retaining wall that was extended and enhanced by unsorted sediments either at the time of construction or at a later stage. Since the deposition of the piled stones was not dated directly, it is not clear if the ages of samples Gi584 and Gi853 represent the initial construction of the retaining wall or its later extension. Therefore, these OSL results should be interpreted as the latest possible ages for the construction of the retaining wall and consequently the cutting of cistern I.

The two upper OSL samples provide ages of 0.32 ± 0.03 ka (Gi582) and 0.19 ± 0.05 ka (Gi581), respectively. Within 2σ errors, the two ages agree with each other. Because no sediment layering was observed, it can be assumed that the sediments were deposited during a single event, although multiple events within the OSL age range cannot be excluded. In any event, these ages indicate that the retaining wall was heightened during the seventeenth to the nineteenth century with material possibly originating from maintenance material from the cistern and the adjacent channel.

To summarize, two deposition events can be distinguished: the older OSL ages are assumed to represent the minimum age of the construction of the retaining wall, and possibly of the construction of the associated cistern I, during the late Byzantine to Early Islamic period or earlier. The younger OSL ages represent a deposition during the seventeenth to the nineteenth century and might reflect the enhancement of the retaining wall, or the cleaning of cistern I and its channel.

The channel fill (BH-1 and BH-2)

Trenches BH-1 and BH-2 were cut into the sediment deposition within a channel directing water into cistern I (Fig. 4). The bottom of both is bounded by bedrock. The overlying sediment is composed of alternating layers of sandy silts and gravels with a few stones (< 15 cm), indicating depositional events of varying magnitude. While the sandy silt layers are interpreted as fluvial deposits, the deposits with larger gravels and stones may be understood as gravitational transported slope debris.

The OSL samples from trench BH-2 yield ages of 0.19 ± 0.01 ka (Gi578), 0.13 ± 0.02 ka (Gi579) and 0.16 ± 0.02 ka (Gi580), while the bottom sample in trench BH-1 yields an age of 0.17 ± 0.03 ka (Gi576). Considering their 2σ errors, all ages are the same, indicating that sediment accumulation in the channel occurred during the nineteenth century. The uppermost sample in trench BH-1 yields an age of 0.66 ± 0.08 ka (Gi577), resulting in an age inversion in the trench. This age overestimation can be explained by poor exposure to sunlight during the sediment transport, e.g., turbid water over short transport distances within short time periods, or transport and deposition during the night. Besides Gi577, samples Gi576, Gi579 and Gi580 also show D_e distributions with characteristics of incomplete bleaching. The application of the MAM for the three samples (Gi576, Gi579 and Gi580) results in the agreement of the ages with the results from the well-bleached sample (Gi578). The use of the MAM for sample Gi577 still results in a strong overestimation of the age. This can be caused by no grains or only very few grains being bleached during transport. When only a few well-bleached grains are mixed with a high number of grains with residual doses, no measured aliquot represents the final transport and deposition, but rather earlier bleaching events. In other words, the MAM emphasizes aliquots with lower doses, but these still overestimate the time of the final deposition. Thus, it is impossible to interpret the age of sample Gi577.

The younger ages obtained from BH-1 and BH-2 point to sediment accumulation after the last cleaning of the channel during the nineteenth century. This latest accumulation within the channel corresponds with the sediment deposition on the retaining wall (BH-3: Gi581 and Gi582, ca. late seventeenth to early nineteenth century CE).

Cistern fill (BH-4)

The sediments within cistern I (BH-4, Fig. 6) are composed of sandy silt with some gravels (< 1 cm) and a few stones (< 20 cm), two sandy layers in the lower part and two shallow organic-rich layers near the top. The stones within the trench most likely fell through the partially collapsed roof of the cistern from the adjacent slope, or are parts of the roof collapse. It is unlikely that stones of this size were washed into the cistern by surface runoff from the channel, because the water and sediments in the channel are slowed by the retaining wall and the reduced transport capacity of the runoff water hampers the further transport of larger stones into the cistern. This assumption is supported by the limited number of gravels and other stones in the layers where the large stones occur. The bottom of the cistern was not reached; excavation was stopped when an enamelled metal bucket (twentieth century) was exposed at a depth of 180 to 200 cm. The material at this depth was compacted due to the overburden in a moist environment, as it can be seen in the bottom part of the micromorphology sample (Figs. 11b–d). The OSL dating at this depth results in an age of 0.27 ± 0.05 ka (Gi585), indicating the last maintenance within cistern I probably took place no later than the eighteenth century. In comparison to OSL ages from BH-1 and BH-2, this would mean that the channel of cistern I was still cleaned for one or two centuries when the cistern itself was no longer maintained. This scenario cannot be ruled out, because the shallow channel is filled with sediments more rapidly than the cistern; thus, the cistern needs to be maintained less often. At the same time, the appearance of plastic and metal trash deep in the trench indicates a very recent sediment accumulation. While this is in accordance with the information shared by a local farmer about cleaning activities in cistern III in the 1960s by members of a nearby kibbutz, it is assumed that Bedouin have been using these cisterns until recently as well. This recent maintenance might have been also carried out in cistern I, hinting towards later utilization. The discrepancy between the OSL age and the stratigraphic evidence in this section indicates that insufficient bleaching occurred that cannot be corrected by the application of the MAM. The reasons for this are similar to the causes of the age overestimation of sample Gi577 in BH-1.

Bleaching

During construction and maintenance, large amounts of material were removed by humans and transported over a very short distance to the spoil pile. Despite the unfavourable conditions for bleaching, the results show that incomplete bleaching is an issue only for one of the construction samples (Gi591). For this sample, the age agreement with other samples from the same event shows the successful application of the MAM to correct for the age overestimation due to residual signals on some of the quartz grains. This better than expected bleaching of the construction material may result from the fact that the quartz grains do not originate from the hewn chalk bedrock, but from dust incorporated either naturally or by humans walking over the spoil pile during ongoing construction work. The long exposure of the spoil pile layers during construction, due to slow construction of the cisterns, supports the bleaching of the incorporated grains.

While the construction material was transported and deposited once, the sediments removed during cleaning were moved twice: first, when they washed into the cisterns and channels, and second, when they were removed from the installations during maintenance. Despite this, all maintenance samples from the site suffer from broad, skewed distributions indicating insufficient bleaching. The resetting of the OSL signal during the fluvial transport often suffers from incomplete bleaching as evidenced by the samples from the sediment accumulations within the channel and cistern. This poor bleaching might be the result of the short transport distances, large amounts of material transported, water turbidity, or a transport and deposition event overnight. This might be amplified by the transport of sediments that accumulated initially in the catchment during the Late Pleistocene or Early Holocene, resulting in an even older OSL signal to be reset. The second transportation and deposition of the maintenance material was carried out by humans. Other than the construction material, the infill sediments were likely unconsolidated and easy to remove from the installations, which potentially made this process faster and limited the exposure of sediments on top of the spoil pile to sunlight, reducing bleaching time.

Furthermore, the younger ages of the maintenance material in general and the final accumulation within the installations in particular are more vulnerable to residual doses, because the dose accumulated since the last deposition is quite small. This can result in considerable age overestimations even with very minor residual doses. For most of the samples, this issue is controllable with the application of MAM, but if no or only very poor bleaching occurs, the MAM still results in an age overestimation, as in the case for the samples Gi577 and Gi585. In these cases, it is necessary to compare them with other samples from the same or similar units and to put them in a stratigraphical context. The handling of the incomplete bleaching as described here, and the incorporation of micromorphological analyses for the interpretation of the mode of deposition, allows the establishment of a chronology of the cistern system at Borot Hazaz.

Overall chronology of the Borot Hazaz cistern system

As described above, the chronology of subterranean cisterns in the Negev Highlands is based on hypotheses regarding architectural similarities, proximity and a handful of inscriptions. This has resulted in an assumption that construction of rock-cut cisterns took place only during the Hellenistic-Roman (Nabatean) to Byzantine Period. The use of OSL allows the dating of sediment transported during construction and cleaning (maintenance) of the cisterns, as well as fluvial sediment accumulation in the installations when maintenance declines or ceases. For cistern IV, the archaeological age assessment is supported by OSL dating, indicating construction during the Late Roman to Byzantine Period. For cistern I, the latest possible date of construction is 600–1000 CE (Late Byzantine to Early Islamic periods). A possible maintenance phase for cistern IV took place during the twelfth century and final maintenance of this cistern is dated to the fifteenth to the sixteenth century. In comparison, cistern I was maintained and utilized at least until the seventeenth to the nineteenth century. These data indicate that the Borot Hazaz cisterns may have been constructed at slightly different times and not as a complete system in one campaign. Additionally, the cisterns studied here were used and maintained differently.

The Byzantine period features unprecedented prosperity in the Negev Highland, with several urban centres and a large number of smaller settlements and farmhouses, being the only period in the history of the Negev Highlands which also supplies textual evidence for agricultural activity (Rubin 1988; Tepper et al. 2020). Scholars debate whether this activity declined relatively abruptly at the end of the Byzantine period (recently Tepper et al. 2018), or gradually during the Early Islamic period (Haiman 1995; Avni 2008, 2014). The study at Borot Hazaz is too limited to shed light on this issue. However, together with a previous study on an open-water reservoir located nearby (Junge et al. 2018), it is shown that cisterns were utilized and maintained by (agro) pastoral groups in the region for centuries after the decline of the Byzantine settlement system.

Conclusion

The dating of the cisterns system of Borot Hazaz benefits from the very suitable characteristics of the coarse-grain quartz fraction for OSL dating. Despite the unfavourable bleaching conditions of short transport distances, the majority of samples were well-bleached. Of the samples insufficiently bleached, the application of the MAM was able to successfully correct for the age overestimation, as confirmed by the agreement of the resulting ages with other OSL ages from associated sediments and events. Only for two samples, the comparison with other ages or the sedimentary context reveals an age overestimation that cannot be corrected. Overall, the interpretation of the OSL ages is supported and enhanced by the micromorphological analyses. The identification of different modes of deposition is necessary to distinguish between sediment accumulation before and during cistern construction, and to differentiate material deposited when the installation was maintained, and sediment accumulation after maintenance ceased.

The combination of OSL dating and micromorphology confirms the archaeological age assessment of cistern IV: construction took place during the late Roman to Byzantine Period. For cistern I, construction can only be given as a minimum age—before or during the Early Islamic Period. A maintenance phase of cistern IV took place during the twelfth century and final maintenance for this cistern was conducted during the fifteenth to the sixteenth centuries. For cistern I, later maintenance and utilization can be dated to the seventeenth to the nineteenth century. It is notable that there are substantial time gaps between the construction phases and the maintenance of the installations, and that the different cisterns of the system were likely constructed and used at different times.

Acknowledgements This research was supported by a grant (No. FU 417/33-1 with M. F. as principal investigator and R. S.-G. and I. F. as co-investigators) from the DFG, German Research Foundation. Excavations were conducted under the Israel Antiquities Authority permit G-17/2018. We would like to thank Abra Spiciarich, Angie Hudson, Brett Cohen and Ronnie Avidov for their relentless work and support during the excavation of Borot Hazaz, and Manfred Fischer from the Bayreuth University for U and Th measurements.

Funding Open Access funding enabled and organized by Projekt DEAL.

Open Access This article is licensed under a Creative Commons Attribution 4.0 International License, which permits use, sharing, adaptation, distribution and reproduction in any medium or format, as long as you give appropriate credit to the original author(s) and the source, provide a link to the Creative Commons licence, and indicate if changes were made. The images or other third party material in this article are included in the article's Creative Commons licence, unless indicated otherwise in a credit line to the material. If material is not included in the article's Creative Commons licence and your intended use is not permitted by statutory regulation or exceeds the permitted use, you will need to obtain permission directly from the copyright holder. To view a copy of this licence, visit http://creativecommons.org/licenses/by/4.0/.

References

Aitken MJ (1998) An introduction to optical dating. Oxford University Press, Oxford

Arnold LJ, Roberts RG, Galbraith RF, DeLong SB (2009) A revised burial dose estimation procedure for optical dating of young and modern-age sediments. Quat Geochronol 4:306–325
Avni G (2008) The Byzantine-Islamic transition in the Negev: an archaeological perspective. Jerus Stud Arab Islam 35:1–26
Avni G (2014) The Byzantine–islamic Transition in Palestine: an Archaeological Approach. Oxford University Press, Oxford
Avni Y, Weiler N (2013) Geological map of Israel 1:50,000: Sede Boqer sheet 18-IV. Jerusalem, Israel: Ministry of Energy and Water Resources, Earth and Marine Research Administration, Geological Survey.
Avni Y, Porat N, Plakht J, Avni G (2006) Geomorphic changes leading to natural desertification versus anthropogenic land conservation in an arid environment, the Negev Highlands. Israel Geomorphology 82(3–4):177–200
Avni Y, Porat N, Avni G (2012) Pre-farming environment and OSL chronology in the Negev Highlands, Israel. J Arid Environ 86:12–27
Avni G, Porat N, Avni Y (2013) Byzantine—Early Islamic agricultural systems in the Negev Highlands: Stages of development as interpreted through OSL dating. J Field Archaeol 38(4):332–346
Bailey RM, Arnold LJ (2006) Statistical modelling of single grain quartz De distributions and an assessment of procedures for estimating burial dose. Quatern Sci Rev 25(19–20):2475–2502
Bailey RM, Smith BW, Rhodes EJ (1997) Partial bleaching and the decay form characteristics of Quartz OSL. Radiat Meas 27(2):123–136
Bar-Matthews M, Ayalon A, Gilmour M, Matthews A, Hawkesworth CJ (2003) Sea–land oxygen isotopic relationships from planktonic Foraminifera and speleothems in the Eastern Mediterranean region and their implication for paleorainfall during interglacial intervals. Geochim Cosmochim Acta 67(17):3181–3199
Bar-Matthews M, Ayalon A (2004) Speleothems as palaeoclimate indicators, a case study from Soreq Cave located in the eastern Mediterranean region, Israel. In: Battarbee RW, Gasse F, Stickley CE (eds) Past climate variability through Europe and Africa. Springer, Dordrecht, Netherlands, pp 363–391
Boaretto E, Finkelstein I, Shahack-Gross R (2010) Radiocarbon results from the Iron IIA site of Atar Haroa in the Negev Highlands and their archaeological and historical implications. Radiocarbon 52:1–12
Bookman R, Enzel Y, Agnon A, Stein M (2004) LateHolocene lake levels of the Dead Sea. Bulletin of the Geological Society of America 116:555–571
Bowman D, Karnieli A, Issar A, Bruins HJ (1986) Residual colluvio-aeolian aprons in the Negev Highlands (Israel) as a paleo-climatic indicator. Palaeogeogr Palaeoclimatol Palaeoecol 56:89–101
Bruins HJ (1986) Desert environment and agriculture in the Central Negev and Kadesh Barnea during historical times (Published PhD dissertation). University of Wageningen, Wageningen, the Netherlands, Stichting Midbar Foundation, Nijkerk, the Netherlands
Bruins HJ (2012) Ancient desert agriculture in the Negev and climate-zone boundary changes during average, wet and drought years. J Arid Environ 86:28–42
Burow C (2020) calc_AliquotSize(): Estimate the amount of grains on an aliquot. Function version 0.31. In: Kreutzer, S., Burow, C., Dietze, M., Fuchs, M.C., Schmidt, C., Fischer, M., Friedrich, J., 2020. Luminescence: Comprehensive Luminescence Dating Data Analysis. R package version 0.9.8.9000–72. https://CRAN.R-project.org/package=Luminescence.
Cohen R (1981) Survey of Sede Boqer Southwest – Map 168. Jerusalem.
Cohen R, Cohen-Amin R (2004) Ancient settlement of the Negev Highlands: the Iron Age and the Persian period (Vol. II, in Hebrew). Jerusalem, Israel: Israel Antiquities Authority.
Crouvi O, Amit R, Enzel Y, Porat N, Sandler A (2008) Sand dunes as a major proximal dust source for Late Pleistocene loess in the Negev Desert. Israel Quaternary Research 70(2):275–282
Cunningham AC, Wallinga J (2012) Realizing the potential of fluvial archives using robust OSL chronologies. Quat Geochronol 12:98–106
Duller GAT (2003) Distinguishing quartz and feldspar in single grain luminescence measurements. Radiat Meas 37:161–165
Dunseth ZC, Junge A, Lomax J, Boaretto E, Finkelstein I, Fuchs M, Shahack-Gross R (2017) Dating archaeological sites in an arid environment: a multi-method case study in the Negev Highlands, Israel. J Arid Environ 144:156–169
Durcan JA, King GE, Duller GAT (2015) DRAC: dose rate and age calculator for trapped charge dating. Quat Geochronol 28:54–61
Evenari M, Aharoni Y, Shanan L, Tadmor NH (1958) The ancient desert agriculture of the Negev: III. Early Beginnings Israel Exploration Journal 8(4):231–268
Evenari M, Shanan L, Tadmor N (1982) The Negev: the challenge of a desert, 2nd edn. Harvard University Press, Cambridge, MA
Faershtein G, Porat N, Avni Y, Matmon A (2016) Aggradation–incision transition in arid environments at the end of the Pleistocene: an example from the Negev Highlands, southern Israel. Geomorphology 253:289–304
Fuchs M, Wagner GA (2003) Optical dating of sediments: recognition of insufficient bleaching by small aliquots of quartz for reconstructing soil erosion in Greece. Quatern Sci Rev 22:1161–1167
Fuchs M, Woda C, Bürkert A (2007) Chronostratigraphy of a sedimentary record from the Hajar mountain range, N-Oman. Quat Geochronol 2:202–207
Galbraith RF, Roberts RG, Laslett GM, Yoshide H, Olley JM (1999) Optical dating of single and multiple grains of quartz from Jinmium Rock Shelter, Northern Australia: Part I, experimental design and statistical models. Archaeometry 41(2):339–364
Goldreich Y (2003) The climate of Israel: observation, research and application. Kluwer Academic/Plenum Publishers, New York, NY
Guérin G, Mercier N, Adamiec G (2011) Dose-rate conversion factors: update. Ancient TL 29:5–8
Haiman M (1991) Archaeological survey of Israel, map of Mizpe Ramon Southwest (200). Jerusalem, Israel: Israel Antiquities Authority.
Haiman M (1995) Agriculture and nomad-state relations in the Byzantine and Early Islamic periods. Bull Am Sch Orient Res 297:29–53
Heim C, Nowaczyk NR, Negendank JFW, Leroy SAG, Ben-Avraham Z (1997) Near East desertification: Evidence from the Dead Sea. Naturwissenschaften 84:398–401
Huntley DJ, Godfrey-Smith DI, Haskell EH (1991) Light-induced emission spectra from some quartz and feldspars. International Journal of Radiation Applications and Instrumentation. Part D. Nuclear Tracks and Radiation Measurements 18(1–2):127–131
Hütt G, Jaek I, Tchonka J (1988) Optical dating: K-feldspars optical response stimulation spectra. Quatern Sci Rev 7:381–385
Itzhaki Y (1971) The geological history of the Negev. In: Evenari M, Shanan L, Tadmor NH (eds) The Negev, the challenge of a desert. Cambridge, MA: Harvard University Press.
Junge A, Lomax J, Shahack-Gross R, Dunseth ZC, Finkelstein I, Fuchs M (2016) OSL age determination of archaeological structures using trapped aeolian sediments: A case study from the Negev Highlands, Israel. Geoarchaeology 31:550–563
Junge A, Lomax J, Shahack-Gross R, Finkelstein I, Fuchs M (2018) Chronology of an ancient water reservoir and the history of human activity in the Negev Highlands, Israel. Geoarchaeology 33:695–707
Kafle HK, Bruins HJ (2009) Climatic trends in Israel 1970–2002: warmer and increasing aridity inland. Clim Change 96(1–2):63–77

Kidron GJ (1999) Altitude dependent dew and fog in the Negev Desert. Israel Agricultural and Forest Meteorology 96(1–3):1–8
Kreutzer S, Burow C, Dietze M, Fuchs M, Schmidt C, Fischer M, Friedrich J (2020) Luminescence: comprehensive luminescence dating data analysis. R package version 0.9.7: https://CRAN.R-project.org/package=Luminescence.
Lender Y (1990). Archaeological Survey of Israel, map of Har Nafha (196). Jerusalem, Israel: Israel Antiquities Authority.
Lomax J, Kreutzer S, Fuchs M (2014) Performance tests using the Lexsyg luminescence reader. Geochronometria 41(4):327–333
Lomax J, Mittelstraß D, Kreutzer S, Fuchs M (2015) OSL, TL and IRSL emission spectra of sedimentary quartz and feldspar samples. Radiat Meas 81:251–256
Mayya YS, Morthekai P, MurariMadhav K, Singhvi AK (2006) Towards quantifying beta microdosimetric effects in single-grain quartz dose distribution. Radiation Measurement 41:1032–1039
Mejdahl V (1979) Thermoluminescence dating: beta-dose attenuation in quartz grains. Archaeometry 21:61–72
Migowski C, Stein M, Prasad S, Negendank JF, Agnon A (2006) Holocene climate variability and cultural evolution in the Near East from the Dead Sea sedimentary record. Quatern Res 66(3):421–431
Murray AS, Wintle AG (2000) Luminescence dating of quartz using an improved single-aliquot regenerative-dose protocol. Radiat Meas 32(1):57–73
Murray AS, Wintle AG (2003) The single aliquot regenerative dose protocol: potential for improvements in reliability. Radiat Meas 37:377–381
Neumann FH, Kagan EJ, Leroy SAG, Baruch U (2010) Vegetation history and climate fluctuations on a transect along the Dead Sea west shore and their impact on past societies over the last 3500 years. J Arid Environ 74:756–764
Ore G, Bruins, HJ, Meir IA (2020) Ancient cisterns in the Negev Highlands: types and spatial correlation with Bronze and Iron Age sites. Journal of Archaeological Science: Reports: 30https://doi.org/10.1016/j.jasrep.2020.102227
Orland IJ, Bar-Matthews M, Kita NT, Ayalon A, Matthews A, Valley JW (2009) Climate deterioration in the Eastern Mediterranean as revealed by ion microprobe analysis of a speleothem that grew from 2.2 to 0.9 ka in Soreq Cave. Israel Quaternary Research 71:27–35
Porat N, Rosen SA, Avni Y, Boaretto E (2006) Dating the Ramat Saharonim late neolithic desert cult site. J Archaeol Sci 33:1341–1355
Prescott JR, Hutton JT (1994) Cosmic ray contributions to dose rates for luminescence and ESR dating: large depths and long-term time variations. Radiat Meas 23(2–3):497–500
Roskin J, Tsoar H, Porat N, Blumberg DG (2011) Palaeoclimate interpretations of Late Pleistocene vegetated linear dune mobilization episodes: Evidence from the northwestern Negev dunefield. Israel Quaternary Science Reviews 30(23–24):3364–3380
Rubin R (1988) Water conservation methods in Israel's Negev desert in late antiquity. J Hist Geogr 14:229–244
Shanan L (2000) Runoff, erosion, and the sustainability of ancient irrigation systems in the Central Negev Desert. In: Hassan MA, Slaymaker O (eds) The hydrology-geomorphology interface: rainfall, floods, sedimentation, land use. IAHS Publications, Jerusalem, Israel, pp 75–106
Starinsky A, Zilberman E, Braun M, Sneh A (2010) Geological map of Israel 1:50,000: Revivim sheet 18-II. Jerusalem: State of Israel, Ministry of National Infrastructure, Geological Survey.
Stoops G (2003) Guidelines for analysis and description of soil and regolith thin sections. Soil Science Society of America, Madison, WI
Survey of Israel (2007) Mapping and GIS. Retrieved from https://www.govmap.gov.il.
Tepper Y, Erickson-Gini T, Farhi Y, Bar Oz G (2018) Probing the Byzantine/Early Islamic transition in the Negev: the renewed Shivta excavations, 2015–2016. Tel Aviv 45:120–152
Tepper Y, Porat N, Bar-Oz G (2020) Sustainable farming in the Roman-Byzantine period: dating an advanced agriculture system near the site of Shivta, Negev Desert, Israel. Journal of Arid Environments 177https://doi.org/10.1016/j.jaridenv.2020.104134

Publisher's Note Springer Nature remains neutral with regard to jurisdictional claims in published maps and institutional affiliations.

Third Study

The Archaeology and History of Rock-cut Cisterns and Open Water Reservoirs in the Negev Highlands

Andrea Junge, Zachary C. Dunseth, Ruth Shahack-Gross,
Israel Finkelstein, & Markus Fuchs

Bulletin of the American Society of Overseas Research, Volume 389, Issue 1, Pages 191-216, 2023

Published Online: 13^{th} April 2023

The Archaeology and History of Rock-cut Cisterns and Open Water Reservoirs in the Negev Highlands

Andrea Junge, Zachary C. Dunseth, Ruth Shahack-Gross, Israel Finkelstein, and Markus Fuchs

This article provides the final assessment of a large-scale optically stimulated luminescence (OSL) dating project of water installations in the arid Negev Highlands, southern Israel. Results from five open reservoirs and five rock-cut cisterns are reported. By sampling spoil piles, feeding channels, and accumulation of sediments within reservoirs and cisterns, their construction and phases of maintenance and abandonment are dated. Conventional wisdom argued for progress from simpler open reservoirs in the Bronze or Iron Ages to the more sophisticated rock-cut cisterns of the Nabatean–Byzantine periods. It is shown that open reservoirs were dug throughout the history of the region, likely from the Early or Intermediate Bronze Ages until the medieval period, including periods with no stone-built remains in the region. The construction of subterranean cisterns, which calls for more resources and skill, characterize the Late Roman/Byzantine to Early Islamic period. The significance of these results for reconstructing the history of human activity in the region is also discussed.

Keywords: water installations; open reservoirs; rock-cut cisterns; Negev Highlands; settlement oscillations; Early Bronze Age; Intermediate Bronze Age; Iron Age; Nabatean period; Byzantine period; Early Islamic period; OSL dating; geoarchaeology

The arid Negev Highlands region in southern Israel is characterized by a series of northeast-to-southwest oriented anticlines and synclines, with elevations ranging between 1000 m above sea level (asl) in the southwest and 350 m asl in the northeast. Bedrock consists of limestone, dolomite, chalk, chert, and marl formations (Starinsky et al. 2010). Annual precipitation ranges between 80 and 150 mm (Kafle and Bruins 2009), with fog and dew adding an equivalent of 10 mm precipitation for each 100 m increase in elevation (Kidron 1999). The majority of the rainfall occurs roughly between October and April with strong year-to-year variations (Evenari, Shanan, and Tadmor 1982; Bruins 2012). Possible oscillations in precipitation in the periods discussed here are still being investigated (brief summary in Junge et al. 2021; see also Bar-Matthews et al. 2003; Migowski et al. 2006; Orland et al. 2009; Langgut et al. 2015; among others) although there are limited paleoenvironmental archives and proxies in the desert itself.

Andrea Junge: Department of Geography, Justus Liebig University Gießen, Senckenberstraße 1, 35390 Gießen, Germany; *andrea.junge@geogr.uni-giessen.de*

Zachary C. Dunseth: Joukowsky Institute for Archaeology and the Ancient World, Brown University, 60 George Street, Providence, RI 02906, United States; *zachary_dunseth@brown.edu*

Ruth Shahack-Gross: Department of Maritime Civilizations, School of Archaeology and Maritime Cultures, University of Haifa, Haifa 3498838, Israel; *rgross@univ.haifa.ac.il*

Israel Finkelstein: School of Archaeology and Maritime Cultures, University of Haifa, Haifa 3498838, Israel and Institute of Archaeology, Tel Aviv University, Tel Aviv 6997801, Israel; *fink2@tauex.tau.ac.il*

Markus Fuchs: Department of Geography, Justus Liebig University Gießen, Senckenberstraße 1, 35390 Gießen, Germany; *markus.fuchs@geogr.uni-giessen.de*

Electronically Published April 13, 2023.

Bulletin of ASOR, volume 389, May 2023. © 2023 American Society of Overseas Research. All rights reserved. Published by The University of Chicago Press for ASOR. https://doi.org/10.1086/724457

From previous research, it seems that historical, economic, and geopolitical factors dictated settlement patterns in the steppe areas of the southern Levant more than climate change (Greener, Finkelstein, and Langgut 2018).

Human activity in this region in the last five millennia is characterized by several "waves" of settlement, which are meant here as periods that left behind stone-built remains. The main phases[1] are:

- The Early and Intermediate Bronze Ages (ca. 3600–1950 B.C.E.): Remains consist of larger and smaller sites, animal pens, and fields of tumuli (e.g., Haiman 1992, 1996; Cohen 1999). To differ from past interpretations, which described two phases of activity in the Early Bronze II and Intermediate Bronze with a gap in the Early Bronze III (e.g., Cohen 1999), recent work shows activity from the Early Bronze I until the middle of the Intermediate Bronze (ca. 3600–2200 B.C.E.; Gidding 2016; Ben-Yosef et al. 2016; Dunseth et al. 2017; Dunseth, Finkelstein, and Shahack-Gross 2018; Finkelstein et al. 2018).
- The Iron IIA (late 10th–late 9th centuries B.C.E.): Remains consist of enclosed structures (described as "forts" in the past, e.g., Cohen and Cohen-Amin 2004), isolated houses and pens, and adjacent settlements. There is debate regarding terraced agricultural activity in the desert during the Iron Age (compare Haiman 2012a; Shahack-Gross and Finkelstein 2015, 2017; and Bruins and van der Plicht 2017a, 2017b; for OSL data from agricultural terraces, see Avni, Porat, and Avni 2012, 2013; Avni, Avni, and Porat 2019). Opportunistic farming has been suggested (e.g., Haiman 1994, 2012a), but the current authors argue subsistence agriculture was not conducted in the Negev Highlands during the Iron Age. Regardless, radiocarbon ages from habitation sites put activity in this period between the late 10th and late 9th centuries B.C.E. (Boaretto, Finkelstein, and Shahack-Gross 2010; Shahack-Gross et al. 2014).
- The Byzantine–Early Islamic periods (4th–11th centuries C.E.): This era is characterized by the entire spectrum of settlements—from animal pens and isolated farms to large towns (Rubin 1990; Avni 2014). Though scholars placed the beginning of this phase of activity in the Hellenistic–Roman periods (the Nabatean period), evidence for widespread permanent sites in the early part of this time span is not obvious (e.g., Tepper et al. 2018, although see Erickson-Gini and Israel 2013). The nature and decline of the Byzantine–Early Islamic settlement systems are debated: either abruptly during the Late Byzantine period or gradually in the Early Islamic period (Haiman 1995; Avni 2014; Avni, Avni, and Porat 2019). Recent studies indicate the gradual decline of farming during the Late Byzantine period (mid-6th century C.E., Bar-Oz et al. 2019; Fuks et al. 2020; although see Avni, Avni, and Porat 2019 for a different perspective). At the same time there appears to be a growth of pastoral activity during the Early Islamic period at town sites (Butler et al. 2020), although the pattern is less clear at other sites in the region (Avni 2014).

Subsistence in the first two settlement waves was based on animal husbandry and the copper industry in the Arabah, with no evidence for agricultural activity in the first (Dunseth, Finkelstein, and Shahack-Gross 2018; Vardi and Rosen 2020: especially pp. 245–46 for the Early and Intermediate Bronze Ages), and no evidence for systematic agricultural activity in the second (Shahack-Gross and Finkelstein 2008; Shahack-Gross et al. 2014 for the Iron IIA, but see above). It seems that during these periods participation in the copper industry, including the transportation of the products to the north, led at least some of the Negev Highlands groups to establish permanent sites (Finkelstein 2014; Ben-Yosef et al. 2016; Finkelstein et al. 2018). Remains on the ground (Avni, Porat, and Avni 2013), textual records (Kraemer 1958; Mayerson 1994), and zooarchaeological, archaeobotanical, and geoarchaeological investigations (Shahack-Gross et al. 2014; Bar-Oz et al. 2019; Dunseth et al. 2019; Marom et al. 2019; Blevis et al. 2020; Butler et al. 2020; Fuks et al. 2020; Lantos, Bar-Oz, and Gambash 2020; Langgut et al. 2021) show that subsistence in the Byzantine–Early Islamic period was more diverse, including animal husbandry, dry-farming and horticulture, and intensive circum-Mediterranean trade—especially the famous Gaza wine.

For the periods between these "waves" of settlement, stone-built constructions have not been identified, or are extremely rare. These include the period from the second half of the Intermediate Bronze through the Middle and Late Bronze Ages and the beginning of the Iron Age (ca. 2200–950 B.C.E.); the Iron IIB–C, Persian (with a few exceptions), and much of the Hellenistic periods (ca. 800–200 B.C.E.); and medieval periods (ca. 11th C.E. until the Ottoman period). Yet, numerous radiocarbon samples collected in Negev sites show that during these periods human activity in the region (probably pastoral-nomadic) did not completely cease (e.g., Rosen et al. 2005; Saidel and Erickson-Gini 2014; Bruins, Segal, and van der Plicht 2018). Even dates with ambiguous (or unpublished) contexts indicate activity, albeit more difficult to determine (e.g., Avner and Carmi 2001). At least for the first two periods "lacking" built remains, a shift in the copper industry away from the Arabah to Cyprus seems to have led the local groups to turn back to traditional animal husbandry (Finkelstein 2014; Finkelstein et al. 2018).

[1] For the early periods, see Finkelstein 1995; Cohen 1999; Cohen and Cohen-Amin 2004; Ben-Yosef et al. 2016; Rosen 2017 and references therein; for the Byzantine–Early Islamic period, see Avni 2014.

The arid environment and nature of the region necessitated that people in the Negev Highlands find solutions for obtaining water, especially in areas away from the few permanent springs and wells. Indeed, hundreds of water installations dot the terrain (most relevantly, Evenari et al. 1958: 241–43; Haiman 1994, 1995; Cohen 1999; Cohen and Cohen-Amin 2004). Most of these belong to two types:[2]

1) Round, open reservoirs dug into the relatively impermeable marl of the Ora or Tamar formations, which functions as an aquiclude for the installations. These reservoirs, which may reach up to 10–12 m in diameter and 4–5 m in depth, are lined with stones for stability.
2) Subterranean or rock-cut cisterns (*kharaba*) cut in the soft chalk of the Horsha or Menuha formations. Most are rectangular, with their roofs often supported by one or more square or rectangular rock-cut pillars.

Both types were dug or hewn along hill slopes, which served as their natural water catchment area. Stone-built channels (in some places partly rock-cut) led water from the slope and in some cases flat areas above the slope to the reservoirs or cisterns. These channels can be up to hundreds of meters in length, collecting water from catchments larger than a few km^2. In both cases, a spoil pile can often be found immediately next to the reservoir/cistern, created by the material removed during construction as well as maintenance (cleaning of sediment infill) over the years of use (Junge et al. 2018, 2021). Today, most installations are infilled by sediments accumulated since the last significant cleaning operation.

According to conventional wisdom, there is an assumed technological and chronological progress from open reservoirs to rock-cut cisterns (Evenari et al. 1958). Based on proximity to settlement sites and sherd scatters, open reservoirs are traditionally associated with the Iron Age (e.g., Evenari et al. 1958: 241–42; Haiman 1994, 2012b; Cohen and Cohen-Amin 2004: 151–53), although some recent research has suggested dating them to the Early and Intermediate Bronze Ages (Ore, Bruins, and Meir 2020). Simple rock-cut cisterns were also once associated with Iron Age sites (Evenari et al. 1958) but are more commonly dated to the Nabatean–Byzantine era based on a few inscriptions and plaster technology (Rubin 1988). These are problematic assertions for several reasons, including: 1) in the case of the open reservoirs, they are based on circumstance rather than direct evidence as most installations are found in proximity to sites from different periods and there is rarely pottery or radiocarbon evidence available for dating them; and 2) many cisterns were maintained and renovated until modern times (e.g., Marx 1967; for documented Mandate-period examples, see Kressel, Ben-David, and Rabi'a 1991: 35, 48, especially nn. 41–42), muddying their long-term chronology.

For these reasons, a geoarchaeological and optically stimulated luminescence (OSL) dating project of water installations in the Negev Highlands was initiated. The use of OSL as the preferred dating technique is based on the fact that the *time of sediment deposition*—fluvial or anthropogenic—can be constrained using this method. The approach presented here focused on trenching three parts of these water collection systems: 1) the spoil piles down to the contact between the paleosurface and construction deposits overlain by maintenance material, 2) the sediments accumulated within the water reservoir/cistern itself, and 3) sediments accumulated in the channels and sedimentation pools. Dating the final exposure of the paleosurface to sunlight provided the time these sediments (i.e., slope or wadi deposits) accumulated before cistern or reservoir construction, while dating the anthropogenic deposits of the spoil pile above this contact indicated the time of construction and maintenance activities. Similar approaches have been used to explore other water management systems in arid regions, including qanats in Iran and Spain (Bailif et al. 2015, 2018; Fattahi 2015).

Dating sediments accumulated within reservoirs, channels, and sedimentation pools provided the time of cessation of maintenance activities. This approach works well in both open reservoirs (Junge et al. 2018) and rock-cut cisterns (Junge et al. 2021; see also Lucke et al. 2019; Tepper, Porat, and Bar-Oz 2020). Altogether, ten installations were examined—five open reservoirs and five rock-cut cisterns (**Fig. 1b**, **Table 1**)—to survey a range of possible construction and maintenance phases at various sites in different micro-regions across the Negev. This of course does not exclude the possibility that installations were built or used during periods not identified in this investigation. The authors' previously published results show that: 1) the open reservoir of Haroa, northeast of Sede Boqer, which had conventionally been associated with the nearby Iron IIA site of Atar Haroa (Cohen and Cohen-Amin 2004: 34), was dug in the Early Islamic period and continued (likely episodically) to function from the medieval period until recent centuries (Junge et al. 2018); and 2) two nearby rock-cut installations at the Borot Hazaz site were hewn in the time centering around the Late Roman/Byzantine transition and maintained until recent centuries (Junge et al. 2021).

This paper presents results from seven additional installations—four open reservoirs and three rock-cut cisterns—which add vital information to the subject matter. It then summarizes the entire project and reflects on the project's

[2] Following Evenari et al. 1958; Evenari, Shannan, and Tadmor 1982; Moran and Palmach 1985; Rubin 1988.

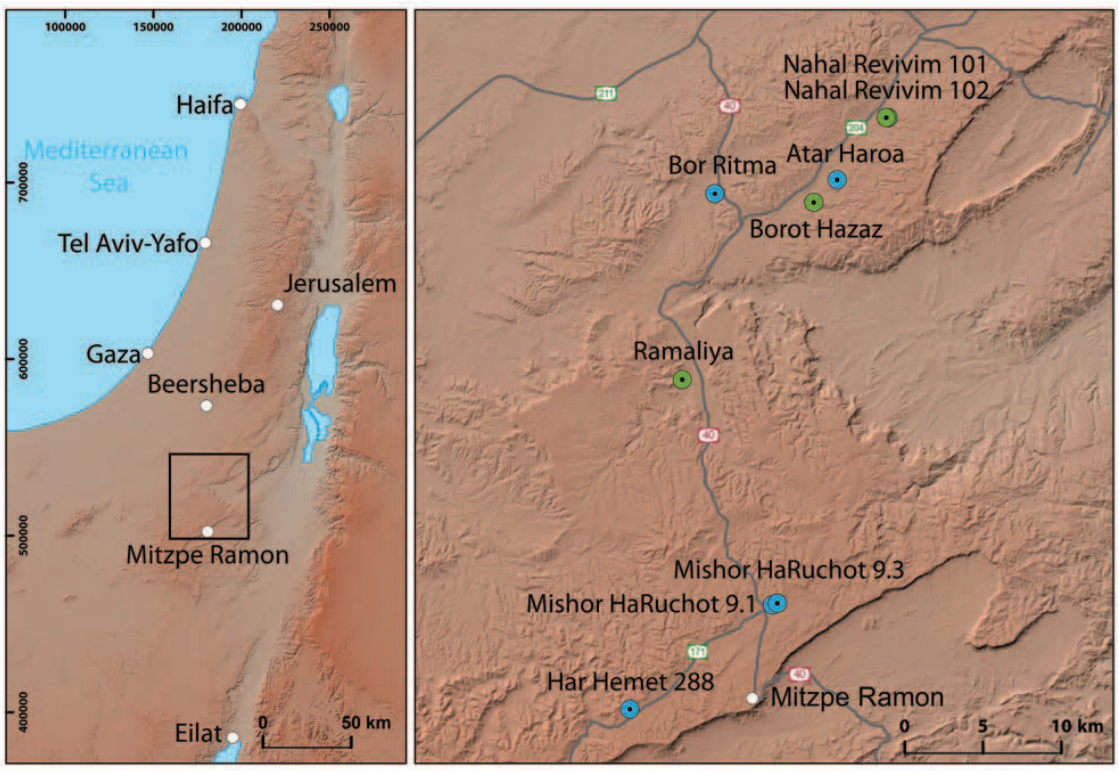


Fig. 1. (a) Map of the southern Levant marking the location of the investigated area; (b) map of the investigated area showing the position of all studied cisterns and reservoirs. Open reservoirs are marked as blue dots; rock-cut cisterns are marked as green dots. (Maps by [a] L. Diehl and [b] B. Ringleb)

implications for reconstructing the history of human activity in the Negev Highlands.

The Sites

Open Reservoirs

Mishor HaRuchot 9.1 and Mishor HaRuchot 9.3. Mishor HaRuchot 9.1 and Mishor HaRuchot 9.3 (**Fig. 2a–b**) are located approximately 330 m apart (the western cistern is located at NIG: 182190 508300), 6 km north of Mizpe Ramon. They are part of a line of such reservoirs dug along the marl layers of the Ora (or Tamar) formation that runs from northeast to southwest at the base of a cuesta 2–3 km north of Makhtesh Ramon. The reservoirs were recorded during the 1950s (Cisterns 3 and 5 respectively in Evenari et al. 1958: figs. 3, 4, 11, pl. 42), and again during the archaeological survey of the area in the 1980s (Rosen and Golan 2016). Importantly, these open reservoirs should not be confused with the reconstructed Bor Haktzinim (The Officer's Cistern)—the sites in this study are approximately 0.5 km to the east. Both include a spoil pile and two channels directing water into them from the slope to the north. Mishor HaRuchot 9.1 also features a small sediment pool between the channels and the reservoir built to decrease the sediment input into the reservoir from the surface runoff by reducing the velocity and sediment transport capacity of the water before it enters the

Table 1. Location (as NIG Coordinates) of All Sites Studied, Including the Haroa Reservoir and the Borot Hazaz Cisterns

Site	*Coordinates NIG*	*Type*
Nahal Revivim 101	189700 539450	Subterranean Cistern
Nahal Revivim 102	189570 539320	Subterranean Cistern
Ramaliya	176450 527560	Subterranean Cistern
Borot Hazaz I & IV	184840 533920	Subterranean Cistern
Har Hemet 288	173050 501640	Open Reservoir
Ritma	178540 534500	Open Reservoir
Mishor HaRuchot 9.1	182190 508300	Open Reservoir
Mishor HaRuchot 9.3	182510 508390	Open Reservoir
Haroa	186330 535360	Open Reservoir

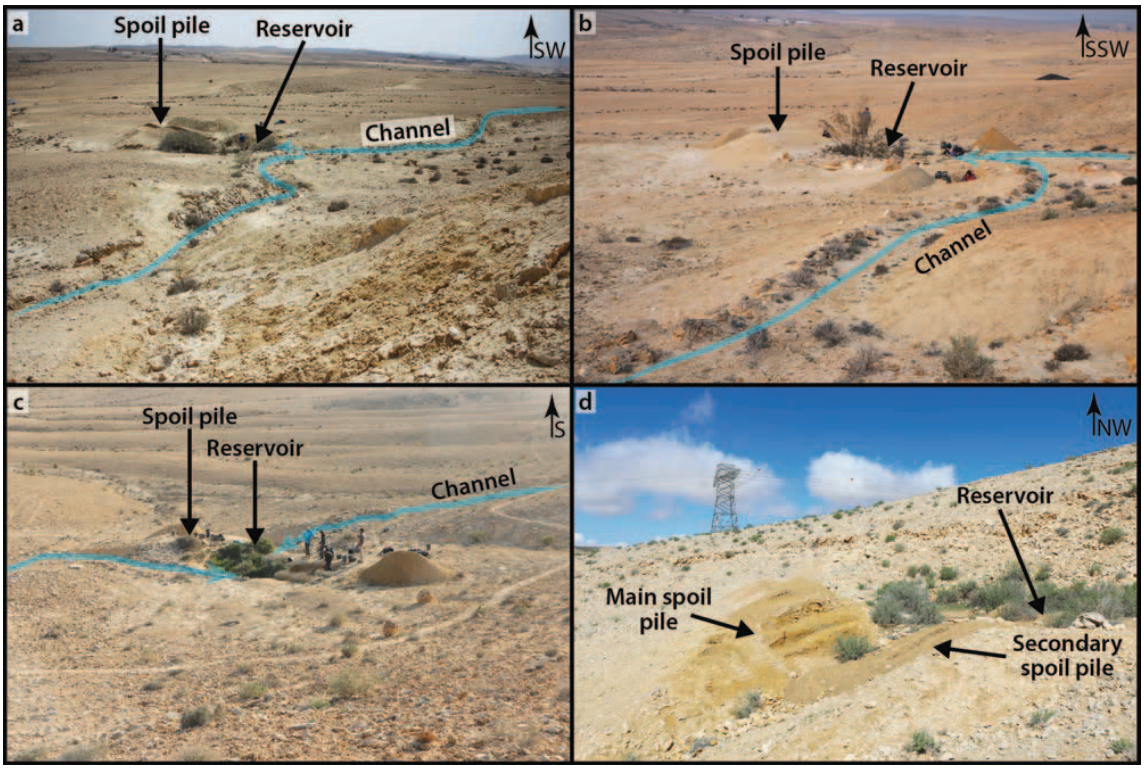


Fig. 2. The open reservoirs with their spoil piles and channels marked: (a) Mishor HaRuchot 9.1; (b) Mishor HaRuchot 9.3; (c) Har Hemet 288 and (d) Ritma. (Photos/image by A. Junge)

structure. Both Mishor HaRuchot 9.1 and 9.3 reservoirs are about 5 m in diameter. Mishor HaRuchot 9.1 is at least 2.5 m deep (the bottom was not reached during our excavation) and Mishor HaRuchot 9.3 is approximately 4 m deep. Note that a schematic sketch of Mishor HaRuchot 9.3 was published in Evenari et al. 1958 (fig. 11, No. 5), which also shows a depth of approximately 4m—it is unclear if the reservoir was cleaned at the time, probed, or merely estimated by the researchers (see below). The reservoirs are surrounded by several archaeological features, especially noteworthy are the remains of an Iron Age "fort" with associated structures and a large open reservoir several hundred meters to their west (Cohen and Cohen-Amin 2004: 90–91). Several round and rectangular structures from the Early and Intermediate Bronze Ages and the Byzantine period are located 200–400 m to the north. Another large reservoir can be found ca. 400 m to the south (for all these, see Rosen and Golan 2016).

Har Hemet 288. Har Hemet 288 (**Fig. 2c**) is located in a similar topographic location as the Mishor HaRuchot reservoirs, about 11 km to the west, ca. 2 km north of the northern rim of Makhtesh Ramon (NIG: 173050 501640; Haiman 1991: 90*). Again, it is important not to confuse this site with Bor Hemet, one of the largest (and reconstructed) open reservoirs in the area, approximately 2 km to the west. Approximately 300 m to the southwest of Har Hemet 288 there is a similar reservoir, and about 400 m to the east are three structures from the Nabatean period with several square rooms and courtyards (Haiman 1991). The Iron IIA "fort" of Har Hemet (Cohen and Cohen-Amin 2004: 107–9) is located on the ridge ca. 1.5 km to the northeast. Har Hemet 288 consists of the reservoir, a spoil pile, and two ca. 100–200 m-long channels that directed water from the catchment area on the slope. Remains of a sedimentation pool can be traced between the western channel and the reservoir. The reservoir is approximately 8 m in diameter, with a minimum depth of 3 m. The bottom was not reached during the excavation.

Ritma. Ritma (**Fig. 2d**) is located on the slope of a small hill, about 3.5 km northwest of Sede Boqer. The Iron IIA "fort" of Horvat Ritma is located ca. 250 m to the northwest of the reservoir (NIG: 178535 534500;

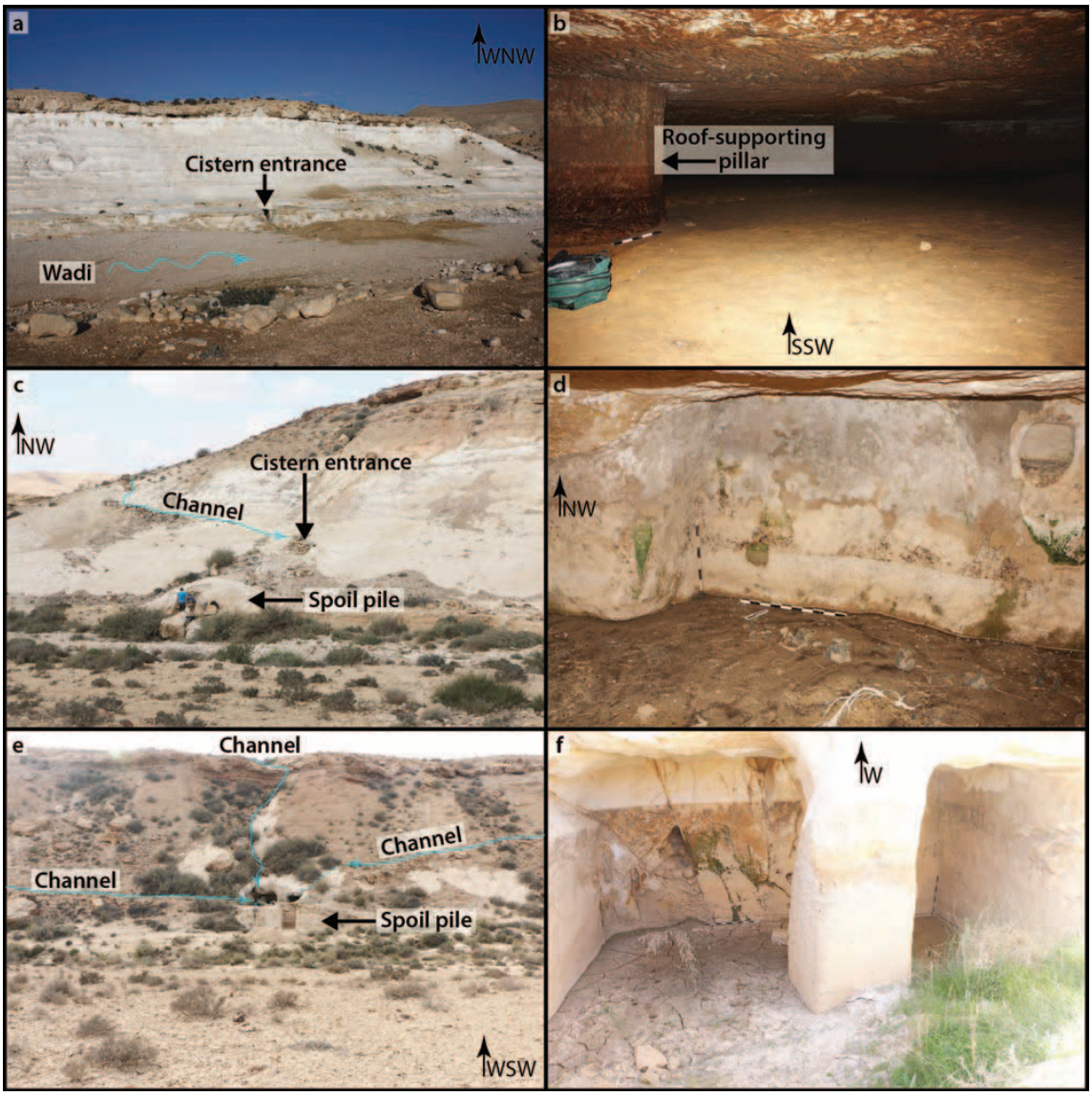


Fig. 3. The rock-cut cisterns: (a) Ramaliya with the wadi it is fed by, Nahal Zin, in the front; (b) Ramaliya from the inside; (c) Nahal Revivim 101 with its spoil pile in the front; (d) the inside of Nahal Revivim 101; (e) Nahal Revivim 102 with its spoil pile in the front; (f) the inside of Nahal Revivim 102. (Photos/image by A. Junge)

Meshel 1977). Two more reservoirs are located in this area. The site consists of the reservoir, the remains of a channel directing water from the slope into the reservoir, and a two-part spoil pile that was either cut by reservoir overflow in antiquity or was two separate spoil piles originally. The size of the reservoir cannot be determined due to complete sediment refill.

Rock-cut Cisterns

Nahal Revivim 101 and Nahal Revivim 102. Nahal Revivim 101 and Nahal Revivim 102 (**Fig. 3c–f**) are located only 100 m apart along the footslopes of the same wadi, 6 km southwest of modern Yeruham (NIG: 189700 539450; Moran and Palmach 1985). Each cistern has a

spoil pile located along the edge of the wadi. Nahal Revivim 101 (the smaller, eastern cistern) is ca. 6 × 5 m in size and about 3 m deep, with a capacity of ca. 90 m^3. This cistern is fed by a stone-built channel on the plateau north of the wadi that leads into a rock-cut channel on the slope. Nahal Revivim 102 is fed by two stone-built channels bringing water from the slope, and a third stone-built channel that collected water from the plateau above the wadi. This cistern is ca. 6–8 m wide and over 5 m from roof to base, although due to a low-lying entrance the capacity is only ca. 140 m^3. The roof is supported by a single hewn central pillar. Moran and Palmach (1985) noted a rock-cut stairway along the western side of the cistern that is not visible today. They also mention use and maintenance by Bedouin until the last few decades.

Ramaliya. Ramaliya (**Fig. 3a–b**) is a rock-cut subterranean cistern located about 1.5 km west of the ancient Nabatean–Byzantine city of Avdat (NIG: 176450 522755; Glueck 1958). It was cut into the soft chalk of the Horsha formation. The cistern measures ca. 16 × 19 m and is 4.7 m in depth, resulting in a capacity of ca. 1400 m^3. In the center of the cistern, a 2 × 2 m pillar supports the roof. In contrast to the other sites in this study, no channels are preserved that direct water into the installation. The cistern's entrance faces Nahal Zin (the largest wadi in the area), which fed it through the entrance with water when flooded. A spoil pile recording either construction or maintenance of the cistern was not preserved; likely it was deposited within the wadi and washed away by winter floods. Consequently, only the sediment accumulation within the cistern was trenched and sampled.

Methods

Profiles exposed in the trenches described above were excavated manually by teams of 5–10 people over the course of a few days each. The profiles were sampled according to their stratigraphy. Our previous studies indicated that the paleosurfaces below the spoil piles are composed of colluvial debris or alluvial fines, which are usually distinguishable from the construction spoils. The latter are characterized by massive accumulation of homogenous, randomly oriented, compact chalk or marl material (**Fig. 4a–b**). These deposits are often overlain by loose, soft, and sometimes thinly bedded deposits that result from regular clean-out maintenance of the installation (**Fig. 4c**). Sampling for OSL dating therefore took these visible stratigraphic and sedimentological parameters into consideration, attempting to sample just below the contact between the paleosurface and the construction spoil, as well as the construction and maintenance material. OSL samples were collected considering stratigraphic observations in the field within the cisterns, water reservoirs, channels, and sedimentation pools. In one instance, OSL dating was conducted on mortar (hydraulic cement) that lined the floor of a cistern.

To further assist age interpretation, sediment micromorphological samples accompanied OSL dating (**Fig. 4**). This method focused on sampling sediments associated with stratigraphic contacts, specifically between the paleosurface and construction deposits, and between the latter and maintenance deposits. Micromorphological samples were also collected within stratigraphic units (e.g., sediments within installations). The purpose of this analysis was to characterize the deposits, for example, identifying paleosurfaces, distinguishing between anthropogenic construction material and material removed from installations during clean-out and (re)deposition on the spoil pile, and characterizing water-lain deposits within the reservoirs/cisterns. Additionally, micromorphological observations assisted in identifying the source(s) of quartz grains in the various deposits dated by OSL—whether windblown, from sheet-wash along cracks, or brought in by (modern or ancient) bioturbation. These observations proved useful for the understanding of the origin of the quartz grains and the interpretation of the ages obtained by OSL dating.

In the case of cisterns hewn into chalk bedrock and reservoirs dug into marl, both of which naturally lack the quartz required for OSL dating, it is assumed that the quartz grains identified and used for dating construction material originate from windblown and/or trampled-in dust mixed into these deposits during construction activities. This is supported by the size of the installations, which necessitate excavation and/or construction longer than a few days' work at any site (e.g., Erasmus 1965). Quartz grains used for dating maintenance material were primarily transported into the installations during rain events by surface runoff, and later removed and deposited on the spoil piles by human activity, with a minor quartz input deposited by wind. Each OSL age was evaluated in comparison with the results of other OSL samples from the same event and surrounding layers, and consideration of statistical properties of the subsample distribution of each sample. In many cases, older-than-expected ages can be explained as the result from insufficient bleaching, while younger-than-expected ages can be associated with post-depositional mixing. While the latter is mainly detected by stratigraphic evidence and cannot be corrected for, the former can be addressed by the use of the minimum age model (MAM) in OSL dating (Cunningham and Wallinga 2012). In cases where the resetting of the OSL signal during deposition is insufficient, samples might still overestimate the actual age even after the application of the MAM (for more details, see Junge et al. 2021).

Six vegetal samples from the Nahal Revivim sites were radiocarbon dated. Details on the preparation and

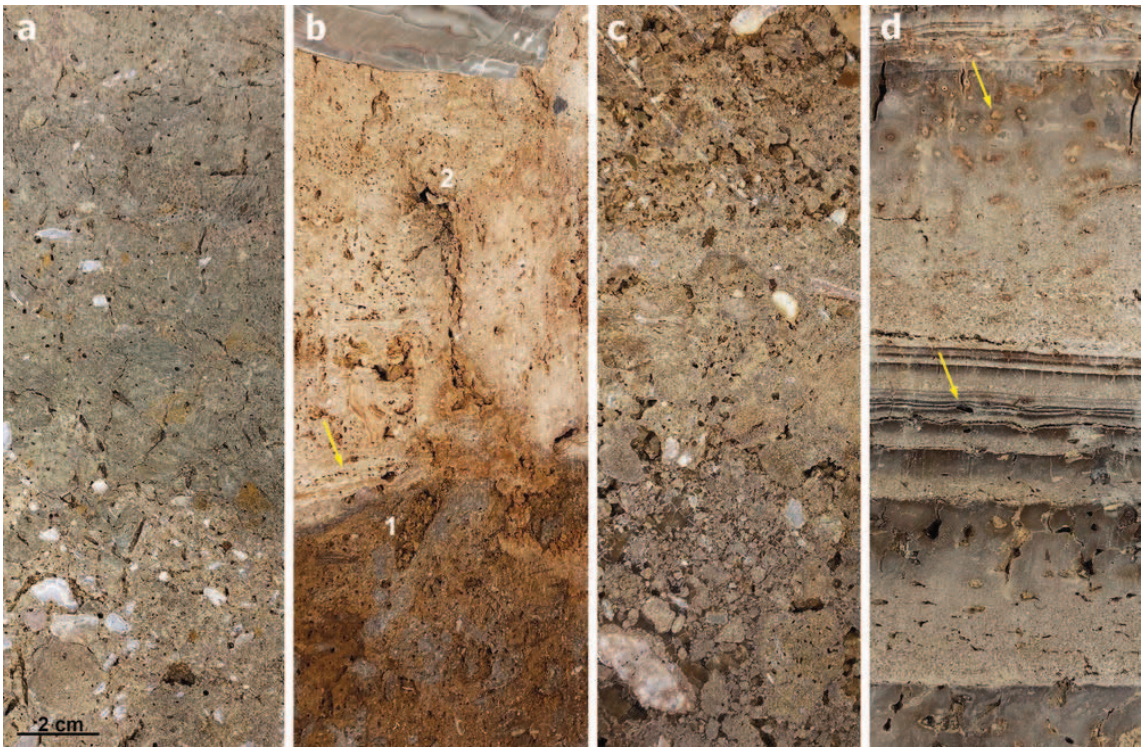


Fig. 4. Consolidated and cut micromorphology monoliths. Scale bar in (a) applies to all panels. (a) Pre-construction (lower deposit, light colored) and construction (upper deposit, greenish-gray) sediments typical of Mishor Haruchot sites situated on marl (example from the Mishor Haruchot 9.1 spoil pile). Pre-construction material is colluvium that includes limestone cobbles (white fragments in image) and colluviated loess deposits (light-colored sediment matrix). Construction material is greenish-gray marl. Note its patchy (fragmented) appearance with occasional lighter areas and limestone cobbles due to mixing with pre-construction deposits during construction activities. Note also that the contact between these units is irregular. The darker brown patches within the marl are oxide nodules typical of this rock formation; (b) Contact between pre-construction (bottom, brown deposit) and construction (upper, light-colored) sediments typical of sites situated on chalk (example from the Nahal Revivim 101 spoil pile). The contact between these two deposits includes disturbances that may affect OSL dating: (1) oval insect burrow infilled with sediments; (2) a vertical crack that goes from the top unit into the lower one, showing infiltration of sediments along it. The arrow indicates a suite of bedded deposits similar to those found within water reservoirs, yet these may in fact be the result of local erosion and deposition by water activity along the voids between the large construction debris; (c) Maintenance deposits (example from the Mishor Haruchot 9.1 spoil pile). Note the granular appearance associated with many voids, giving this deposit its fluffy nature; (d) Sediments accumulating within water reservoirs (example from the Nahal Revivim 101 cistern). These sediments are typified by laminations of various thicknesses representing depositions after rain/flood events. Most layers exhibit graded bedding: coarser grains of sand and occasional gravel at the bottom (lighter-colored beds) and fining upwards to silt and clay (darker-colored beds). Black and orange-colored nodules (examples indicated by arrows) are manganese and iron oxides that formed in hydromorphic (long-term inundation) conditions typical to water reservoirs and cisterns. (Photos/image by R. Shahack-Gross)

measurements are given in the online supplementary material and results can be found in supplementary Table S3.

Preparation of the micromorphology blocks for the thin section analyses, sample preparation of the coarse-grain quartz fraction for OSL dating, as well as information on the OSL measurements and statistical analyses are described in detail elsewhere (Junge et al. 2018, 2021). The OSL preparation steps are presented in the online supplementary material; these differ slightly from those deployed in the authors' previous studies.

OSL results are reported with higher accuracy (rounded to tens of years) for the last 1,000 years and lower accuracy (rounded to hundreds of years) for earlier periods. All OSL data is provided in Tables S1 and S2 in the online supplementary material and all OSL ages are presented in a diagram in **Figure 5**. For all the figures presented below, orthophotos were created using Agisoft Metashape following Megiddo Expedition protocols based on Prins 2016. In the photos and drawings of the sections dug through the spoil piles and inside the installations, the locations of the OSL samples are marked by black boxes,

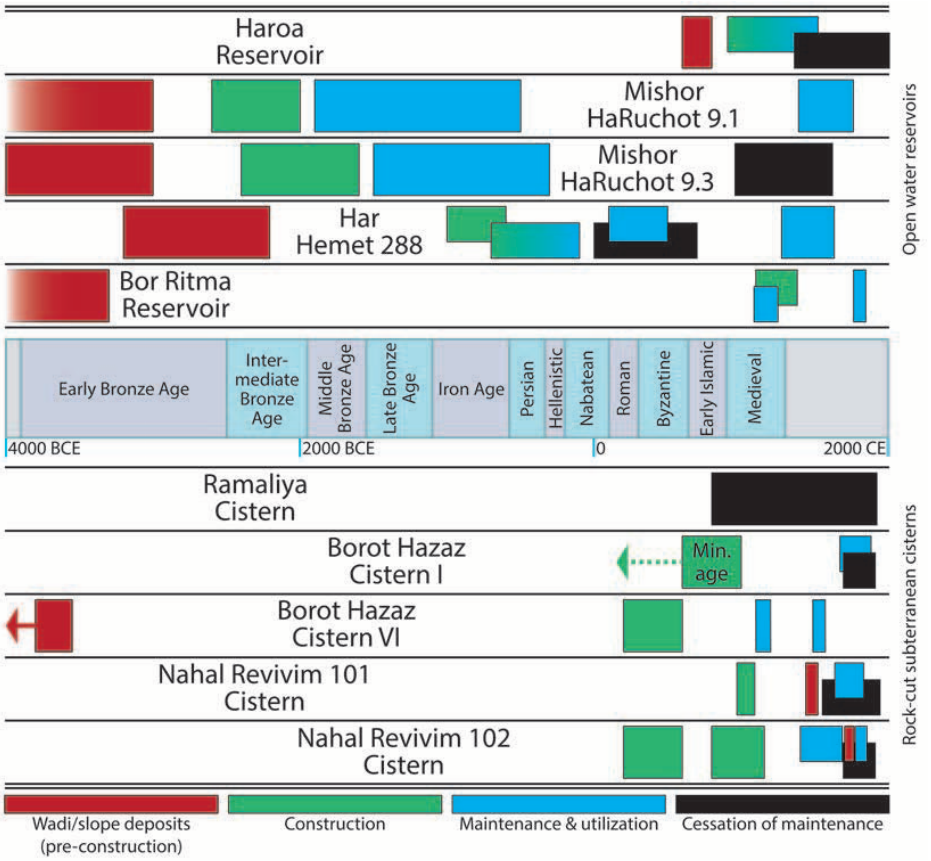


Fig. 5. Summary figure showing the OSL ages from all studied open water reservoirs (top) and rock-cut subterranean cisterns (bottom). The ages are assigned to the different events the deposition of sampled sediments is linked to: pre-construction wadi or slope deposits (red), construction (green), maintenance and utilization (blue), and cessation of maintenance (black). Detailed data from the Haroa reservoir can be found in Junge et al. 2018 and for the Borot Hazaz cisterns in Junge et al. 2021. (Image by A. Junge)

micromorphology samples by white boxes, and positions of radiocarbon samples by red boxes. Red arrows mark the location of modern (20th century) plastic and metal trash.

Results and Discussion

Open Reservoirs

Open reservoirs are described in chronological order of construction.

Mishor Haruchot 9.3. A trench was cut approximately 1.5 × 7.5 m through the ca. 2 m-high spoil pile (**Fig. 6**). At its base, it was not possible to extract a sufficient amount of quartz grains from the green-grayish marl bedrock for OSL measurements. The layer above it is composed of weathered marl bedrock fragments mixed with limestone gravels, as noted micromorphologically. This layer, representing pre-construction deposits, yielded an OSL age of 5.5 ± 0.5 ka (4000–3000 B.C.E.; Sample Gi845), meaning it was last exposed to sunlight during the late Chalcolithic or Early Bronze Age I. The remaining samples in this section yielded ages of 2.7 ± 0.4 ka (1100–300 B.C.E.; Sample Gi846), 3.1 ± 0.2 ka (1300–900 B.C.E.; Sample Gi847), 3.2 ± 0.3 ka (1500–900 B.C.E.; Sample Gi848), and 2.7 ± 0.2 ka (900–500 B.C.E.; Sample Gi849). They are identified as maintenance operations of the reservoir by micromorphological analyses. All four ages are consistent within their errors. They point to activities in the Late Bronze–Iron I–early

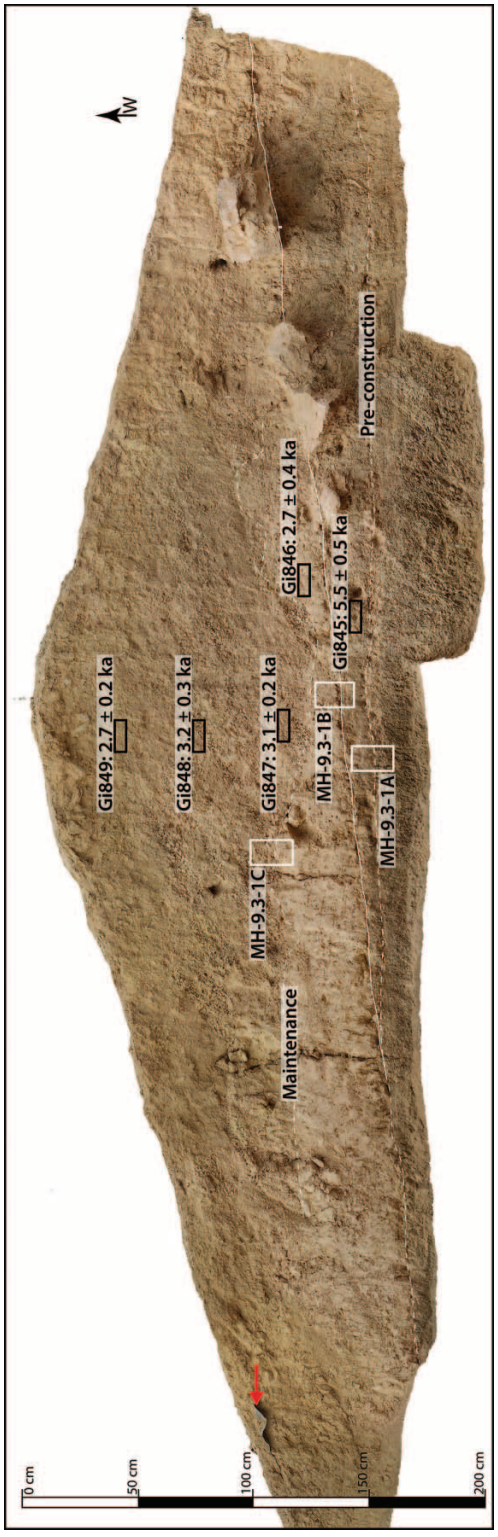


Fig. 6. The section in the trench dug through the spoil pile of Mishor HaRuchot 9.3. (Photos/image by A. Junge)

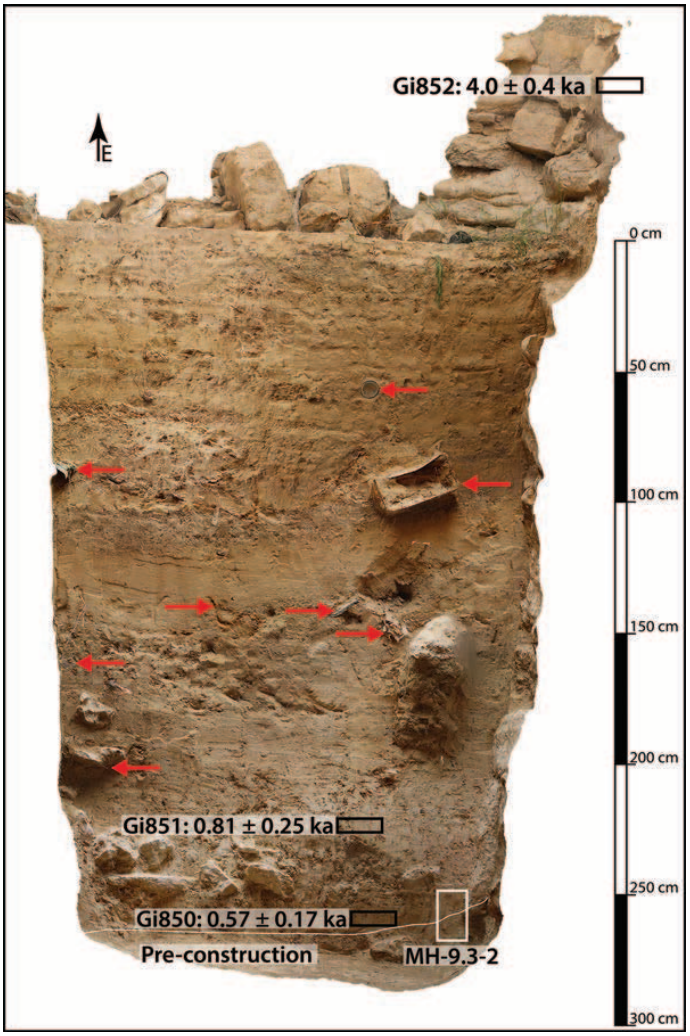


Fig. 7. The section in the trench dug inside Mishor HaRuchot 9.3. Note OSL Sample Gi852, collected from the sediments between the stones lined up to reinforce the reservoir walls at the top. (Photos/image by A. Junge)

Iron IIA time span, possibly related to the Iron Age "fort" with associated structures located several hundred meters to the west (Cohen and Cohen-Amin 2004: 90–91).

With the intention of dating the construction of the stone lining of the reservoir, at Mishor Haruchot 9.3 the upper three courses of the reservoir's stone lining was removed in one location to sample sediments between the stones for OSL dating (**Fig. 7**). This sample resulted in an age of 4.0 ± 0.4 ka (2400–1600 B.C.E.; Sample Gi852). This age can be interpreted as indicating the time of construction of the reservoir or later renovations of the stone lining. This sample is older than the maintenance material in the spoil pile, indicating that the earliest possible time of initial construction was sometime between the Intermediate and Middle Bronze Ages, while maintenance took place (likely episodically) during the Late Bronze–Iron IIA.

The sediment accumulation within the reservoir displayed modern trash down to a depth of 2 m (**Fig. 7**). Sediments below 2 m were free of modern material, all the way down to the hard green-gray marl that is assumed to have served as the reservoir's aquiclude. The micromorphological

sample identified water-lain deposits above the marly bedrock, indicating that the bottom of the reservoir was indeed reached. The bottommost sediments yielded ages of 0.57 ± 0.17 ka (1280–1620 C.E.; Sample Gi850) and 0.81 ± 0.25 ka (960–1460 C.E.; Sample Gi851), which overlap in the late 13th–mid-15th centuries C.E. They represent the last complete cleaning of the cistern during the medieval period.

Mishor HaRuchot 9.1. The 2.2 m spoil pile of this reservoir was cut by an 8 × 1.5 m trench, exposing the greengrayish paleosurface at the southern and northern ends of the trench, construction material throughout the studied section, and sediments removed from the reservoir during maintenance in the center and southern part of the trench (**Fig. 8**). The OSL samples from the paleosurface yielded ages of 6.6 ± 0.3 ka (4900–4300 B.C.E.; Sample Gi394) and 5.6 ± 0.6 ka (3900–3300 B.C.E.; Sample Gi387). The construction material was sampled for OSL dating in three locations, resulting in ages of 5.5 ± 0.3 ka (3800–3200 B.C.E.; Sample Gi388), 4.3 ± 0.3 ka (2600–2000 B.C.E.; Sample Gi391), and 3.0 ± 0.5 ka (1500–500 B.C.E.; Sample Gi392).

Sample Gi388 (construction) agrees with pre-construction Sample Gi387 extracted from the paleosurface. Since there is an expected time gap between the natural deposition of the colluvial sediments and the construction material, the age of Gi388 hints that there was insufficient bleaching of this particular sample, resulting in an age overestimation for the construction. For Gi392, the micromorphological analysis shows that coarse quartz grains were only incorporated into the construction layer through cracks when it had already been deposited. Consequently, Gi392 underestimates the construction time and should be interpreted as indicating an early maintenance phase. Therefore, Sample Gi391 is the most secure, and allows placing the construction of the reservoir in the Early Bronze III or Intermediate Bronze Age. In addition to Gi392, OSL Samples Gi389 (3.5 ± 0.3 ka, 1800–1200 B.C.E.), Gi390 (3.2 ± 0.2 ka, 1400–1000 B.C.E.), and Gi393 (3.7 ± 0.2 ka, 1900–1500 B.C.E.) date maintenance operations (likely punctuated) at the reservoir between the Middle Bronze and Iron Age I. The topmost part of the spoil pile includes modern plastic and glass materials, indicating modern maintenance activities.

The accumulation in a sedimentation pool and sediments below the stones lining the water-leading channels were also sampled for OSL dating. The shallow sedimentation pool accumulation (**Fig. 9a**) yielded an age of 0.52 ± 0.11 ka (1390–1610 C.E.; Sample Gi397) indicating that the last cleaning of this feature took place in the medieval period. The sediments below the channel stones accumulated 0.37 ± 0.11 ka ago (1540–1760 C.E.; Sample Gi398, **Fig. 9b**) in the western channel, and 0.47 ± 0.09 ka ago (1460–1640 C.E.; Sample Gi399, **Fig. 9c**) in the eastern channel. Within the error range, the three ages agree with each other, and thus it is implied that the channels were repaired and the sedimentation pool was cleaned in the medieval period.

The sediment inside this reservoir was dug down to a depth of 2 m. OSL dating was not conducted due to space limitations and the occurrence of modern metal and plastic trash throughout the trench.

Har Hemet 288. The ca. 2 m-high spoil pile was probed in a 2 × 1.7 m trench (**Fig. 10**). The surface of the spoil pile showed significant bioturbation (likely by desert mammals), and care was taken to trench where it appeared undisturbed. The paleosurface material at the bottom was identified by micromorphological analyses as colluvium capped by water-lain deposits from slope sheetwash. OSL dating of the colluvium resulted in an age of 4.7 ± 0.5 ka (3200–2200 B.C.E.; Sample Gi832), meaning a surface exposed to sunlight at some point during the Early Bronze I–Intermediate Bronze Age. The deposits corresponding to Sample Gi833 as construction material were identified by micromorphology due to the occurrence of marly rock fragments. Its deposition is dated to 2.8 ± 0.2 ka (1000–600 B.C.E.). This age allows us to constrain the construction of the reservoir to the Iron Age IIA, the beginning of this time span, overlapping with the nearby Har Hemet "fort" (Cohen and Cohen-Amin 2004: 107–9). Several layers in the center and top part of the section resulted in the following ages: 2.4 ± 0.3 ka (700–100 B.C.E., Sample Gi834), 0.57 ± 0.18 ka (1270–1630 C.E.; Sample Gi835), and 1.7 ± 0.2 ka (100–500 C.E.; Sample Gi836). Gi834 represents either a second phase of construction to deepen the reservoir or an early phase of cleaning operation sometime in the Iron IIB–Hellenistic. The stratigraphy does not provide a clear shift from construction to maintenance material, preventing a definite interpretation of this sample. An age inversion occurs in the upper two samples, where Gi836 is older than the underlying Gi835. The older-than-expected age can be explained by insufficient bleaching of Gi836.

The sediment accumulation within the reservoir (**Fig. 11**) was excavated to a depth of 3 m without reaching the bottom of the installation. The lower 1.3 m of the excavation is made of fine-grained sediments (Samples Gi837–841) similar to the sediments within other installations of the same type. The five OSL ages from this lower unit span 2.0–1.3 ka (0–700 C.E.). The 1.7 m upper unit of material is primarily debris dominated by gravels and stones (Samples Gi842–843) yielding a deposition age of 4.9 ± 0.9 ka (3800–2000 B.C.E.; Sample Gi842) and 1.9 ± 0.3 ka (200 B.C.E. to 400 C.E.; Sample Gi843). Gi842 is the only clear outlier in this chronostratigraphy; it may be assumed that the age from this sample is overestimated due to incomplete

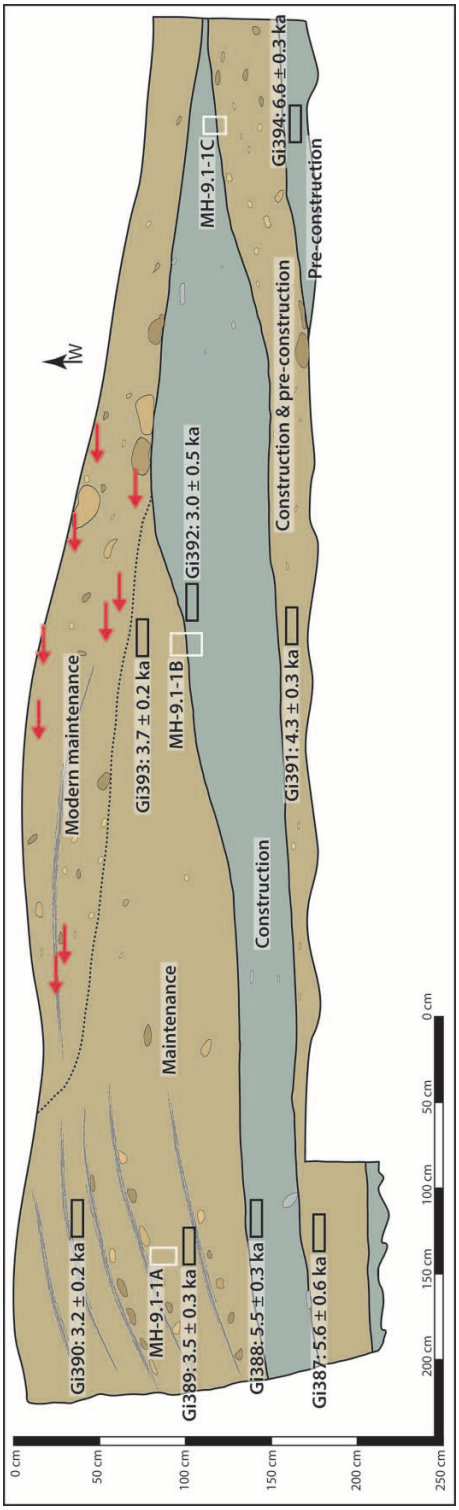


Fig. 8. Schematic drawing of the section in the trench through the spoil pile of Mishor HaRuchot 9.1. (Image by A. Junge)



Fig. 9. (a) The section in the sedimentation pool of Mishor HaRuchot 9.1. For the western (b) and eastern (c) channels, a construction stone was moved and the material below was sampled for OSL dating. (Photos/image by A. Junge)

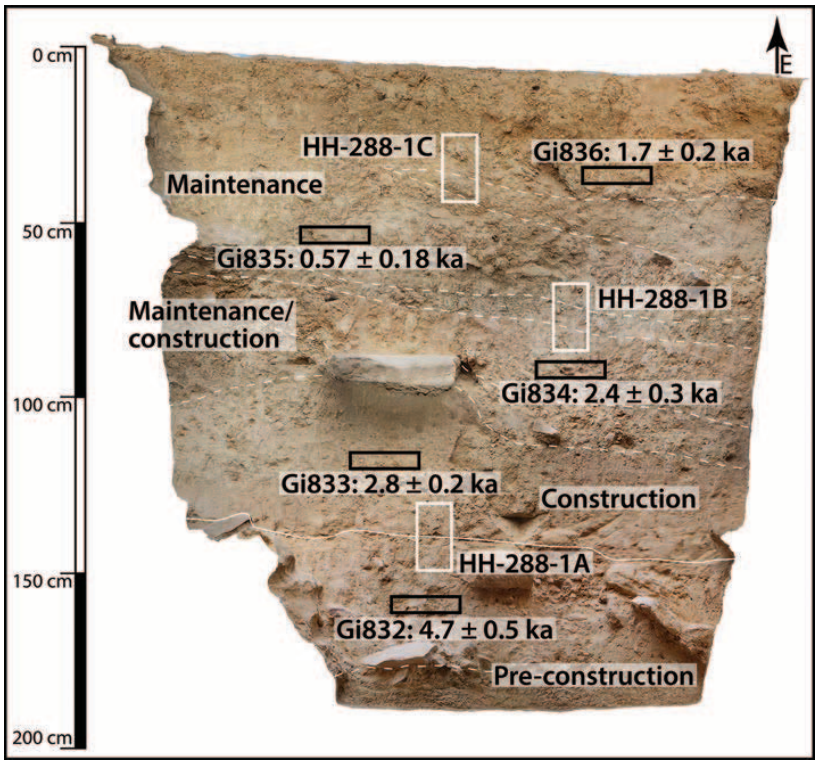


Fig. 10. The section in the trench excavated through the spoil pile of the Har Hemet 288 reservoir. (Photos/image by A. Junge)

bleaching. All other ages from the reservoir are older compared to the maintenance layer in the spoil pile (**Fig. 10**, Gi835: 0.57 ± 0.18 ka). This might hint towards a general bleaching issue of the sediments that were washed into the reservoir at this site. Consequently, the time of cessation is more securely constrained by the last maintenance event dated (Gi835: 0.57 ± 0.18 ka) than by the infill sediments within the installation.

Ritma. The main spoil pile of the Ritma reservoir (**Fig. 12a**) was cut in steps to preserve its original shape. The bottom of the lowermost step is composed of pre-construction material with an OSL age of 5.9 ± 0.6 ka (4500–3300 B.C.E.; Sample Gi605). The overlying construction material was deposited 0.78 ± 0.14 ka ago (1100–1380 C.E.; Sample Gi607), meaning that the reservoir was initially constructed during the medieval period. The very shallow accumulation at the very top of this section yielded evidence for maintenance activity at 0.85 ± 0.08 ka (1090–1250 B.C.E., Sample Gi610), also during the medieval period. The secondary spoil pile (**Fig. 12b**) was cut until large stones were exposed at the bottom of the trench (interpreted as construction or pre-construction deposits). This secondary pile is composed of loose maintenance material. At the contact of the large stones with the maintenance material at the southern end of the trench, diagnostic sherds of an Ottoman Gaza Gray Ware vessel were found, generally accepted as dating between the 17th or 18th and early 20th centuries C.E. (Rosen and Goodfriend 1993; Saidel and Erickson-Gini 2014). The OSL ages in this section showed deposition at 0.22 ± 0.04 ka (1760–1840 C.E.; Sample Gi611) at the bottom and 1.1 ± 0.08 ka (840–1000 C.E.; Sample Gi612) at the top. In combination with the Ottoman sherds at the base of the studied section and the age inversion between the two OSL results, an age overestimation for the upper sample is assumed. At Ritma the inside of the reservoir was not excavated.

All this seems to imply construction of the reservoir in the 12–14th centuries C.E., initial maintenance shortly after construction and a much later cleaning operation in the late 18th or early 19th century C.E.

Haroa. The results from the open reservoir at Haroa were published and discussed elsewhere (Junge et al. 2018). They indicate construction of the reservoir in the

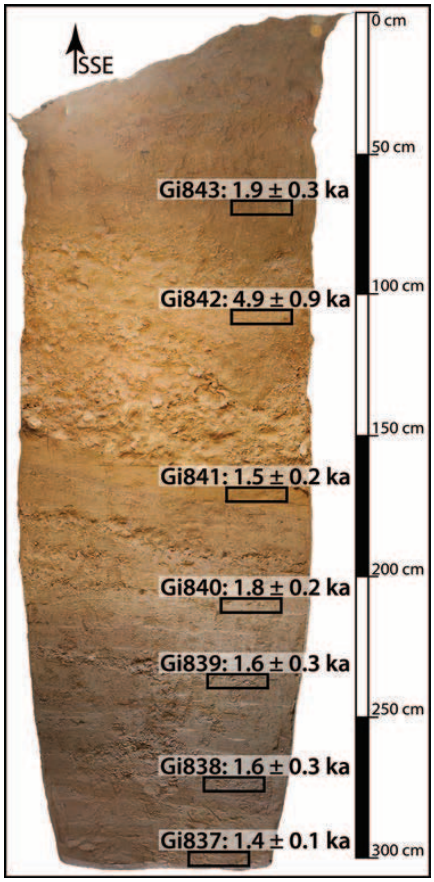


Fig. 11. The section of the trench dug inside Har Hemet 288. (Photos/image by A. Junge)

Early Islamic period (8th–11th centuries C.E.) and final maintenance in the 15th century C.E.

Rock-cut Cisterns

Nahal Revivim 101. The spoil pile was trenched along the side of the wadi, where it was cut by earlier wadi floods. The trench was about 1.5 m deep and 1.6 m long (**Fig. 13**). The fluvial deposits of the wadi were OSL dated to 0.54 ± 0.04 ka (1440–1520 C.E.; Sample Gi823) and the corresponding radiocarbon sample resulted in an age of 460 ± 30 years cal BP (1460–1520 C.E.; Sample NR-101-S-147). The overlying construction material consists of a fine-grained deposit at the bottom, overlain by cut gravels, stones, and boulders originating from the chalk bedrock. The fine-grained sediments were OSL dated to 0.99 ± 0.06 ka (970–1090 C.E.; Sample Gi824), while the radiocarbon age of plant remains from the upper unit resulted in 255 ± 30 years cal BP (late 17th and early 18th century B.C.E.; Sample NR-101-S-84). An age of 0.29 ± 0.10 ka (1720–1740 C.E.; Sample Gi825) for the maintenance material at the topmost part of the spoil pile shows pre-modern cleaning activity at this site. Obviously, the OSL ages of pre-construction and construction material are inversed. The construction material Sample Gi824 does not show typical signs of age overestimation caused by incomplete bleaching. However, it is possible that the underlying pre-construction OSL Sample Gi823 is affected by post-depositional mixing, resulting in an age underestimation. This is suggested by micromorphological evidence for bioturbation, including substantial insect burrowing and root penetration that may have transported younger grains into the pre-construction material (**Fig. 4b**). On the other hand, the radiocarbon age from the pre-construction material is similar to the OSL dating of Gi823. A final explanation for the age inversion cannot be given, hence both the pre-construction and construction ages should be considered with caution.

Inside the cistern, a sediment accumulation of ca. 130 cm was trenched to bedrock (**Fig. 14**). The laminated sediments were sampled for radiocarbon dating in the lower part and for OSL dating throughout the section. The OSL dating yielded stratigraphically disordered ages, from bottom up: modern (Gi826), submodern (Gi827), modern (Gi828, supported by radiocarbon Sample NR-101-C-110), medieval to submodern (Gi829), and modern (Gi830–331). Even though the ages agree with each other when considering a two-sigma error range, the age provided by the maintenance material (0.29 ± 0.10 ka; Sample Gi825) and the radiocarbon dating, as well as the modern trash within the sediment accumulation hint towards an age overestimation of Sample Gi829. This indicates that cessation of maintenance took place in the 18th–20th century C.E.

Overall, it seems plausible that the cistern was cut in the later years of the Early Islamic period (Gi824) and maintenance ceased in submodern times.

Nahal Revivim 102. The spoil pile, already truncated by floods, was cut on the wadi-facing side (**Fig. 15**). The trench is ca. 2 m deep and ca. 1.5 m wide. The fluvial fines of the paleosurface provided an age of 0.27 ± 0.04 ka (1710–1790 C.E.; Sample Gi810). Construction was dated to 0.94 ± 0.10 ka (980–1180 C.E.; Sample Gi811) and 1.1 ± 0.1 ka (800–1000 C.E.; Sample Gi812). This corresponds to the Early Islamic period, or less likely, the medieval period. The age inversion between construction and pre-construction observed in the spoil pile of Nahal Revivim 101 appears here as well. Again, there are no signs of

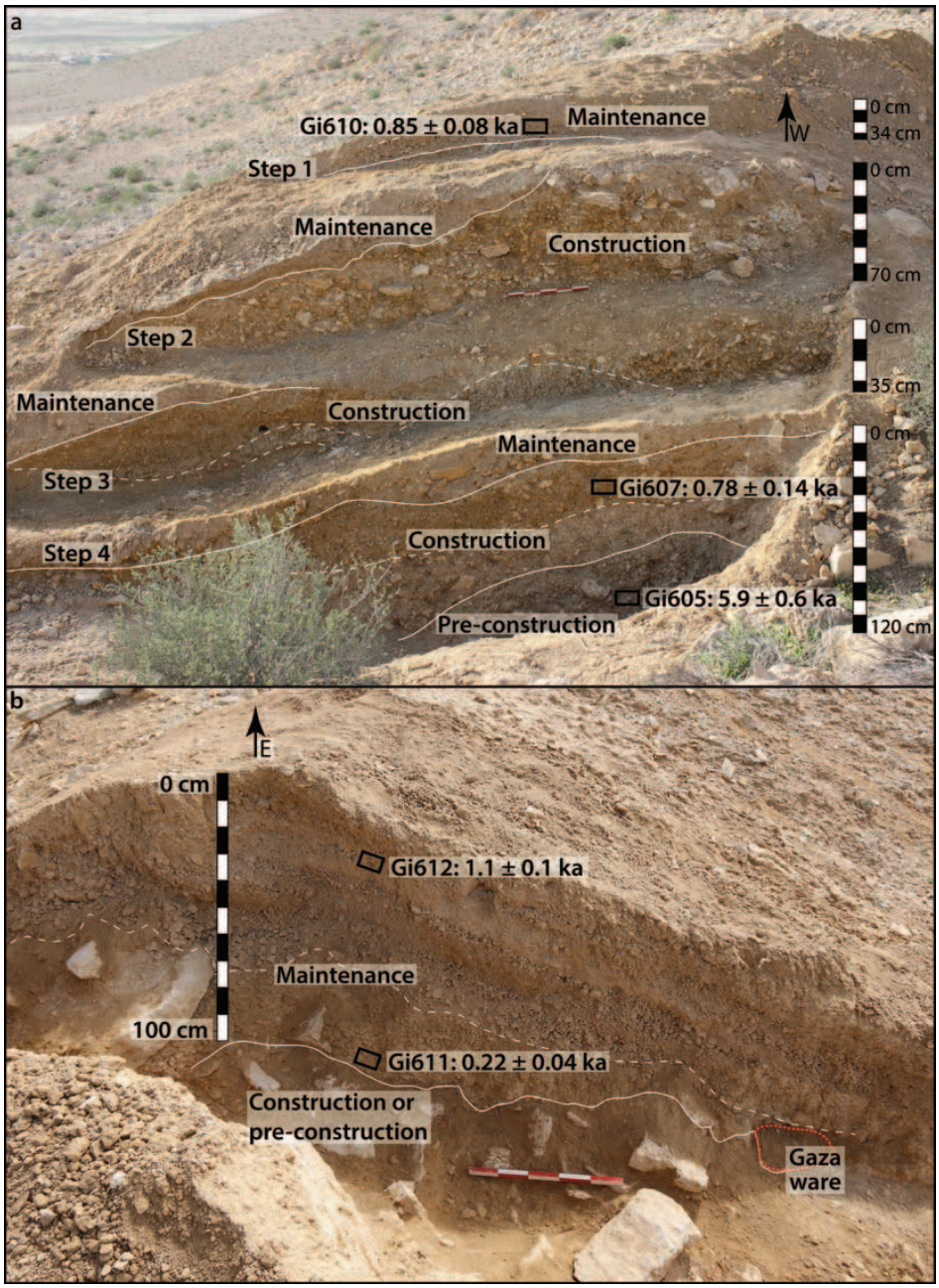


Fig. 12. Trenches through the two spoil piles of the Ritma: the main spoil pile in the west (a), cut by a stepped trench, and the secondary spoil pile in the east (b). The dashed red line marks the position of sherds of an Ottoman Gaza Gray Ware vessel found in the trench through the secondary spoil pile. (Photos/image by A. Junge)

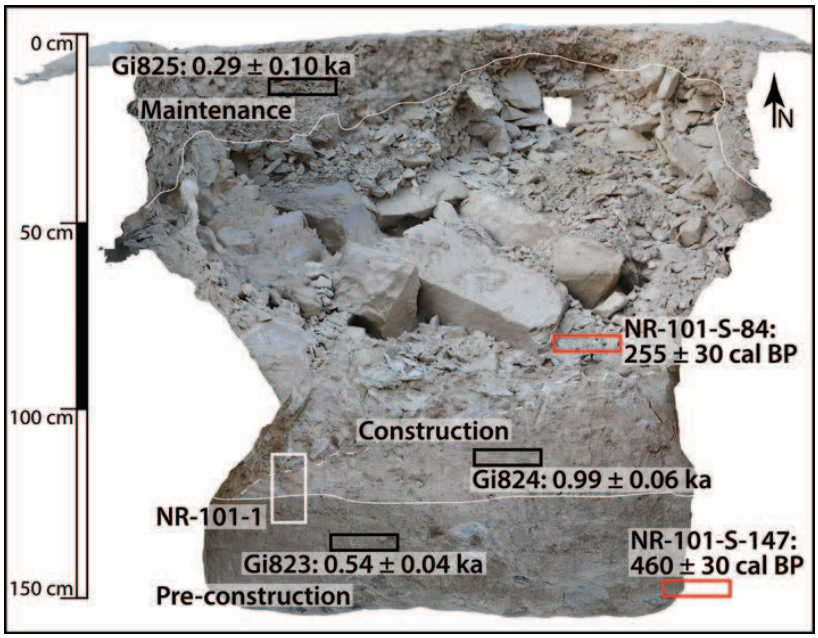


Fig. 13. The section in the trench dug through the spoil pile of Nahal Revivim 101. (Photos/image by A. Junge)

incomplete bleaching that would result in an age overestimation of the construction material. Additionally, the micromorphology analysis does not show any indication of animal borrowing or root penetration into the pre-construction wadi deposits, dismissing the possibility of post-depositional mixing in this case. Although the age inversion at the bottom of the section cannot be explained, the other four ages are chronostratigraphically consistent, suggesting construction between 800 and 1180 C.E. and maintenance dated to 0.49 ± 0.13 ka (1400–1660 C.E.; Sample Gi813) and 0.20 ± 0.03 ka (1790–1850 C.E.; Sample Gi812), indicating cleaning and use of the installation in the late medieval period and up to the modern era.

The excavation inside the cistern exposed over 2 m of sediment accumulation of laminated clay and sandy loam with lenses consisting of gravels and a few stones (**Fig. 16**). The bottom sediments rested on a 3–4 cm-thick plastered mortar surface. A piece of this mortar was sampled for OSL dating. It is assumed that it was applied when the cistern was constructed or shortly thereafter. The dating resulted in an age of 1.6 ± 0.2 ka (200–600 C.E.; Sample Gi815), earlier than the date of construction deposits in the spoil pile (Gi811 and Gi812). This discrepancy may be explained by a slight overestimation of the mortar's age due to incomplete bleaching during manufacture. Plant remains (roots) found between the mortar and the bedrock at the bottom of the trench were sampled for radiocarbon

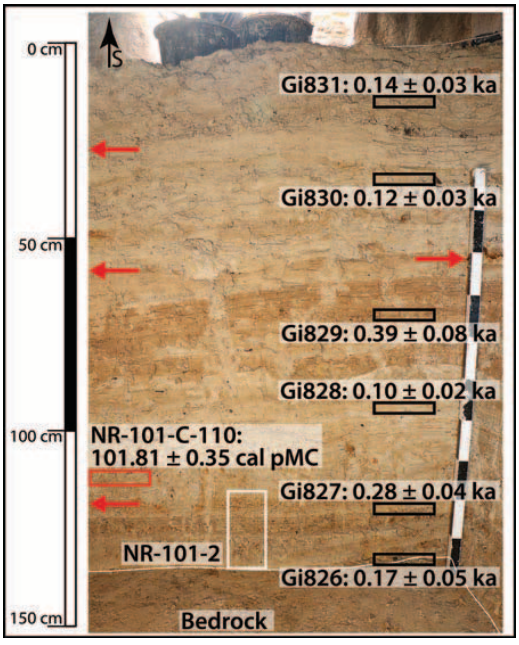


Fig. 14. The section in the trench inside Nahal Revivim 101. (Photos/image by A. Junge)

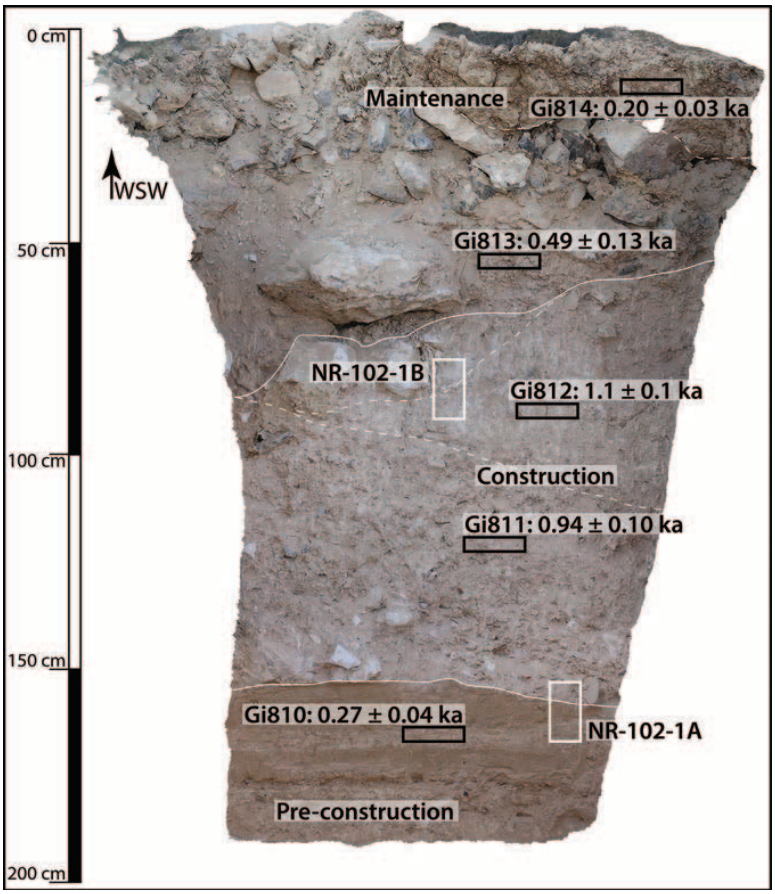


Fig. 15. The section in the trench through the spoil pile of Nahal Revivim 102. (Photos/image by A. Junge)

dating (NR-102-C-217) yielding a modern age, which indicates recent growth in the small gap between bedrock and mortar. The sediment accumulation was constrained by six overlapping OSL ages ranging between 0.28 ± 0.04 ka (1700–1780 B.C.E., Gi820; the oldest sample) and 0.13 ± 0.02 ka (ca. 1900 C.E.; Sample Gi821; the youngest sample), the latter supported by a radiocarbon age (NR-102-C-190) of 180 ± 30 cal BP. Like Nahal Revivim 101, some sort of activity took place here during the last few centuries.

Ramaliya. A deep ca. 3 m trench was cut through the cistern sediments down to bedrock (**Fig. 17**). The OSL age of the lowermost sediment accumulation is 1.0 ± 0.2 ka (800–1200 C.E.; Sample Gi594). Since no spoil pile was preserved at this site, this sample serves as a minimum construction age. The ca. 600-year gap in sedimentation between this sample (Gi594) and those above it (Gi595–Gi604) can best be interpreted as an anthropogenic truncation during an incomplete cleaning of the cistern during past maintenance activities. This also follows the stratigraphic sequence exposed, where an inclined surface (possibly cut) can be observed in the lower deposits. The overlying ages show a short temporal gap between the initial accumulation and the following layers. The OSL ages from Sample Gi595 upwards are not in chronological order. This might by caused by incomplete bleaching of some of the layers due to rapid and turbid sediment transport by wadi flash floods. If these flooding and sediment relocation events occurred overnight, bleaching of the quartz grains would further be reduced.

Borot Hazaz. The results from the rock-cut cisterns at Borot Hazaz are published in Junge et al. 2021. There, one sample from Cistern IV indicates its construction sometime between the late Roman and Byzantine period (200–600 C.E.; Sample Gi589 in Junge et al. 2021: fig. 7), while two other

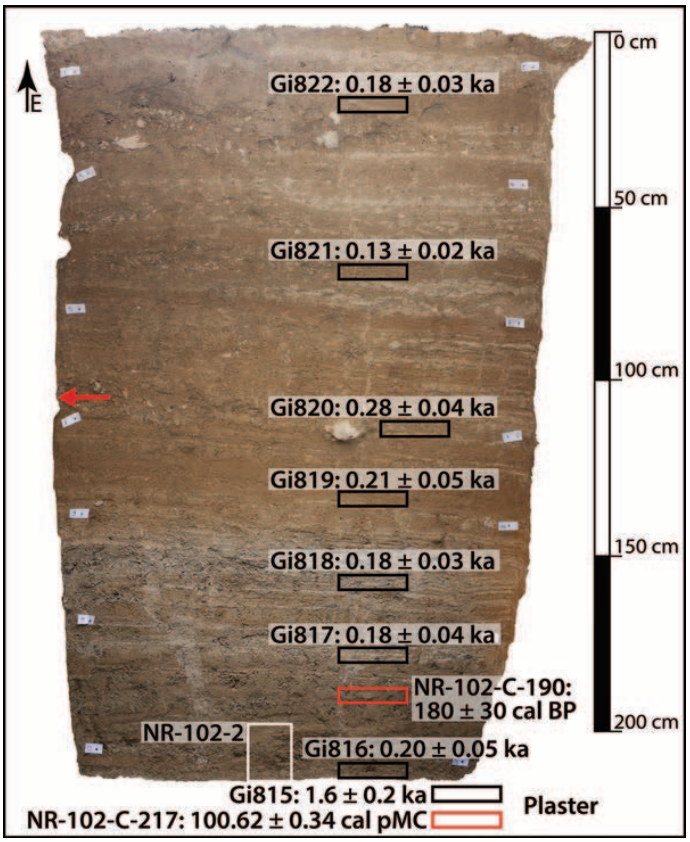


Fig. 16. The section in the trench inside Nahal Revivim 102. (Photos/image by A. Junge)

samples indicate construction in the Byzantine period (400–600 C.E.; Samples Gi591 and Gi592 in Junge et al. 2021: fig. 7). Maintenance took place in the 12th to 16th centuries C.E. For Cistern I, a minimum age for construction was established in the Byzantine/Early Islamic period or earlier (600–1000 B.C.E.; Samples Gi584 and Gi583 in Junge et al. 2021: fig. 5).

Summary

This paper offers an overall interpretation for the history of water storage installations in the Negev Highlands. While this work covers ten out of hundreds of cisterns and water reservoirs in the region, it is the largest study on dating these water installations to date. This interpretation is caged by the acknowledgment that it is likely to change in the future with more data.

This study shows that the use and construction of open reservoirs characterize the entire history of the region. Mishor HaRuchot 9.1 was probably dug in Early Bronze III or the Intermediate Bronze Age, Mishor HaRuchot 9.3 sometime between the Intermediate Bronze, Middle Bronze and Late Bronze, Har Hemet 288 dates to the Iron I–IIA (possibly in relation to the nearby located "fort"), the reservoir near Atar Haroa to the Early Islamic period, and Ritma in the medieval period. Interestingly, the open reservoirs of Ritma and (possibly) Mishor HaRuchot 9.3 were dug in periods that did not leave behind permanent remains (medieval for the former and Middle Bronze or Late Bronze for the latter).

In contrast to previous interpretations, this study shows that the Negev open reservoirs are not simply replaced by more "sophisticated" rock-cut cisterns. The sudden appearance of rock-cut cisterns as a new and fully developed water collection and storage technology, the limited timespan of their construction, and their association with specific sociopolitical circumstances, suggests that this is a diffusion of water management technology into the Negev Highlands. For open reservoirs, once the basic idea of digging into impermeable chalk or marl was established, it was evident in the terrain and relatively easy to imitate and maintain, even by small numbers of

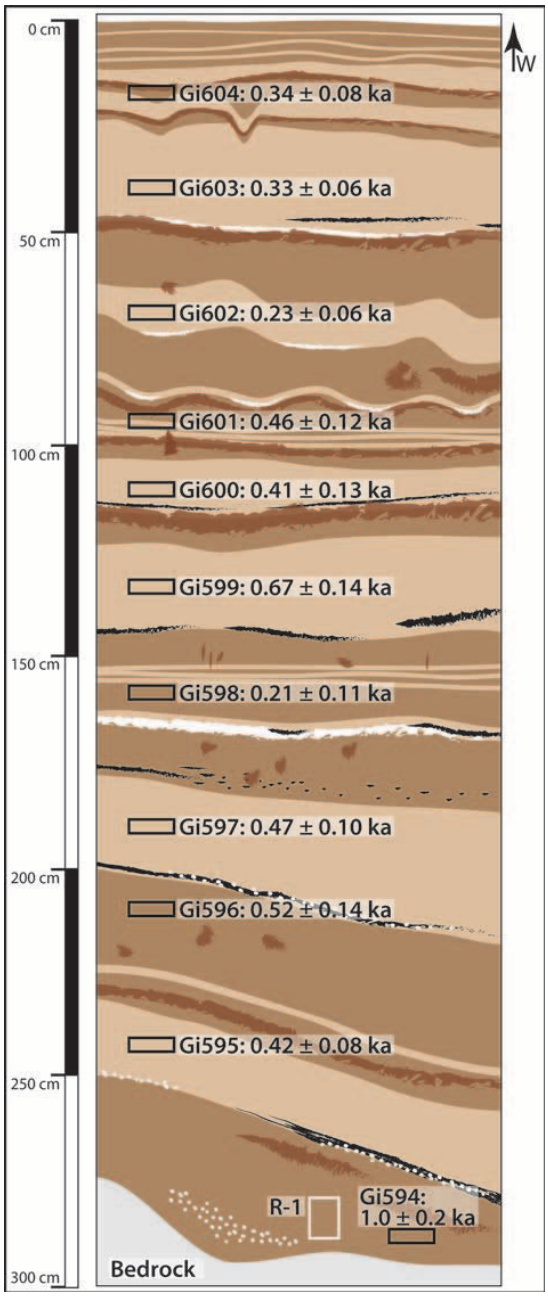


Fig. 17. Schematic drawing of the section in the trench excavated inside the Ramaliya cistern. The coloration of the accumulation shows alternating grain sizes (silty clay in darker brown; sandy silt in lighter brown) with secondary calcium carbonate accumulations (white spots and lines), oxidation (reddish-brown spots and lines), and manganese compounds (black spots and lines). (Image by A. Junge)

people. Given these begin in the late 4th or early 3rd millennium B.C.E., it is proposed they were developed by pastoral groups. Future investigation of open reservoirs is expected to yield additional construction dates, likely in periods not attested in this study. While the data provided here partially support the spatial analysis as outlined in Ore, Bruins, and Meir 2020, spatial correlation is limited. In general, this work contradicts the usual assumption that the Negev open reservoirs can be simply dated according to their proximity to archaeological remains (contra Cohen and Cohen-Amin 2004: 151–53; Haiman 2012b). The same has been shown for the dating of agricultural terraces (Avni, Porat, and Avni 2012, 2013).

The ages from the open reservoir spoil piles show that periodic maintenance continued for many centuries in every single case: at Mishor HaRuchot 9.1 probably throughout the Middle Bronze Age and Iron Age I, at Mishor Haruchot 9.3 in the Late Bronze to Iron Age II, at Har Hemet 288 in the Iron IIB and later, in Haroa until the medieval period, and at Ritma even later. Also note that the channels leading to Mishor HaRuchot 9.1 were repaired in the medieval period. As for the rock-cut cisterns, the spoil piles of Nahal Revivim 101 and Nahal Revivim 102 indicate a date of construction in the Early Islamic period. The age of the mortar inside the Nahal Revivim 102 cistern seems to indicate construction during the Late Byzantine period, but this age might overestimate the timing of mortar manufacture. Our previous work on the system of cisterns at the Borot Hazaz site indicates a date of construction for Cistern IV in the Late Roman or Early Byzantine period and for Cistern I during or before the Late Byzantine/Early Islamic period (Junge et al. 2021). The very large cistern of Ramaliya was constructed during or before the time interval of 800–1200 C.E.

In contrast to the open reservoirs, which could have possibly been dug by small groups of people over a relatively short period of time (e.g., in the authors' experience, a team of 3 people can carefully excavate an average 3 m^3 of sediment infill per day), hewing subterranean cisterns represents considerable commitment of manpower and skill. The large Byzantine–Early Islamic towns and villages of the Negev feature elaborate stone architecture, urban planning, and infrastructure, including large churches and other indications for involvement of the central authorities. Three of the five rock-cut cisterns investigated indeed point to construction in the Byzantine–Early Islamic period. One was constructed either in the same period or slightly earlier (possibly late Roman: Borot Hazaz IV), and in one (Ramaliya) there was no spoil pile preserved to allow the dating of its construction. Still, the range of rock-cut cistern construction is narrow, strongly pointing to construction in the Byzantine–Early Islamic period, rather than the ongoing and continual construction of the open reservoirs.

The work presented here sheds light on two historical questions. First, for now, there is no evidence for cutting subterranean cisterns in the Nabatean period (Hellenistic–Early Roman periods). It is assumed that in this period the population of the Negev Highlands continued to dig, use, and maintain open reservoirs. Second, the results support the notion of a gradual decline of the Byzantine–Early Islamic settlement system, showing construction primarily throughout this period, followed only by maintenance after the decline of the villages and towns (Haiman 1995; Avni 2008; Butler et al. 2020).

Maintenance of the rock-cut cisterns continued through the medieval period, with sediments inside the installations primarily accumulating in recent centuries (though earlier in the Ramaliya cistern). Logic dictates that accumulation of sediments within the water installations—open reservoirs and rock-cut alike—mark periods when maintenance ceased. However, it is likely that the installations continued to be used while only partly cleaned out, even after regular maintenance was abandoned. Hence, dating the complete or final abandonment of water reservoirs and cisterns remains difficult to establish.

Evidence presented here shows that some of the open reservoirs were constructed and maintained during the so-called of Negev Highlands settlement. This therefore provides another indication (in addition to radiocarbon dates; e.g., Avner and Carmi 2001; Rosen et al. 2005) for human activity in the Negev Highlands in periods with no archaeologically visible stone-built constructions. Arguably, the type of activity carried out during "empty periods" was mainly nomadic pastoralism (Finkelstein 1995). In other words, there was continuous human presence in this region over the last five millennia.

Future research should investigate reservoir deposits as environmental archives, as micromorphology shows water-logging features and thus a sedimentary environment conducive for preservation of organic and inorganic environmental proxies such as pollen and phytoliths.

Acknowledgments

This research was supported by a grant (No. FU 417/33-1, with Fuchs as principal investigator and Shahack-Gross and Finkelstein as co-investigators) from the Deutsche Forschungsgemeinschaft (DFG, German Research Foundation). Excavations were conducted under the Israel Antiquities Authority, permit G-17/2018. The authors would like to thank students from Tel Aviv University, Justus-Liebig-University Gießen, and Sacramento State who volunteered in the field for their relentless work and support during the numerous excavations. Special thanks go to Hadar Azrad, Ronnie Avidov, Omer Ze'evi-Berger, and Eli Itkin. Additionally, thanks are due to the anonymous reviewers for their helpful comments that improved this paper.

References

Avner, U., and Carmi, I.
2001 "Settlement Patterns in the Southern Levant Deserts during the 6th–3rd millennia BC: A Revision Based on ^{14}C Dating." *Radiocarbon* 43(3): 1203–16. https://doi.org/10.1017/S0033822200038492

Avni, G.
2008 "The Byzantine-Islamic Transition in the Negev: An Archaeological Perspective." *Jerusalem Studies in Arabic and Islam* 35: 1–26.
2014 *The Byzantine-Islamic Transition in Palestine: An Archaeological Approach*. Oxford Studies in Byzantium. Oxford: Oxford University.

Avni, Y., Avni, G., and Porat, N.
2019 "A Review of the Rise and Fall of Ancient Desert Runoff Agriculture in the Negev Highlands – A Model for the Southern Levant Deserts." *Journal of Arid Environment* 163: 127–37. https://doi.org/10.1016/j.jaridenv.2019.01.010

Avni, G., Porat, N., and Avni, Y.
2013 "Byzantine–Early Islamic Agricultural Systems in the Negev Highlands: Stages of Development as Interpreted through OSL Dating." *Journal of Field Archaeology* 38(4): 332–46. https://doi.org/10.1179/0093469013Z.00000000052

Avni, Y., Porat, N., and Avni, G.
2012 "Pre-farming Environment and OSL Chronology in the Negev Highlands, Israel." *Journal of Arid Environment* 86: 12–27. https://doi.org/10.1016/j.jaridenv.2012.01.002

Bailiff, I. K., Gerrard, C. M., Gutiérrez, A., Snape-Kennedy, L. M., and Wilkinson, K. N.
2015 "Luminescence Dating of Irrigation Systems: Application to a Qanat in Aragón, Spain." *Quaternary Geochronology* 30: 452–59. https://doi.org/10.1016/j.quageo.2015.02.016

Bailiff, I. K., Jankowski, N., Snape, L. M., Gerrard, C. M., Gutiérrez, A., and Wilkinson, K. N.
2018 "Luminescence Dating of Qanat Technology: Prospects for Further Development." *Water History* 10: 73–84. https://doi.org/10.1007/s12685-018-0213-x

Bar-Matthews, M., Ayalon, A., Gilmour, M., Matthews, A., and Hawkesworth, C. J.
2003 "Sea-land Oxygen Isotopic Relationships from Planktonic Foraminifera and Speleothems in the Eastern Mediterranean Region and Their Implication for Paleorainfall during Interglacial Intervals." *Geochimica et Cosmochimica Acta* 67(17): 3181–99. https://doi.org/10.1016/s0016-7037(02)01031-1

Bar-Oz, G., Weissbrod, L., Erickson-Gini, T., Tepper, Y., Malkinson, D., Benzaquen, M., Langgut, D., Dunseth, Z. C., Butler, D. H., Shahack-Gross, R., Roskin, Y., Fuks, D., Weiss, E., Marom, N., Ktalav, I., Blevis, R., Zohar, I., Farhi, Y., Filatova, A., Gorin-Rosen, Y., Xin, Y., and Boaretto, E.
2019 "Ancient Trash Mounds Unravel Urban Collapse a Century before the End of Byzantine Hegemony in the Southern Levant." *Proceedings of the National Academy of Science* 116(17): 8239–48. https://doi.org/10.1073/pnas.1900233116

Ben-Yosef, E., Gidding, A., Tauxe, L., Davidovich, U., Najjar, M., and Levy, T. E.
2016 "Early Bronze Age Copper Production Systems in the Northern Arabah Valley: New Insights from Archaeomagnetic Study of Slag Deposits in Jordan and Israel." *Journal of Archaeological Science* 72: 71–84. https://doi.org/10.1016/j.jas.2016.05.010

Blevis, R., Bar-Oz, G., Tepper, Y., and Zohar, I.
2020 "Fish in the Desert: Identifying Fish Trade Routes and the Role of Red Sea Parrotfish (Scaridae) during the Byzantine and Early Islamic Periods." *Journal of Archaeological Science: Reports* 36: 102808. https://doi.org/10.1016/j.jasrep.2021.102808

Boaretto, E., Finkelstein, I., and Shahack-Gross, R.
2010 "Radiocarbon Results from the Iron IIA Site of Atar Haroa in the Negev Highlands and Their Archaeological and Historical Implications." *Radiocarbon* 52(1): 1–12. https://doi.org/10.1017/S0033822200044982

Butler, D., Dunseth, Z. C., Tepper, Y., Erickson-Gini, T., Bar-Oz, G., and Shahack-Gross, R.
2020 "Byzantine–Early Islamic Resource Management Detected through Micro-geoarchaeological Investigations of Trash Mounds (Negev, Israel)." *PLoS ONE* 15 (10): e0239227 https://doi.org/10.1371/journal.pone.0239227

Bruins, H. J.
2012 "Ancient Desert Agriculture in the Negev and Climate-Zone Boundary Changes during Average, Wet and Drought Years." *Journal of Arid Environments* 86: 28–42. https://doi.org/10.1016/j.jaridenv.2012.01.015

Bruins, H. J., and van der Plicht, J.
2017a "Iron Age Agriculture — A Critical Rejoinder to 'Settlement Oscillations in the Negev Highlands Revisited: The Impact of Microarchaeological Methods'." *Radiocarbon* 59(1): 1–16. https://doi.org/10.1017/RDC.2016.95
2017b "Dating of Iron Age Agriculture in the Negev Highlands: A Response to Shahack-Gross and Finkelstein." *Radiocarbon* 59(4): 1233–39. https://doi.org/10.1017/RDC.2017.57

Bruins, H. J., Segal, I., and van der Plicht, J.
2018 "Bronze Chisel at Horvat Haluqim (Central Negev Highlands) in a Sequence of Radiocarbon Dated Late Bronze to Iron I Layers." Pp. 297–308 in E. Ben-Yosef (ed.), *Mining for Ancient Copper: Essays in Memory of Beno Rothenberg*. Tel Aviv University Sonia and Marco Nadler Institute of Archaeology Monograph Series 37. Tel Aviv: Tel Aviv University, Sonia and Marco Nadler Institute of Archaeology.

Cohen, R.
1999 *Ancient Settlements of the Central Negev: The Chalcolithic Period, the Early Bronze Age and the Middle Bronze I*. Israel Antiquities Authority Reports 6. Jerusalem: Israel Antiquities Authority.

Cohen, R., and Cohen-Amin, R.
2004 *Ancient Settlement of the Negev Highlands: The Iron Age and the Persian Period*. Israel Antiquities Authority Reports 20. Jerusalem: Israel Antiquities Authority.

Cunningham, A. C., and Wallinga, J.
2012 "Realizing the Potential of Fluvial Archives Using Robust OSL Chronologies." *Quaternary Geochronology* 12: 98–106.

Dunseth, Z. C., Finkelstein, I., and Shahack-Gross, R.
2018 "Intermediate Bronze Age Subsistence Practices in the Negev Highlands, Israel: Macro- and Micro-archaeological Results from the sites of Ein Ziq and Nahal Boqer 66." *Journal of Archaeological Science: Reports* 19: 712–26. https://doi.org/10.1016/j.jasrep.2018.03.025

Dunseth, Z. C., Fuks, D., Langgut, D., Weiss, E., Melamed, Y., Butler, D., Yan, X., Boaretto, E., Tepper, Y., Bar-Oz, G., and Shahack-Gross, R.
2019 "Archaeobotanical Proxies and Archaeological Interpretation: A Comparative Study of Phytoliths, Pollen and Seeds in Dung Pellets and Refuse Deposits at Early Islamic Shivta, Negev, Israel." *Quaternary Science Reviews* 211: 166–85. https://doi.org/10.1016/j.quascirev.2019.03.010

Dunseth Z. C., Junge, A., Lomax, J., Boaretto, E., Finkelstein, I., Fuchs, M., and Shahack-Gross, R.
2017 "Dating Archaeological Sites in an Arid Environment: A Multi-Method Case Study in the Negev Highlands, Israel." *Journal of Arid Environments* 144: 156–69. https://doi.org/10.1016/j.jaridenv.2017.05.006

Erasmus, C. J.
1965 "Monument Building: Some Field Experiments." *Southwestern Journal of Anthropology* 21(4): 277–301.

Erickson-Gini, T., and Israel, Y.
2013 "Excavating the Nabataean Incense Road." *Journal of Eastern Mediterranean Archaeology and Heritage Studies* 1(1): 24–53.

Evenari, M., Aharoni, Y., Shanan, L., and Tadmor, N. H.
1958 "The Ancient Desert Agriculture of the Negev: III. Early Beginnings." *Israel Exploration Journal* 8(4): 231–68.

Evenari, M., Shanan, L., and Tadmor, N.
1982 *The Negev: The Challenge of a Desert*. Cambridge:

Harvard University. https://doi.org/10.4159/harvard.9780674419254

Fattahi, M.
2015 "OSL Dating of the Miam Qanat (KĀRIZ) System in NE Iran." *Journal of Archaeological Science* 59: 54–63. https://doi.org/10.1016/j.jas.2015.04.006

Finkelstein, I.
1995 *Living on the Fringe: The Archaeology and History of the Negev, Sinai and Neighbouring Regions in the Bronze and Iron Ages*. Sheffield: Sheffield Academic.
2014 "The Southern Steppe of the Levant ca. 1050–750 BCE: A Framework for a Territorial History." *Palestine Exploration Quarterly* 146(2): 89–104. https://doi.org/10.1179/0031032814Z.00000000092

Finkelstein, I., Adams, M. J., Dunseth, Z. C., and Shahack-Gross, R.
2018 "The Archaeology and History of the Negev and Neighbouring Areas in the Third Millennium BCE: A New Paradigm." *Tel Aviv* 45(1): 63–88. https://doi.org/10.1080/03344355.2018.1412054

Fuks, D., Bar-Oz, G., Tepper, Y., Erickson-Gini, T., Langgut, D., Weissbrod, L., and Weiss, E.
2020 "The Rise and Fall of Viticulture in the Late Antique Negev Highlands Reconstructed from Archaeobotanical and Ceramic Data." *Proceedings of the National Academy of Science* 117(33): 19780–91. https://doi.org/10.1073/pnas.1922200117

Gidding, A.
2016 "Approaches to Production and Distribution in Anthropological Archaeology: Views from the Early Bronze Age of Jordan and Israel." Ph.D. dissertation, University of California, San Diego.

Glueck, N.
1958 "The Seventh Season of Archaeological Exploration in the Negeb." *Bulletin of the American Schools of Oriental Research* 152: 18–38. https://doi.org/10.2307/1356041

Greener, A., Finkelstein, I., and Langgut, D.
2018 "Settlement Oscillations along the Desert Fringes of the Southern Levant: Impact of Climate Versus Economic and Historical Factors." *Ugarit-Forschungen* 49: 165–96.

Haiman, M.
1991 "Archaeological Survey of Israel: Map of Mizpe Ramon—Southwest (200)." Jerusalem: Department of Antiquities.
1992 "Cairn Burials and Cairn Fields in the Negev." *Bulletin of the American Schools of Oriental Research* 287: 25–45. https://doi.org/10.2307/1357137
1994 "The Iron Age II Sites of the Western Negev Highlands." *Israel Exploration Journal* 44(1/2): 36–61.
1995 "Agriculture and Nomad-State Relations in the Negev Desert in the Byzantine and Early Islamic Periods." *Bulletin of the American Schools of Oriental Research* 297: 29–53. https://doi.org/10.2307/1357388
1996 "Early Bronze Age IV Settlement Pattern of the Negev and Sinai Deserts: View from Small Marginal Temporary Sites." *Bulletin of the American Schools of Oriental Research* 303: 1–32. https://doi.org/10.2307/1357468
2012a "Geopolitical Aspects of the Negev Desert in the 11th–10th centuries BCE." Pp: 199–206 in G. Galil, A. Gilboa, A. M. Maeir, and D. Kahn (eds.), *The Ancient Near East in the 12th-10th Centuries BCE: Culture and History, Proceedings of the International Conference Held at the University of Haifa, 2–5 May, 2010*. Alter Orient und Altes Testament Band 392. Münster: Ugarit.
2012b "Dating the Agricultural Terraces in the Southern Levantine Deserts—The Spatial-Contextual Argument." *Journal of Arid Environments* 86: 43–49. https://doi.org/10.1016/j.jaridenv.2012.01.003

Junge, A., Dunseth, Z. C., Shahack-Gross, R., Finkelstein, I., and Fuchs, M.
2021 "Construction and Usage of Rock-Cut Cisterns: A Chronological OSL Approach in the Arid Negev Highlands, Israel." *Archaeological and Anthropological Sciences* 13: 150. https://doi.org/10.1007/s12520-021-01366-5

Junge, A., Lomax, J., Shahack-Gross, R., Finkelstein, I., and Fuchs, M.
2018 "Chronology of an Ancient Water Reservoir and the History of Human Activity in the Negev Highlands, Israel." *Geoarchaeology* 33(6): 695–707. https://doi.org/10.1002/gea.21682

Kafle, H. K., and Bruins, H. J.
2009 "Climatic Trends in Israel 1970–2002: Warmer and Increasing Aridity Inland." *Climatic Change* 96(1–2): 63–77. https://doi.org/10.1007/s10584-009-9578-2

Kidron, G. J.
1999 "Altitude Dependent Dew and Fog in the Negev Desert, Israel." *Agricultural and Forest Meteorology* 96(1–3): 1–8. https://doi.org/10.1016/S0168-1923(99)00043-X

Kraemer, G. J.
1958 *Excavations at Nessana*, Vol. 3, *Non-Literary Papyri*. Princeton: Princeton University.

Kressel, G. M., Ben-David, J., and Rabiʿa, K. A.
1991 "Changes in Land Usage by the Negev Bedouin since the Mid-19th Century." *Nomadic Peoples* 28: 28–55.

Langgut, D., Finkelstein, I., Litt, T., Neumann, F. H., and Stein, M.
2015 "Vegetation and Climate Changes during the Bronze and Iron Ages (~3600–600 BCE) in the Southern Levant Based on Palynological Records." *Radiocarbon* 57(2): 217–36. https://doi.org/10.2458/azu_rc.57.18555

Langgut, D., Tepper, Y., Benzaquen, M., Erickson-Gini, T., and Bar-Oz, G.
2021 "Environment and Horticulture in the Byzantine Negev Desert, Israel: Sustainability, Prosperity and Enigmatic Decline." *Quaternary International* 593–594: 160–77. https://doi.org/10.1016/j.quaint.2020.08.056

Lantos, S., Bar-Oz, G., and Gambash, G.
2020 "Wine from the Desert: Late-Antique Negev Viniculture and the Famous Gaza Wine." *Near Eastern Archaeology* 83(1): 56–64. https://doi.org/10.1086/707483

Lucke, B., Sandler, A., Vanselow, K. A., Bruins, H. J., Abu-Jaber, N., Bäumler, R., Porat, N., and Kouki, P.
2019 "Composition of Modern Dust and Holocene Aeolian Sediments in Archaeological Structures of the Southern Levant." *Atmosphere* 10(12): 762. https://doi.org/10.3390/atmos10120762

Marom, N., Meiri, M., Tepper, Y., Erickson-Gini, T., Reshef, H., Weissbrod, L., and Bar-Oz, G.
2019 "Zooarchaeology of the Social and Economic Upheavals in the Late Antique-Early Islamic Sequence of the Negev Desert." *Scientific Reports* 9: 6702. https://doi.org/10.1038/s41598-019-43169-8

Marx, E.
1967 *Bedouin of the Negev*. New York and Washington: Praeger.

Mayerson, P.
1994 *Monks, Martyrs, Soldiers and Saracens: Papers on the Near East in Late Antiquity (1962–1993)*. Jerusalem: Israel Exploration Society.

Meshel, Z.
1977 "Horvat Ritma – An Iron Age Fortress in the Negev Highlands." *Tel Aviv* 4(3–4): 110–35. https://doi.org/10.1179/033443577788497731

Migowski, C., Stein, M., Prasad, S., Negendank, J. F., and Agnon, A.
2006 "Holocene Climate Variability and Cultural Evolution in the Near East from the Dead Sea Sedimentary Record." *Quaternary Research* 66(3): 421–31. https://doi.org/10.1016/j.yqres.2006.06.010

Moran, O., and Palmach, D.
1985 "The Water Cisterns in the Negev Highlands." Sede Boker: The Society for Protection the Nature in Israel (Hebrew).

Ore, J., Bruins, H. J., and Meir, I. A.
2020 "Ancient Cisterns in the Negev Highlands: Types and Spatial Correlation with Bronze and Iron Age Sites." *Journal of Archaeological Science Reports* 30: 102227. https://doi.org/10.1016/j.jasrep.2020.102227

Orland, I. J., Bar-Matthews, M., Kita, N. T., Ayalon, A., Matthews, A., and Valley, J. W.
2009 "Climate Deterioration in the Eastern Mediterranean as Revealed by Ion Microprobe Analysis of a Speleothem That Grew from 2.2 to 0.9 ka in Soreq Cave, Israel." *Quaternary Research* 71(1): 27–35. https://doi.org/10.1016/j.yqres.2008.08.005

Prins, A. B.
2016 "3D Modelling for Archaeological Documentation: Using the JVRP Method to Record Archaeological Excavations with Millimeter-Accuracy (Version 3.0)." *JVRP White Papers in Archaeological Technology*, www.jezreelvalleyregionalproject.com/3d-modeling

Rosen, S. A.
2017 *Revolutions in the Desert: The Rise of Mobile Pastoralism in the Southern Levant*. New York: Routledge. https://doi.org/10.4324/9781315399942

Rosen, S. A., and Golan, K.
2016 "Map of Mizpe Ramon (201). Archaeological Survey of Israel." http://survey.antiquities.org.il/index_Eng.html#/MapSurvey/2151

Rosen, S. A., and Goodfriend, G. A.
1993 "An Early Date for Gaza Ware from the Northern Negev." *Palestine Exploration Quarterly* 125(2): 143–48. https://doi.org/10.1179/peq.1993.125.2.143

Rosen, S. A., Savinetsky, A. B., Plakht, Y., Kisseleva, N. K., Khassanov, B. F., Pereladov, A. M., and Haiman, M.
2005 "Dung in the Desert: Preliminary Results of the Negev Holocene Ecology Project." *Current Anthropology* 46(2): 317–27. https://doi.org/10.1086/428789

Rubin, R.
1988 "Water Conservation Methods in Israel's Negev Desert in Late Antiquity." *Journal of Historical Geography* 14(3): 229–44. https://doi.org/10.1016/S0305-7488(88)80220-2
1990 *The Negev as a Settled Land: Urbanization and Settlement in the Desert in the Byzantine Period*. Jerusalem: Yad Izhak Ben-Zvi (Hebrew).

Saidel, B. A., and Erickson-Gini, T.
2014 "A Note on the Excavation of an Ottoman and British Mandate Period Bedouin Campground at Nahal Beʿrotayim West in the Negev Desert, Israel." *Arabian Archaeology and Epigraphy* 25(1): 138–45. https://doi.org/10.1111/aae.12032

Shahack-Gross, R., Boaretto, E., Cabanes, D., Katz, O., and Finkelstein, I.
2014 "Subsistence Economy in the Negev Highlands: The Iron Age and the Byzantine/Early Islamic Period." *Levant* 46(1): 98–117. https://doi.org/10.1179/00758914 13Z.00000000034

Shahack-Gross, R., and Finkelstein, I.
2008 "Subsistence Practices in an Arid Environment: A Geoarchaeological Investigation in an Iron Age Site, the Negev Highlands, Israel." *Journal of Archaeological Science* 35(4): 965–82. https://doi.org/10.1016/j.jas.2007.06.019
2015 "The Settlement Oscillations in the Negev Highlands Revisited: The Impact of Micro-Archaeological Methods." *Radiocarbon* 57(2): 253–64. https://doi.org/10.2458/azu_rc.57.18561
2017 "Iron Age Agriculture in the Negev Highlands? Methodological and Factual Comments on Bruins and van der Plicht 2017a (*Radiocarbon* Vol. 59, Nr. 1)." *Radiocarbon* 59(4): 1227–31. https://doi.org/10.1017/RDC.2017.56

Starinsky, A., Zilberman, E., Braun, M., and Sneh, A.
2010 Geological map of Israel 1:50,000: Revivim sheet 18-II. Jerusalem: State of Israel, Ministry of National Infrastructure, Geological Survey.

Tepper, Y., Erickson-Gini, T., Farhi, Y., and Bar Oz, G.
2018 "Probing the Byzantine/Early Islamic Transition in the Negev: The Renewed Shivta Excavations, 2015–2016." *Tel Aviv* 45(1): 120–52. https://doi.org/10.1080/03344355.2018.1412058

Tepper, Y., Porat, N., and Bar-Oz, G.
2020 "Sustainable Farming in the Roman-Byzantine Period: Dating an Advanced Agriculture System near the Site of Shivta, Negev Desert, Israel." *Journal of Arid Environments* 177: 104134. https://doi.org/10.1016/j.jaridenv.2020.104134

Vardi, J., and Rosen, S. A.
2020 "The Intermediate Bronze Age Lithic Industry from Ein Ziq: Implications for Cultural Affinities, Function, and Chronology." *Journal of the Israel Prehistoric Society* 50: 223–52.

The Archaeology and History of Rock-cut Cisterns and Open Water Reservoirs in the Negev Highlands

ONLINE SUPPLEMENTARY MATERIAL

ANDREA JUNGE, ZACHARY C. DUNSETH, RUTH SHAHACK-GROSS, ISRAEL FINKELSTEIN, AND MARKUS FUCHS

I. Methods

Preparation of the micromorphology blocks for the thin section analyses, sample preparation of the coarse-grain quartz fraction for OSL dating, as well as information on the OSL measurements and statistical analyses are described in detail elsewhere (Junge et al. 2018, 2021). This supplement describes the preparation steps that differ from those deployed in the authors' previous studies.

Preparation of an OSL Sample from Mortar

The mortar sample Gi815 from the bottom of the Nahal Revivim 102 cistern was collected as an entire block and brought to the OSL preparation laboratory. There, the outermost layer was removed by chiseling, to discard the light exposed material, followed by calcium carbonate dissolution with 10% HCl. The remaining grains were prepared similarly to the OSL preparations described in Junge et al. 2021.

Radionuclide Concentrations

For the OSL dating of the Ritma and Mishor HaRuchot open reservoirs and the Ramaliya rock-cut cistern, α-counting (U and Th) and ICP-OES (K) were used to determine the radionuclide concentrations. For Har Hemet 288, Mishor HaRuchot 9.3, Nahal Revivm 101 and 102 reservoirs and cisterns, the concentrations of Th, U, and K were assessed using the µDose system (Miłosz et al. 2017; Tudyka et al. 2018). The calculation of the cosmic dose rate as well as the conversion factors are equal to those used in Junge et al. 2021.

Water Content

The water content used for dose rate calculations (**Table S1**) for OSL dating from samples collected from the sediment fill within cisterns and reservoirs (15 ± 7.5%), sediment accumulations within channels (10 ± 5%) and spoil piles (6 ± 3%) has been extensively discussed in Junge et al. (2018, 2021). In the current study, different sampling positions are introduced and water contents assigned to them: 10 ± 5% for the sediment accumulation in the sedimentation pool (Gi397) and 6 ± 3% for sediments below channel stones (Gi398 and

Gi399) at Mishor HaRuchot 9.1, and the fines between the stone lining within the reservoir Mishor HaRuchot 9.3 (Gi852), 15 ± 7.5% for the mortar from the bottom of the cistern Nahal Revivim (Gi815).

For the sediments below channel stones (Gi398 and Gi399) at Mishor HaRuchot 9.1 and the fines between the stone lining within the reservoir Mishor HaRuchot 9.3 (Gi852), the water content was set to 6 ± 3%. This low water content is based on the comparably high amount of sand in these samples and their well-drained positions. The water content of the mortar from the bottom of the cistern Nahal Revivim (Gi815) was set to 15 ± 7.5%, because water can enter the porous mortar and when the cistern is flooded, a high water content is maintained over long periods of time (days to months). The saturation with water of the accumulation in the sedimentation pool of reservoir Mishor HaRuchot 9.1 (Gi397) is comparable with the channel fill at Borot Hazaz (Junge et al. 2021): the structure is fed by water from the slope but is not designed to hold the water over long periods of time, resulting in a water content of 10 ± 5%. All assigned water contents are supported by the measured water contents from samples collected in the field.

Cosmic Dose Rate Attenuation

To evaluate the attenuation of the cosmic dose rate, the thickness of the overlying material since the sediment was deposited needs to be estimated (**Table S2**). For gradual accumulation within cisterns, reservoirs and pools, half of the depth of the OSL sample location within a section is assumed to be the average depth below surface of the samples since deposition, while for the spoil piles that accumulated rapidly the total depth is used for the calculations. Due to the massive bedrock formation covering the entire Ramaliya cistern (**Fig. 3a**), 25 m was added to the depth of each sample to account for the strong reduction of cosmic dose rate at this site.

Radiocarbon Dating

The preparation of the samples was carried out according to Piotrowska 2013 at the Institute of Physics (Division of Geochronology and Environmental Isotopes) of the Silesian University of Technology in Gliwice. The AMS measurements were performed at the Poznan Radiocarbon Laboratory with use of NEC 0.5MV spectrometer (Goslar, Czernik, and Goslar 2004). The calibration of the radiocarbon ages was conducted using OxCal 4.4 (Bronk Ramsey 2009, 2021) and the IntCal20 calibration curve for radiocarbon ages BP (Reimer et al. 2020) or the post-bomb curve for NH1 zone for modern samples (Hua, Barbetti, and Rakowski 2013).

References

Bronk Ramsey, C.

2009 "Bayesian Analysis of Radiocarbon Dates." *Radiocarbon* 51(1): 337–60. https://doi.org/10.1017/S0033822200033865

2021 OxCal 4.4. https://c14.arch.ox.ac.uk/oxcal/OxCal.html

Goslar, T., Czernik, J., and Goslar, E.

2004 "Low-Energy 14C AMS in Poznań Radiocarbon Laboratory, Poland." *Nuclear Instruments and Methods in Physics Research Section B: Beam Interactions with Materials and Atoms* 223–24: 5–11. https://doi.org/10.1016/j.nimb.2004.04.005

Hua, Q., Barbetti, M., and Rakowski, A. J.

2013 "Atmospheric Radiocarbon for the Period 1950–2010." *Radiocarbon* 55(4): 2059–72. https://doi.org/10.2458/azu_js_rc.v55i2.16177

Junge, A., Dunseth, Z. C., Shahack-Gross, R., Finkelstein, I., and Fuchs, M.

2021 "Construction and Usage of Rock-Cut Cisterns: A Chronological Approach in the Arid Negev Highlands, Israel." *Archaeological and Anthropological Sciences* 13: 150. https://doi.org/10.1007/s12520-021-01366-5

Junge, A., Lomax, J., Shahack-Gross, R., Finkelstein, I., and Fuchs, M.

2018 "Chronology of an Ancient Water Reservoir and the History of Human Activity in the Negev Highlands, Israel." *Geoarchaeology* 33(6): 695–707. https://doi.org/10.1002/gea.21682

Miłosz, S., Tudyka, K., Walencik-Łata, A., Barwinek, S., Bluszcz, A., and Adamiec, G.

2017 "Pulse Height, Pulse Shape, and Time Interval Analyzer for Delayed α/β Coincidence Counting." *IEEE Transactions on Nuclear Science* 64: 2536–42. https://doi.org/10.1109/TNS.2017.2731852

Piotrowska, N.

2013 "Status Report of AMS Sample Preparation Laboratory at GADAM Centre, Gliwice, Poland." *Nuclear Instruments and Methods in Physics Research Section B: Beam Interactions with Materials and Atoms* 294: 176–81. https://doi.org/10.1016/j.nimb.2012.05.017

Reimer, P., Austin, W., Bard, E., Bayliss, A., Blackwell, P., Bronk Ramsey, C., Butzin, M., Cheng, H., Edwards, R., Friedrich, M., Grootes, P., Guilderson, T., Hajdas, I., Heaton, T., Hogg, A., Hughen, K., Kromer, B., Manning, S., Muscheler, R., Palmer, J., Pearson, C., van der Plicht, J., Reimer, R., Richards, D., Scott, E., Southon, J., Turney, C., Wacker, L., Adolphi, F., Büntgen, U., Capano, M., Fahrni, S., Fogtmann-

Schulz, A., Friedrich, R., Köhler, P., Kudsk, S., Miyake, F., Olsen, J., Reinig, F., Sakamoto, M., Sookdeo, A., and Talamo, S.

2020 "The IntCal20 Northern Hemisphere Radiocarbon Age Calibration Curve (0–55 cal kBP)." *Radiocarbon* 62(4): 725–57. https://doi.org/10.1017/RDC.2020.41

Tudyka, K., Miłosz, S., Adamiec, G., Bluszcz, A., Poręba, G., Paszkowski, Ł., and Kolarczyk, A.

2018 "μDose: A Compact System for Environmental Radioactivity and Dose Rate Measurement." *Radiation Measurements* 118: 8–13. https://doi.org/10.1016/j.radmeas.2018.07.016

II. Tables

Table S1. Sample ID, K-, Th- and U-content, cosmic dose rate, water content and the resulting dose rate (Ḋ).

Sample ID	K [%]	Th [ppm]	U [ppm]	Cosmic dose rate [Gy/ka]	Water content [%]	Total dose rate [Gy/ka]
Mishor HaRuchot 9.1 reservoir						
Spoil Pile						
Gi387	0.38 ± 0.02	2.37 ± 0.35	1.44 ± 0.11	0.18 ± 0.02	6 ± 3	1.00 ± 0.04
Gi388	0.43 ± 0.02	3.22 ± 0.40	0.94 ± 0.12	0.19 ± 0.02	6 ± 3	1.00 ± 0.04
Gi389	0.46 ± 0.02	2.80 ± 0.38	1.16 ± 0.12	0.20 ± 0.02	6 ± 3	1.06 ± 0.04
Gi390	0.51 ± 0.03	2.06 ± 0.30	1.65 ± 0.09	0.25 ± 0.03	6 ± 3	1.21 ± 0.05
Gi391	0.34 ± 0.02	1.76 ± 0.27	1.09 ± 0.08	0.20 ± 0.02	6 ± 3	0.87 ± 0.04
Gi392	0.46 ± 0.02	1.85 ± 0.27	1.15 ± 0.08	0.24 ± 0.02	6 ± 3	1.04 ± 0.04
Gi393	0.47 ± 0.02	2.24 ± 0.31	1.57 ± 0.10	0.30 ± 0.03	6 ± 3	1.15 ± 0.05
Gi394	0.46 ± 0.02	2.19 ± 0.29	1.25 ± 0.09	0.21 ± 0.02	6 ± 3	1.05 ± 0.04
Pool						
Gi397	0.31 ± 0.02	1.86 ± 0.27	1.21 ± 0.09	0.26 ± 0.03	10 ± 5	0.89 ± 0.04
Channels						
Gi398	0.31 ± 0.02	1.77 ± 0.27	1.19 ± 0.08	0.26 ± 0.03	6 ± 3	0.91 ± 0.04
Gi399	0.29 ± 0.01	1.09 ± 0.19	1.25 ± 0.06	0.26 ± 0.03	6 ± 3	0.86 ± 0.03
Mishor HaRuchot 9.3 reservoir						
Spoil pile						
Gi845	0.26 ± 0.05	0.80 ± 0.50	0.93 ± 0.15	0.20 ± 0.02	6 ± 3	0.69 ± 0.06
Gi846	0.41 ± 0.06	2.40 ± 0.60	0.90 ± 0.16	0.20 ± 0.02	6 ± 3	0.93 ± 0.07
Gi847	0.42 ± 0.05	2.90 ± 0.30	1.14 ± 0.11	0.20 ± 0.02	6 ± 3	1.02 ± 0.05
Gi848	0.52 ± 0.05	2.10 ± 0.60	1.09 ± 0.17	0.21 ± 0.02	6 ± 3	1.07 ± 0.06
Gi849	0.49 ± 0.06	2.50 ± 0.60	1.11 ± 0.17	0.24 ± 0.02	6 ± 3	1.10 ± 0.07
Reservoir fill						
Gi850	0.47 ± 0.06	4.40 ± 0.40	1.18 ± 0.12	0.19 ± 0.02	15 ± 7.5	1.08 ± 0.07
Gi851	0.51 ± 0.05	2.90 ± 0.60	0.75 ± 0.17	0.20 ± 0.02	15 ± 7.5	0.95 ± 0.07
Stone lining/wall						
Gi852	0.31 ± 0.05	2.40 ± 0.60	1.19 ± 0.16	0.24 ± 0.02	6 ± 3	0.93 ± 0.06
Har Hemet 288 reservoir						
Spoil pile						
Gi832	0.42 ± 0.05	2.40 ± 0.60	0.86 ± 0.217	0.19 ± 0.02	6 ± 3	0.92 ± 0.06
Gi833	0.37 ± 0.05	3.90 ± 0.40	1.28 ± 0.12	0.20 ± 0.02	6 ± 3	1.07 ± 0.06
Gi834	0.43 ± 0.05	1.80 ± 0.70	1.38 ± 0.20	0.21 ± 0.02	6 ± 3	1.02 ± 0.07
Gi835	0.47 ± 0.06	2.20 ± 0.40	1.65 ± 0.13	0.23 ± 0.02	6 ± 3	1.17 ± 0.06
Gi836	0.40 ± 0.06	6.70 ± 0.50	1.46 ± 0.16	0.25 ± 0.03	6 ± 3	1.36 ± 0.07
Reservoir fill						
Gi837	0.42 ± 0.06	5.00 ± 0.50	1.28 ± 0.14	0.19 ± 0.02	15 ± 7.5	1.09 ± 0.07
Gi838	0.38 ± 0.05	2.80 ± 0.50	0.64 ± 0.15	0.19 ± 0.02	15 ± 7.5	0.81 ± 0.06
Gi839	0.42 ± 0.06	3.00 ± 0.50	0.75 ± 0.15	0.20 ± 0.02	15 ± 7.5	0.88 ± 0.07
Gi840	0.42 ± 0.05	1.50 ± 0.50	0.80 ± 0.15	0.20 ± 0.02	15 ± 7.5	0.80 ± 0.06
Gi841	0.37 ± 0.05	4.30 ± 0.40	1.08 ± 0.12	0.21 ± 0.02	15 ± 7.5	0.98 ± 0.06
Gi842	0.29 ± 0.05	2.20 ± 0.50	0.60 ± 0.14	0.23 ± 0.02	10 ± 5	0.74 ± 0.06

Gi843	0.32 ± 0.05	3.50 ± 0.30	0.78 ± 0.10	0.24 ± 0.02	10 ± 5	0.90 ± 0.05
Bor Ritma reservoir						
Spoil pile (main)						
Gi605	0.68 ± 0.03	4.38 ± 0.74	2.38 ± 0.23	0.19 ± 0.02	6 ± 3	1.62 ± 0.07
Gi607	1.69 ± 0.08	7.45 ± 0.86	2.18 ± 0.26	0.24 ± 0.02	6 ± 3	2.75 ± 0.11
Gi610	0.81 ± 0.04	4.06 ± 0.64	2.15 ± 0.20	0.25 ± 0.03	6 ± 3	1.71 ± 0.07
Spoil pile (secondary)						
Gi611	0.84 ± 0.04	4.04 ± 0.71	2.35 ± 0.22	0.19 ± 0.02	6 ± 3	1.74 ± 0.07
Gi612	0.89 ± 0.04	3.91 ± 0.72	2.77 ± 0.22	0.26 ± 0.03	6 ± 3	1.89 ± 0.08
Ramaliya cistern						
Cistern fill						
Gi594	0.90 ± 0.04	4.21 ± 0.19	2.81 ± 0.20	0.02 ± 0.00	15 ± 7.5	1.58 ± 0.10
Gi595	0.82 ± 0.04	3.83 ± 0.19	2.29 ± 0.19	0.02 ± 0.00	15 ± 7.5	1.38 ± 0.09
Gi596	0.88 ± 0.04	3.43 ± 0.19	3.07 ± 0.20	0.02 ± 0.00	15 ± 7.5	1.57 ± 0.10
Gi597	0.89 ± 0.04	5.30 ± 0.19	2.30 ± 0.22	0.02 ± 0.00	15 ± 7.5	1.53 ± 0.10
Gi598	0.90 ± 0.05	2.97 ± 0.19	3.50 ± 0.20	0.02 ± 0.00	15 ± 7.5	1.64 ± 0.11
Gi599	0.82 ± 0.04	3.85 ± 0.19	2.61 ± 0.12	0.02 ± 0.00	15 ± 7.5	1.45 ± 0.09
Gi600	0.87 ± 0.04	3.73 ± 0.19	2.75 ± 0.12	0.02 ± 0.00	15 ± 7.5	1.51 ± 0.09
Gi601	0.95 ± 0.05	3.82 ± 0.19	3.23 ± 0.23	0.02 ± 0.00	15 ± 7.5	1.68 ± 0.11
Gi602	0.96 ± 0.05	3.92 ± 0.19	3.66 ± 0.24	0.02 ± 0.00	15 ± 7.5	1.78 ± 0.12
Gi603	0.83 ± 0.04	3.62 ± 0.19	3.05 ± 0.22	0.02 ± 0.00	15 ± 7.5	1.53 ± 0.10
Gi604	0.95 ± 0.05	4.40 ± 0.19	2.83 ± 0.24	0.02 ± 0.00	15 ± 7.5	1.63 ± 0.11
Nahal Revivim 101 cistern						
Spoil pile						
Gi823	0.38 ± 0.06	5.10 ± 1.10	5.74 ± 0.30	0.18 ± 0.02	6 ± 3	2.10 ± 0.10
Gi824	0.00 ± 0.06	0.00 ± 0.50	8.84 ± 0.21	0.19 ± 0.02	6 ± 3	2.09 ± 0.07
Gi825	0.05 ± 0.06	0.23 ± 0.24	5.58 ± 0.13	0.26 ± 0.03	6 ± 3	1.49 ± 0.07
Cistern fill						
Gi826	0.67 ± 0.07	8.70 ± 1.30	5.34 ± 0.40	0.20 ± 0.02	15 ± 7.5	2.32 ± 0.15
Gi827	0.48 ± 0.07	6.40 ± 1.40	6.75 ± 0.40	0.21 ± 0.02	15 ± 7.5	2.31 ± 0.15
Gi828	0.47 ± 0.07	3.90 ± 1.00	7.15 ± 0.30	0.22 ± 0.02	15 ± 7.5	2.24 ± 0.14
Gi829	0.31 ± 0.07	3.70 ± 0.60	9.85 ± 0.24	0.23 ± 0.02	15 ± 7.5	2.63 ± 0.15
Gi830	0.26 ± 0.07	2.80 ± 0.90	7.22 ± 0.29	0.26 ± 0.03	15 ± 7.5	2.01 ± 0.12
Gi831	0.29 ± 0.06	4.70 ± 1.40	6.55 ± 0.40	0.28 ± 0.03	15 ± 7.5	1.94 ± 0.13
Nahal Revivim 102 cistern						
Spoil pile						
Gi810	0.55 ± 0.06	5.00 ± 0.80	4.25 ± 0.23	0.18 ± 0.02	6 ± 3	1.92 ± 0.09
Gi811	0.16 ± 0.06	4.60 ± 1.30	6.75 ± 0.40	0.19 ± 0.02	6 ± 3	2.08 ± 0.11
Gi812	0.09 ± 0.06	4.60 ± 1.10	6.45 ± 0.30	0.20 ± 0.02	6 ± 3	1.96 ± 0.10
Gi813	0.25 ± 0.06	1.80 ± 0.90	6.38 ± 0.27	0.21 ± 0.02	6 ± 3	1.93 ± 0.09
Gi814	0.67 ± 0.06	7.80 ± 0.90	4.23 ± 0.28	0.26 ± 0.03	6 ± 3	2.24 ± 0.09
Mortar						
Gi815	0.20 ± 0.06	7.20 ± 1.20	4.83 ± 0.40	0.16 ± 0.02	15 ± 7.5	1.85 ± 0.11
Cistern fill						
Gi816	0.62 ± 0.07	7.80 ± 1.20	5.44 ± 0.30	0.19 ± 0.02	15 ± 7.5	2.23 ± 0.14
Gi817	0.50 ± 0.06	5.40 ± 1.00	5.34 ± 0.30	0.20 ± 0.02	15 ± 7.5	1.98 ± 0.12
Gi818	0.18 ± 0.06	2.10 ± 0.40	6.81 ± 0.18	0.20 ± 0.02	15 ± 7.5	1.80 ± 0.11
Gi819	0.42 ± 0.07	4.10 ± 0.50	6.70 ± 0.18	0.20 ± 0.02	15 ± 7.5	2.11 ± 0.12
Gi820	0.64 ± 0.06	5.50 ± 0.90	4.92 ± 0.27	0.21 ± 0.02	15 ± 7.5	2.03 ± 0.12
Gi821	0.67 ± 0.06	10.60 ± 1.20	4.23 ± 0.40	0.23 ± 0.02	15 ± 7.5	2.24 ± 0.14
Gi822	0.61 ± 0.07	4.00 ± 0.40	5.54 ± 0.17	0.27 ± 0.03	15 ± 7.5	2.02 ± 0.12

Table S2. Sample ID, deposition mode, sampling depth below surface, equivalent dose (D_e), number of measured aliquots, aliquot diameter, overdispersion, relative standard deviation, transformation for De calculation (logged or unlogged), used age models (CAM = central age model, MAM = minimum age model) and the resulting OSL age.

Sample ID	Section location/ deposition mode	Sampling depth [cm]	D_e [Gy]	Number of aliquots	Aliquot diameter [mm]	Overdispersion [%]	Rel. standard deviation [%]	Logged or unlogged	Age model	Age [ka]	Age in calendar years*
Mishor HaRuchot 9.1 reservoir											
	Spoil pile										
Gi387	Pre-construction	160	5.59 ± 0.52	25	2	21	24	logged	MAM	5.6 ± 0.6	4200–3000 B.C.E.
Gi388	Construction (OE)	128	5.49 ± 0.21	25	2	10	13	logged	CAM	5.5 ± 0.3	3800–3200 B.C.E.
Gi389	Maintenance	98	3.70 ± 0.25	24	2	29	29	logged	CAM	3.5 ± 0.3	1800–1200 B.C.E.
Gi390	Maintenance	30	3.85 ± 0.19	23	2	18	18	logged	CAM	3.2 ± 0.2	1400–1000 B.C.E.
Gi391	Construction	141	3.69 ± 0.25	36	2	17	19	logged	MAM	4.3 ± 0.3	2600–2000 B.C.E.
Gi392	Maintenance	75	3.15 ± 0.46	9	2	41	43	logged	CAM	3.0 ± 0.5	1500–500 B.C.E.
Gi393	Maintenance	57	4.18 ± 0.18	31	2	16	16	logged	CAM	3.7 ± 0.2	1900–1500 B.C.E.
Gi394	Pre-construction	81	6.95 ± 0.23	25	2	16	17	logged	CAM	6.6 ± 0.3	4900–4300 B.C.E.
	Pool										
Gi397	Cessation of maintenance	19	0.48 ± 0.10	31	2	78	82	unlogged	MAM	0.52 ± 0.11	1390–1610 C.E.
	Channels										
Gi398	Maintenance	31	0.33 ± 0.12	22	3	66	68	unlogged	MAM	0.37 ± 0.11	1540–1760 C.E.
Gi399	Maintenance	28	0.41 ± 0.07	19	2	99	104	unlogged	MAM	0.47 ± 0.09	1460–1640 C.E.
Mishor HaRuchot 9.3 reservoir											
	Spoil pile										
Gi845	Pre-construction	115	3.80 ± 0.17	31	1	16	19	logged	CAM	5.5 ± 0.5	4000–3000 B.C.E.
Gi846	Maintenance	97	2.52 ± 0.28	34	1	26	30	logged	MAM	2.7 ± 0.4	1100–300 B.C.E.
Gi847	Maintenance	105	3.11 ± 0.14	33	1	18	21	logged	CAM	3.1 ± 0.2	1300–900 B.C.E.
Gi848	Maintenance	68	3.39 ± 0.27	25	2	17	21	logged	MAM	3.2 ± 0.3	1500–900 B.C.E.
Gi849	Maintenance	35	2.96 ± 0.15	33	2	23	24	logged	CAM	2.7 ± 0.2	900–500 B.C.E.
	Reservoir fill										
Gi850	Cessation of maintenance	258	0.61 ± 0.17	28	2	89	90	unlogged	MAM	0.57 ± 0.17	1280–1620 C.E.
Gi851	Cessation of maintenance	223	0.77 ± 0.23	31	2	57	61	unlogged	MAM	0.81 ± 0.25	960–1460 C.E.

	Stone lining/wall										
Gi852	Construction	39	3.72 ± 0.27	25	1	52	103	logged	MAM	4.0 ± 0.4	2400–1600 B.C.E.
Har Hemet 288 reservoir											
	Spoil pile										
Gi832	Pre-construction	155	4.28 ± 0.32	27	1	17	20	logged	MAM	4.7 ± 0.5	3200–2200 B.C.E.
Gi833	Construction	115	2.96 ± 0.17	26	1	24	25	logged	CAM	2.8 ± 0.2	1000–600 B.C.E.
Gi834	Construction/Maintenance	85	2.44 ± 0.31	27	1	40	46	logged	MAM	2.4 ± 0.3	700–100 B.C.E.
Gi835	Maintenance	50	0.67 ± 0.20	31	2	54	56	unlogged	MAM	0.57 ± 0.18	1270–1630 C.E.
Gi836	Maintenance (OE)	29	2.32 ± 0.23	29	1	57	68	logged	MAM	1.7 ± 0.2	100–500 C.E.
	Reservoir fill										
Gi837	Cessation of maintenance	300	1.55 ± 0.11	31	1	45	61	logged	MAM	1.4 ± 0.1	500–700 C.E.
Gi838	Cessation of maintenance	275	1.29 ± 0.24	29	2	73	77	unlogged	MAM	1.6 ± 0.3	100–700 C.E.
Gi839	Cessation of maintenance	240	1.41 ± 0.21	35	2	68	76	logged	MAM	1.6 ± 0.3	100–700 C.E.
Gi840	Cessation of maintenance	210	1.45 ± 0.15	36	3	27	30	logged	MAM	1.8 ± 0.2	0–400 C.E.
Gi841	Cessation of maintenance	175	1.43 ± 0.17	69	1	85	89	logged	MAM	1.5 ± 0.2	300–700 C.E.
Gi842	Cessation of maintenance (OE)	110	3.61 ± 0.63	39	1	77	85	logged	MAM	4.9 ± 0.9	3800–2000 B.C.E.
Gi843	Cessation of maintenance	70	1.74 ± 0.26	40	2	61	67	logged	MAM	1.9 ± 0.3	200 B.C.E–400 C.E.
Bor Ritma reservoir											
	Spoil pile (main)										
Gi605	Pre-construction	105	9.50 ± 0.79	22	2	37	40	logged	CAM	5.9 ± 0.6	4500–3400 B.C.E.
Gi607	Construction	26	2.13 ± 0.36	32	1	72	78	logged	MAM	0.78 ± 0.14	1100–1380 C.E.
Gi610	Maintenance	20	1.45 ± 0.12	24	2	38	41	unlogged	CAM	0.85 ± 0.08	1090–1250 C.E.
	Spoil pile (secondary)										
Gi611	Maintenance	95	0.38 ± 0.06	29	3	44	50	unlogged	MAM	0.22 ± 0.04	1760–1840 C.E.
Gi612	Maintenance (OE)	15	2.11 ± 0.22	28	3	44	45	unlogged	MAM	1.1 ± 0.1	800–1000 C.E.
Ramaliya cistern											
	Cistern fill										
Gi594	Cessation of maintenance	280	1.63 ± 0.24	29	2	48	49	unlogged	MAM	1.0 ± 0.2	800–1200 C.E.
Gi595	Cessation of maintenance	240	0.58 ± 0.10	34	2	82	84	unlogged	MAM	0.42 ± 0.08	1520–1680 C.E.
Gi596	Cessation of maintenance	215	0.81 ± 0.21	42	2	69	71	unlogged	MAM	0.52 ± 0.14	1360–1640 C.E.
Gi597	Cessation of maintenance	191	0.72 ± 0.15	28	2	68	70	unlogged	MAM	0.47 ± 0.10	1450–1650 C.E.
Gi598	Cessation of maintenance	163	0.34 ± 0.18	28	2	88	90	unlogged	MAM	0.21 ± 0.11	1700–1920 C.E.
Gi599	Cessation of maintenance	135	0.98 ± 0.19	28	2	47	48	unlogged	MAM	0.67 ± 0.14	1210–1490 C.E.
Gi600	Cessation of maintenance	113	0.62 ± 0.19	36	2	86	90	unlogged	MAM	0.41 ± 0.13	1480–1740 C.E.

Gi601	Cessation of maintenance	95	0.78 ± 0.20	32	2	60	63	unlogged	MAM	0.46 ± 0.12	1440–1680 C.E.
Gi602	Cessation of maintenance	70	0.41 ± 0.09	37	2	91	93	unlogged	MAM	0.23 ± 0.06	1730–1850 C.E.
Gi603	Cessation of maintenance	45	0.50 ± 0.09	33	2	94	96	unlogged	MAM	0.33 ± 0.06	1630–1750 C.E.
Gi604	Cessation of maintenance	20	0.56 ± 0.13	31	2	65	67	unlogged	MAM	0.34 ± 0.08	1600–1760 C.E.
Nahal Revivim 101 cistern											
	Spoil pile										
Gi823	Pre-Construction	142	1.12 ± 0.06	30	3	58	60	unlogged	MAM	0.54 ± 0.04	1440–1520 C.E.
Gi824	Construction	116	2.06 ± 0.10	58	2	27	27	unlogged	CAM	0.99 ± 0.06	970–1090 C.E.
Gi825	Maintenance	15	0.43 ± 0.15	37	2	66	66	unlogged	MAM	0.29 ± 0.10	1630–1830 C.E.
	Cistern fill										
Gi826	Cessation of maintenance	133	0.40 ± 0.11	32	3	73	74	unlogged	MAM	0.17 ± 0.05	1800–1900 C.E.
Gi827	Cessation of maintenance	120	0.65 ± 0.07	32	3	56	58	unlogged	MAM	0.28 ± 0.04	1700–1780 C.E.
Gi828	Cessation of maintenance	94	0.23 ± 0.05	32	3	173	179	unlogged	MAM	0.10 ± 0.02	1900–1940 C.E.
Gi829	Cessation of maintenance	70	1.01 ± 0.20	35	3	49	50	unlogged	MAM	0.39 ± 0.08	1550–1710 C.E.
Gi830	Cessation of maintenance	35	0.23 ± 0.05	30	3	106	108	unlogged	MAM	0.12 ± 0.03	1870–1930 C.E.
Gi831	Cessation of maintenance	15	0.28 ± 0.06	29	3	92	94	unlogged	MAM	0.14 ± 0.03	1850–1910 C.E.
Nahal Revivim 102 cistern											
	Spoil pile										
Gi810	Pre-construction	162	0.52 ± 0.07	29	2	86	94	unlogged	MAM	0.27 ± 0.04	1710–1790 C.E.
Gi811	Construction	117	1.95 ± 0.18	30	1	24	28	logged	MAM	0.94 ± 0.10	980–1180 C.E.
Gi812	Construction	88	2.15 ± 0.18	35	1	28	35	logged	MAM	1.1 ± 0.1	800–1000 C.E.
Gi813	Maintenance	57	0.95 ± 0.24	29	1	56	60	unlogged	MAM	0.49 ± 0.13	1400–1660 C.E.
Gi814	Maintenance	17	0.46 ± 0.06	31	2	85	90	unlogged	MAM	0.20 ± 0.03	1790–1850 C.E.
	Mortar										
Gi815	Construction	217	2.88 ± 0.23	26	1	17	21	logged	MAM	1.6 ± 0.2	200–600 C.E.
	Cistern fill										
Gi816	Cessation of maintenance	214	0.45 ± 0.10	30	2	75	78	unlogged	MAM	0.20 ± 0.05	1770–1870 C.E.
Gi817	Cessation of maintenance	180	0.35 ± 0.06	32	2	99	103	unlogged	MAM	0.18 ± 0.04	1800–1880 C.E.
Gi818	Cessation of maintenance	159	0.33 ± 0.05	30	3	90	96	unlogged	MAM	0.18 ± 0.03	1810–1870 C.E.
Gi819	Cessation of maintenance	135	0.45 ± 0.11	31	3	61	63	unlogged	MAM	0.21 ± 0.05	1760–1860 C.E.
Gi820	Cessation of maintenance	115	0.57 ± 0.07	31	3	68	70	unlogged	MAM	0.28 ± 0.04	1700–1780 C.E.
Gi821	Cessation of maintenance	70	0.29 ± 0.05	34	4	117	119	unlogged	MAM	0.13 ± 0.02	1870–1910 C.E.
Gi822	Cessation of maintenance	22	0.37 ± 0.05	37	7	102	103	unlogged	MAM	0.18 ± 0.03	1810–1870 C.E.

*The range covers the OSL ages with one σ error range; OE = Overestimation

Table S3. Results of radiocarbon analyses from Nahal Revivim 101 and 102. All samples are plant remains.

Sample ID	Lab. number	Section location/ deposition mode	^{14}C age [cal BP or pMC]	Ranges of calendar age for 68.2% confidence level	Ranges of calendar age for 95.4% confidence level
Nahal Revivim 101					
NR-101-S-147	GdA-6369	Spoil pile	460 ± 30 BP	1427 C.E. (68.3%) 1452 C.E.	1412 C.E. (95.4%) 1471 C.E.
NR-101-S-84	GdA-6370	Spoil pile	255 ± 30 BP	1530 C.E. (6.4%) 1538 C.E. 1636 C.E. (48.9%) 1666 C.E. 1783 C.E. (12.9%) 1796 C.E.	1520 C.E. (22.4%) 1586 C.E. 1622 C.E. (54.4%) 1676 C.E. 1742 C.E. (0.9%) 1751 C.E. 1764 C.E. (17.8%) 1800 C.E.
NR-101-S-43	GdA-6371	Spoil pile	185 ± 30 BP	1664 C.E. (13.6%) 1684 C.E. 1734 C.E. (35.4%) 1784 C.E. 1794 C.E. (6.0%) 1804 C.E. 1928 C.E. (13.3%) …	1653 C.E. (20.6%) 1696 C.E. 1724 C.E. (52.0%) 1812 C.E. 1838 C.E. (5.3%) 1878 C.E. 1915 C.E. (17.6%) …
NR-101-C-110	GdA-6368	Cistern fill	101.81 ± 0.35 pMC	1953 C.E. (68.3%) 1957 C.E.	1951 C.E. (95.4%) 1959 C.E.
Nahal Revivim 102					
NR-102-C-217	GdA-6366	Cistern fill	100.62 ± 0.34 pMC	1953 C.E. (68.3%) 1957 C.E.	1951 C.E. (95.4%) 1959 C.E.
NR-102-C-190	GdA-6367	Cistern fill	180 ± 30 BP	1666 C.E. (13.3%) 1686 C.E. 1732 C.E. (34.4%) 1784 C.E. 1795 C.E. (6.2%) 1806 C.E. 1926 C.E. (14.4%) ...	1655 C.E. (19.3%) 1698 C.E. 1722 C.E. (50.1%) 1814 C.E. 1836 C.E. (7.5%) 1883 C.E. 1910 C.E. (18.6%) …

Declaration

I declare that I have completed this dissertation single-handedly without the unauthorized help of a second party and only with the assistance acknowledged therein. I have appropriately acknowledged and cited all text passages that are derived verbatim from or are based on the content of published work of others, and all information relating to verbal communications. I consent to the use of an anti-plagiarism software to check my thesis. I have abided by the principles of good scientific conduct laid down in the charter of the Justus Liebig University Giessen „Satzung der Justus-Liebig-Universität Gießen zur Sicherung guter wissenschaftlicher Praxis“ in carrying out the investigations described in the dissertation.

Place and Date: **Signature:**